PALEOCLIMATE MODELS FOR WESTERN NORTH AMERICA AS INFERRED FROM SPELEOTHEM ISOTOPE RECORDS

By

FERIDE SEREFIDDIN, B.S., M.A.

A Thesis

Submitted to the School of Graduate Studies

in Partial Fulfillment of the Requirements

for the Degree

Doctor of Philosophy

McMaster University

PALEOCLIMATE MODELS FOR WESTERN NORTH AMERICA

DOCTOR OF PHILOSOPHY (2002) McMaster University

(Geology) Hamilton, Ontario

TITLE: Paleoclimate models for western North America as inferred from speleothem isotope records.

AUTHOR: Feride Serefiddin, B.S. (University of California, Berkeley), M.A. (San Francisco State University)

SUPERVISORS: Dr. Henry P. Schwarcz, Dr. Derek C. Ford

NUMBER OF PAGES: 156, xix

ABSTRACT

Prediction of future climate change relies on the accuracy of models that can be calibrated using paleoclimate proxy data. The longest and most continuous records are based on marine sediment and ice cores, but cannot be dated using absolute radiometric techniques. Analyses of speleothems from western North America were used to develop well-dated isotope records for Quaternary paleoclimate reconstructions. This research uses the oxygen and carbon isotope records of speleothems from Reed's Cave, in the Black Hills of South Dakota, to determine the presence of high resolution and long-term climate cycles. δD analyses of fluid inclusion water extracted from speleothem were used to estimate absolute paleotemperature change.

Oxygen and carbon isotope analysis of two Wisconsin age speleothems shows different $\delta^{18}O_{ct}$ ($\delta^{18}O$ of calcite) records for their coeval period of growth. The growth rates for the speleothems also differ and suggest that local environmental factors may have produced the divergent isotopic variation. Spectral analysis of the oxygen isotope record reveals the presence of millennial-scale cycles and Heinrich events. Good correlation with speleothem isotope records from Missouri and Israel confirm that global climate is being recorded.

Three mid-Pleistocene speleothems from Reed's Cave grew from 550,000 to 150,000 years ago have divergent isotope records but show evidence of global climate change. Local differences in hydrology and topography are attributed to the different records. Two speleothems show large isotopic variation during marine isotope stages

(MIS) 11 and 13. These results show the sensitivity of the speleothem isotope record to climate change on the continents. There is evidence that MIS 13 was warmer than MIS 11, information that rejects the theory that MIS 11 was the warmest Quaternary interglacial.

The measurement of δD variations in speleothem fluid inclusion water gives a record of paleoprecipitation for two sites in western North America. The temperatures calculated show large magnitude changes in temperature during the Wisconsin glacial period of up to 10 °C. The temperature shift for the coeval period of the growth for the two speleothems shows synchronous warming and cooling events between 60 and 55 ka BP. Results of δD analyses of a speleothem from the central California coast show Holocene cooling that was initiated at approximately 8 ka BP and may be evidence of the hypsithermal.

This research was initially intended to develop paleoclimate records for western North America but also succeeded in providing additional insight on speleothem geochemistry. Divergent isotope records in coeval speleothems is not necessarily evidence of non-equilibrium deposition. We found corresponding differences in the deposited calcite and the fluid inclusion water, which is likely a preserved sample of the original dripwaters. Therefore it is possible to uncover global climate signals in speleothems with divergent $\delta^{18}O_{ct}$ records. The influence of local, small scale variables on the isotope record has been underestimated. There is strong evidence that terrestrial proxies record high resolution paleoclimate that cannot be captured by the marine and ice core records.

ACKNOWLEDGEMENTS

I would like to thank my two supervisors, Dr. Derek Ford and Dr. Henry Schwarcz for everything they have done for me over the last four years. I was very lucky to be able to work with the world experts of the geochemistry of caves and speleothems. I was trained to be a good scientist both in the field and in the laboratory. Derek gave me the opportunity to meet and work with many cavers and cave scientists. Henry has worked with me, through endless revisions, on improving my writing and my scientific thought process. I am so grateful for everything they have done for me. Most important, they made me feel like family while I was so far away from mine.

There are so many people that helped me the past four years, I would like to believe they all know who they are. Martin Knyf and Nicki Robinson taught me everything I needed to know about laboratory analyses and even ran many of my samples for me when I needed help. Martin was critical in getting my fluid inclusion crushing cell and vacuum line built. Janice Wade and Nancy Brand made administrative things easier and were always good for a laugh. Chas Yonge was so helpful during field work and provided insight during our discussions about trying to analyze fluid inclusions in speleothems. Peter Rowe and his laboratory welcomed my visit to learn how to build a fluid inclusion crushing cell. I was blessed with the help of many cavers, especially Steve Baldwin, Steve Langendorf, Sammi Langendorf, Brian Bischoff, Brad Wilson, Louise Clearwater and Jim Cochrane.

The friendship of many people in Hamilton and the department helped me to enjoy these last four years. I was blessed with two wonderful housemates - Adriana Zdyrko and Tracy Morkin during most of my stay here. Heather Jones, Chris Giovis, Pat DeLuca and Emmanuelle Arnaud were excellent companions for the much needed musical, dining and beverage rehabilitation. I want to thank all my friends in California for all their support and attempt at understanding what it is I do here at McMaster. Special thanks to Paul Amato for always being my biggest fan and Nyla Comisso for making sure I checked in every now and then.

Lastly, but most importantly, I need to thank my family for all their support. My mother and father are my greatest supporters and always tried to make things easier for me so that I could finish my degree. Ravs, Talia and Timur took care of me when I was home and helped me relax when I needed to most. My niece Leyla always made me smile, even when things were rough. My cousin Adile provided the necessary wine country trips and bottles of vintage wine to keep me happy. The rest of my family was always cheering me on and I am lucky to have such a big support system. Finally, I would like to thank Casey Schroeder for all his love and support when I needed it most.

TABLE OF CONTENTS

LIST OF ILLUSTRATIONS

LIST OF TABLES

PREFACE

Chapters 2 - 4 have been prepared for publication in scientific journals. Chapter 2 has been submitted to the journal Palaeogeography, Palaeoclimatology, Palaeoecology but not yet been accepted for publication. All papers are written entirely by the candidate.

Chapter 2

Title:
Late Pleistocene paleoclimate in the Black Hills of South Dakota from isotope records in speleothems

Journal status:
Submitted to Palaeogeography, Palaeocclimatology, Palaeoecology

Authors:
F. Serefiddin, H.P. Schwarcz, D.C. Ford, and S. Baldwin

Candidate's contribution:
All sample collection, nearly all laboratory work and writing. Editorial assistance by second and third author and assistance with sampling by fourth author.

Chapter 3

Title:
Terrestrial records of climate change in the mid-continent of North America from 530,000 to 150,000 years ago

Journal status:
Being prepared for submission to Quaternary Science Reviews

Authors:
F. Serefiddin, D.C. Ford, and H.P. Schwarcz

Candidate's contribution:
All sample collection, nearly all laboratory work and writing. Editorial assistance by second and third author.

Chapter 4

Title:
Records of climate change in central and western North America from δD variations in speleothem fluid inclusions

Journal status:
Being prepared for submission to Geology

Authors:
F. Serefiddin, H.P. Schwarcz, D.C. Ford, M. Knyf, and H. Seywerd

Candidate's contribution:
All sample collection, nearly all laboratory work and writing. Assistance in development of laboratory equipment by fourth and fifth authors. Editorial assistance by second and third author.

LIST OF TERMS

δ Delta notation used for expressing variation of isotopic ratio of sample from standard. Example for oxygen:

$$\delta^{18}O = \frac{\{(^{18}O/^{16}O_{sample}) - (^{18}O/^{16}O_{standard})\}}{(^{18}O/^{16}O_{standard})} * 10^3$$

‰ Per mil (parts per thousand), units for δ values

α_{AB} Fractionation factor = R_A/R_B where $R = (^{18}O/^{16}O)$

γ $d(\delta^{18}O_{ct})/dT$ = change in $\delta^{18}O_{ct}$ with temperature

BP before present

ct calcite, used as subscript for $\delta^{18}O$

d_0 $\delta D - 8\delta^{18}O$ deuterium excess value

Dansgaard-Oeschger or D-O cycles Millennial scale cycles or interstadial (warm) events discovered in spectral analysis of ice cores

DTAP Distilled tap water used a laboratory standard for isotopic analyses of water in McMaster Isotope Laboratory

fi fluid inclusions, used as subscript for δD

flowstone speleothem formed by water running down a wall or along the floor in the cave

Heinrich or H event Layers discovered in North Atlantic sediments representing major ice rafting events related instabilities in Laurentide Ice Sheet or major climate change

ka thousands of years ago

LGM last glacial maximum at 20,000 years ago

MC-ICP-MS or MC/ICP-MS or MCICP-MS multi-collector inductively coupled plasma mass spectrometer

meteoric water water from rain or snow

MEXIS Iceland Spar from Chihuahua, Mexico

Milankovitch cycles Climate cycles with frequencies of eccentricity (100,000 years), obliquity (41,000 years) or precession (23,000 or 18,000 years) of earth's orbit

MIS marine isotope stages as determined by cycles of $\delta^{18}O$ in foraminifera from sediment record in oceans; odd numbers are interglacial stages, even numbers are glacial stages

MWL meteoric water line relationship $\delta D = 8\delta^{18}O + d_0$

Pleistocene Epoch in geologic time scale from 2.3 million years ago to 10,000 years ago

ppt precipitation, used as subscript for $\delta^{18}O$

Quaternary Period in geologic time scale from 2.3 million years ago to present (current period)

SLAP standard light Antarctic precipitation used as calibration standard for isotopic analyses of water

SPECMAP Spectral Mapping Project (stacked record of $\delta^{18}O$ of foraminifera) based on low and middle latitude marine sediment cores

speleothem mineral deposit formed in a cave from seepage water, generally in the form of calcite or aragonite as stalagmites, stalactites or flowstones

stalactite speleothem hanging from the cave ceiling of cylindrical or conical form, with a central drip tube

stalagmite speleothem growing vertically upwards from the cave floor, forming from cave seepage waters

sw seawater, used as subscript for $\delta^{18}O$

T temperature

TIMS thermal ionization mass spectrometry

VPDB Vienna PDB, artificial standard created with value similar to PeeDee belemnite standard

VSMOW Vienna standard mean ocean water, artificial standard created with value similar to SMOW standard

w water, used as subscript for $\delta^{18}O$

Wisconsin name for glacial stage in North America from approximately 80,000 to 10,000 years ago

CHAPTER ONE. INTRODUCTION

1.1 BACKGROUND

Models attempting to predict the impact of global warming on natural climate cycles are developed from understanding processes in past climate. Proxy records are the only records of Quaternary climate change for the period before written records (few thousand years). Speleothems are useful for paleoclimate studies because they can be absolutely dated using radiometric techniques and have been shown to record climate change in their stable isotope geochemistry during formation. This research uses oxygen, carbon and hydrogen isotope variations in speleothem calcite to reconstruct climate change in North America. The use of stable isotopes is a major component of speleothem paleoclimate research and has advanced with fluid inclusion studies to provide estimates of absolute paleotemperatures. The objectives of this work are threefold: use coeval speleothem records to determine the consistency of speleothem climate records, provide information on Pleistocene climate change in the mid-continent and advance studies using δD variations in fluid inclusions for calculating paleotemperatures.

The main site selected for this research is Reed's Cave in the Black Hills of South Dakota (Figure 1.1). The Black Hills are in the heart of the continent and are located at the convergence of air masses originating in the Pacific, Gulf of Mexico and the Arctic (Bryson 1966). The Black Hills caves formed in the limestone of the Mississippian Pahasapa formation that were uplifted during the late Cretaceous and early Tertiary. The

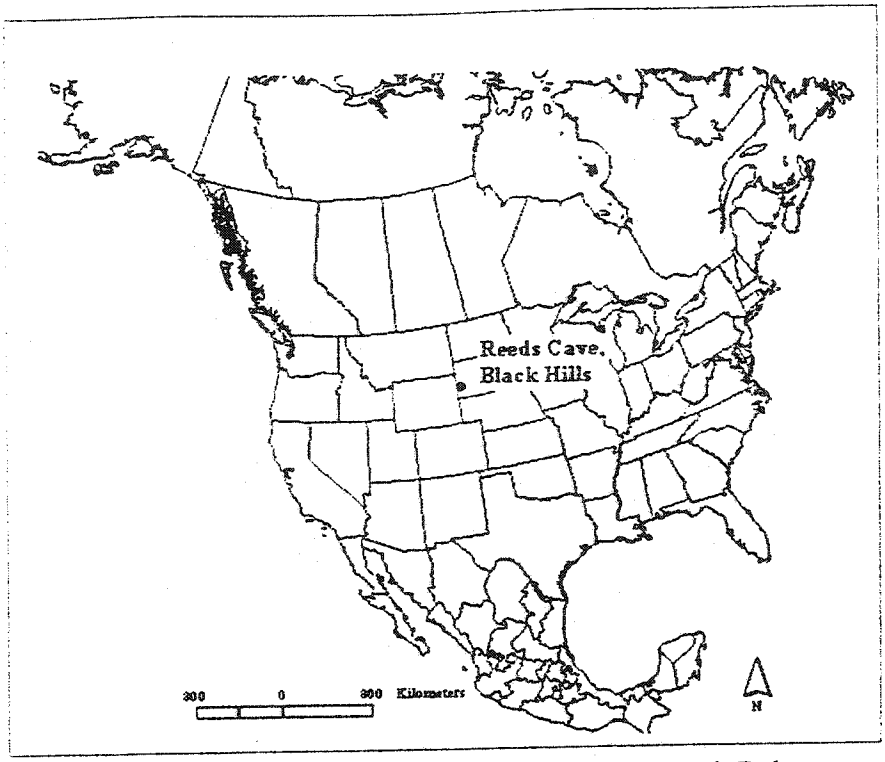

Figure 1.1. Location of Reed's Cave, Black Hills, South Dakota

uplift exposed the limestone unit to aggressive meteoric waters, which resulted in cave development along prominent joints and faults in the rock. Reed's Cave, like all other Black Hills caves, is a multi-level network maze with varied passage cross section that is unique to each level. The caves of the Black Hills contain speleothems in the form of thick hydrothermal spar coating the walls of Wind and Jewel Caves and also in the form of vadose stalagmites, flowstones and stalactites. Vadose speleothems from Reed's Cave have formed in both mid- and late-Pleistocene time, giving well-dated records of climate change for these periods.

Caves provide a unique opportunity for study because they are extremely stable environments that preserve chemical signatures of geological processes that occurred in the past. Speleothems, calcite precipitates that form in caves, can be used for reconstructing climatic conditions because the isotope chemistry of speleothem can give information on conditions at the time of deposition. Isotopic variation in speleothems provides information about climate because the fractionation of oxygen isotopes in the calcite-water system is temperature dependent. Cave temperatures are found to be long-term averages of surface temperatures (Wigley and Brown 1976) which can be used to reconstruct past climates (Schwarcz 1986, Gascoyne 1992). Climate history can also be investigated by looking at variations in the carbon isotopes of speleothems. The $\delta^{13}C$ of speleothem calcite is controlled by changes in overlying vegetation, changes in CO_2 availability and infiltration time for meteoric waters. Changes in productivity and

vegetation types are recorded by changes in $\delta^{13}C$ and can identify periods of warmer (or cooler) temperatures.

1.2 SPELEOTHEM GEOCHEMISTRY AND CLIMATE

Speleothems are chemical precipitates, generally in the form of calcite or aragonite, as flowstone, stalactites or stalagmites. The following chemical reactions are involved in the process of speleothem formation:

$$CO_2(g) \Leftrightarrow CO_2(aq) \quad (1.1)$$

$$H_2O + CO_2(aq) \Leftrightarrow HCO_3^- + H^+ \quad (1.2)$$

$$CO_3^{2-} + Ca^{2+} \Leftrightarrow CaCO_3 \quad (1.3)$$

As meteoric water passes through the soil it becomes enriched in CO_2 respired from by plant roots in the soil. As it passes through the bedrock substrate, the acidic water is able to dissolve limestone (equation 1.2). If the dripwater entering the cave has a higher CO_2 content than the cave air, the water releases CO_2. The degassing reduces the acidity of the water and causes $CaCO_3$ to precipitate, forming speleothem (equation 1.3). The process of speleothem formation can occur at isotopic equilibrium or disequilibrium. If formed in equilibrium, the sample can be used to derive paleoclimatic information. The water percolating through the substrate can also pick up trace elements including uranium, which can be used for dating the speleothem.

1.3 ANALYTICAL METHODS

There have been many advances in dating techniques for paleoclimatology applications. Radiometric dating of speleothem using uranium-series techniques has been significantly improved from the earlier alpha counting methods. During formation, parent uranium isotopes (^{234}U, ^{238}U) are incorporated into the speleothem and ^{234}U decays to the daughter isotope (^{230}Th). The accumulation of the daughter isotopes can be used to calculate the time passed since the calcite was deposited. Using the equation

$$^{230}Th/^{234}U = {}^{234}U/^{238}U(1-e^{-\lambda 230t}) + (\lambda_{230}/\lambda_{230}-\lambda_{234})^* (1-{}^{234}U/^{238}U)(1-e^{-(\lambda 230-\lambda 234)t}) \quad (1.1)$$

time (t) since deposition can be determined. ^{230}Th, ^{234}U and ^{238}U are the abundance of the isotope in activity units (in disintegrations per minute per gram). λ_{230} and λ_{234} are the decay constants for the isotopes ($\lambda_{230} = \ln 2 / t_{1/2}(230)$). Their respective half-lives ($t_{1/2}$) are 75,200 years and 247,000 years. Using the measured values of $^{230}Th/^{234}U$ and $^{238}U/^{234}U$ equation 1.1 is solved iteratively for t.

Thermal Ionization Mass Spectrometry (TIMS) has improved the analytical precision from the 5-10 % obtainable with alpha spectrometry, to less than +/- 1% (Li et al. 1989, Chen et al. 1992). Recent progress in the development of multi-collector ICP inductively coupled plasma) mass spectrometry enables the analysis of up to five isotopes at one time and further improvement in precision (Stirling et al. 2000).

1.4 TEMPORAL ASPECTS

The time slices that are represented include the marine isotope stage (MIS) 11 interval from 425,000 to 325,000 years ago and the late Pleistocene Wisconsin glacial period from 80,000 to 20,000 years ago. The MIS 11 problem (Imbrie et al. 1993) has been a very contentious issue because there is lack of agreement whether this interglacial period was warmer and of longer duration than the present interglacial. Using the Reed's Cave speleothems we hope to give absolute dates on the initiation and duration of this interglacial, and compare it with changes occurring in the North Atlantic. The Reed's Cave isotope record is a much higher resolution record of change than deep-sea cores, so the presence of millennial-scale variability was investigated as well. Oscillations that are over half the interglacial/glacial magnitude are recorded, supporting the idea that there was significant climate instability during this period.

The more recent Wisconsin glacial age records from speleothems and the North Atlantic deep sea sediment and ice core records display millennial scale variability (Dansgaard et al. 1993, Bond et al. 1999, Dorale 2000). It is believed this period was a time of great instability compared to previous glacial periods (Dansgaard et al. 1993). Our study of Wisconsin glacial age samples from Reed's Cave focuses on these millennial-scale oscillations and ice-rafting events. Early on there was some question as to whether this variability was a North Atlantic phenomenon, but this research as well as other global records show that is was more widespread (Leuschner and Sirocko 2000). Speleothem records of millennial-scale variability and Heinrich events may give more precise ages on their timing and duration.

The characterization of paleoclimate in mid-latitude continental areas cannot be done using the ocean and ice records alone. Most terrestrial records were interrupted by surface processes such as glaciation and erosion, but in the past few decades long term continuous records have been found, some of which have the advantage of yielding absolute chronologies. Two long records that exist are the Devil's Hole thermal calcite record and the Chinese loess profile (Rutter et al. 1991, Winograd et al. 1997). Devil's Hole was dated very precisely using uranium-series disequilibrium dating, but because it is a very slow forming groundwater calcite, the records are fairly smoothed. The loess records are dated less precisely using paleomagnetism and optical luminescence. Both records agree well with the SPECMAP reconstruction of climate over the past 500,000 years with minor improvements in resolution.

1.5 FLUID INCLUSIONS AND PALEOTEMPERATURE RECONSTRUCTION

The temperature-controlled fractionation between calcite and water in speleothems is a strong paleothermometer to compliment existing $\delta^{18}O_{ct}$ records. Paleotemperature reconstructions from terrestrial proxies such as ecological indicators (packrat middens, pollen assemblages) and groundwater suffer from significant problems in both accuracy and precision. The temperature shifts associated with ecological indicators are rather coarsely estimated because individual species can thrive in rather large temperature ranges. Groundwater paleotemperature estimates are much more robust due to the very well understood relationship between noble gas solubility and temperature in water, but are dated by radiocarbon ages that may be offset by mixing

processes (Stute et al. 1992). The δD values of speleothem fluid inclusions can be directly measured and are well dated by uranium-series disequilibrium techniques. Using these data and $\delta^{18}O$ of the calcite, we can calculate the temperature of deposition of the calcite (Schwarcz et al. 1976). Earlier problems with extraction have been overcome by new methods that reduce the error associated with reduced inclusion water recovery. The most important problem that remains is the determination of the pre-Holocene meteoric water line (MWL) relationship for each cave site. Successful paleotemperature reconstructions with errors less than the full range of temperature change for an interglacial-glacial transition and good age control allow for high precision estimates of paleotemperature change.

1.6 OUTLINE OF THESIS

The thesis is composed of three papers prepared for publication in scientific journals. The first paper looks at two Reed's Cave speleothems that grew through the Wisconsin glacial age. There is a coeval period of growth over approximately 12,000 years through which we are able to compare the isotope records to determine if there is variability at different sites within the same cave. The oxygen and carbon isotope profiles are compared from within the cave as well as with proxy records from other parts of the world. This global comparison provides further evidence that speleothems are recording major climate change in similar ways. I show that dissimilar isotope records do not necessarily indicate kinetic fractionation in one of the samples, but also that the local environment can have a major influence on the isotope records, by influencing the

isotopic composition of drip waters forming a speleothem. Spectral analysis of the oxygen isotope records confirms the presence of millennial-scale variability seen in the North Atlantic sediment and Greenland ice cores records.

The second manuscript focuses on 200,000 years of speleothem growth in Reed's Cave in the mid-Pleistocene. Three speleothems are recording major climate transitions but in different ways. The response of $\delta^{18}O_{ct}$ to temperature ($d[\delta^{18}O]/dT$) in two speleothems have opposite signs but the oxygen isotope variations are synchronous. The third speleothem shows a muted signal in early stages of growth but a good response to climate in the final 100,000 years of formation. Spectral analysis of the oxygen isotopes shows the presence of long-term Milankovitch climate cycles.

The third paper focuses on the δD records of fluid inclusions from the two Wisconsin age speleothems from Reed's Cave and one Holocene age speleothem from the central California Coast. Paleotemperatures calculated from the coeval period of growth in the Reed's Cave samples, from 62,000 to 49,000 years ago, show that although the oxygen and carbon isotope records in the calcite differ, but they are recording similar temperature shifts and climate change. The Holocene record from Santa Cruz reveal a temperature maximum at 8,000 years ago, with temperatures decreasing to a minimum at 3,000 years ago. Exaggeration of the paleotemperature shifts that we calculated may be due to inaccurate estimations of the MWL relationship in the past.

CHAPTER TWO. LATE PLEISTOCENE PALEOCLIMATE IN THE BLACK HILLS OF SOUTH DAKOTA FROM ISOTOPE RECORDS IN SPELEOTHEMS

2.1. ABSTRACT

Two coeval speleothems from the Black Hills are used to investigate $\delta^{18}O$ and $\delta^{13}C$ variations within Reed's Cave and reconstruct climate during the Wisconsin glacial period from 82,000 to 24,000 years ago. Variation in growth rates between the two speleothems reveals a strong control of hydrology and surface vegetation on isotopic variability and response of the $\delta^{18}O$ to climate. High resolution $\delta^{18}O$ and $\delta^{13}C$ data show that local environmental conditions can produce an offset of $\delta^{18}O$ values of up to 4 ‰ in coeval speleothems but still reveal important climate events. The transition from warmer to cooler periods results in an enrichment of ^{18}O in speleothem 99902. The $\delta^{18}O_{ct}$ record of sample 20000, another equilibrium deposit coeval to part of the 99902 record, is offset from 99902 by between 0 and -3.5 ‰, and shows much higher frequency isotopic variation. Both speleothems record short-term interstadial and ice rafting events that are also present in speleothems from North America and Europe. Spectral analysis of the $\delta^{18}O_{ct}$ records reveals periodicity at 1,000 to 2,000 years, similar to millennial scale variability seen in the North Atlantic sediments and the Greenland ice cores.

2.2. INTRODUCTION

Stable isotope variations in speleothem calcite are precisely datable records that may record major interglacial/glacial transitions and lesser climatic events (Gascoyne 1992, Bar-Matthews et al. 1999, Frumkin et al. 1999, McDermott et al. 1999, Dorale 2000). The validity of the oxygen isotope signal may be problematic because variables controlling isotopic variation in the local cave environment can mask global climate signals present in the record. Recent studies of coeval samples in Israel and Missouri correlate well with ice core records and confirm that global climate signals are present (Bar-Matthews et al. 1999, Frumkin et al. 1999, Dorale et al. 1998). It has been widely presumed that discordant oxygen isotope records are the result of non-equilibrium deposition occurring in the cave. This assumes that the relationship of isotopic variation to climate is invariant at any given site. In this paper two samples from Reed's Cave in the Black Hills of South Dakota with discordant but coeval growth are examined to show that within a cave different models may be necessary for interpreting isotopic change.

The relationship between the speleothem isotope record and climate may change over time because of sensitivity to local conditions. The variability of isotopic composition at different drip sites within a cave can offer different, but still useful, isotope records that can be used as paleoclimate proxies. Application of spectral analysis to the oxygen isotope time series has revealed millennial scale variability in both Reed's Cave speleothems described below. Comparison of their time series to records from ocean sediments, ice cores and terrestrial proxies confirm that both local- and global-scale events are being recorded by the oxygen isotope variations.

2.3. SITE DESCRIPTION

The speleothem samples were collected from Reed's Cave (43° 34' 12" N, 103° 38' 36" W, 1400 m asl) in the Black Hills of South Dakota (Figure 2.1). The Black Hills are a dissected dome exposing a sequence of sedimentary rocks with significant cave development in the Mississippian limestones (Palmer and Palmer 1989). Nearby Jewel and Wind Caves are two of the longest cave systems in the world but contain few vadose speleothems formed by drip waters because they are largely covered by impermeable clastic strata (Bakalowicz et al. 1987). Reed's Cave is at shallow depth because the cover and upper limestone has been eroded, permitting significant amounts of speleothem deposition from vadose dripwaters, some of which are actively depositing today. Part of the cave underlies a quarry that has been active for the past 20 years. The blasting activities have dislodged hundreds of speleothems, enabling us to remove samples without destroying any intact specimens. Cave conservation and preservation ethics discourage the destruction of speleothem formations.

The modern vegetation surrounding the area is a mixed-grass prairie and pine forest. It is an ecosystem transition area and has likely shifted back and forth across the range from full forest to full grassland conditions in the past. The average annual surface temperature is 8 °C and the range between winter and summer average temperature is 28°C. Average annual precipitation is 783 mm with 476 mm from rain and 307 mm (water equivalent) from snow. Seasonality is seen in more active infiltration and dripping during the cooler seasons. Theoretical losses in moisture during summer from increased

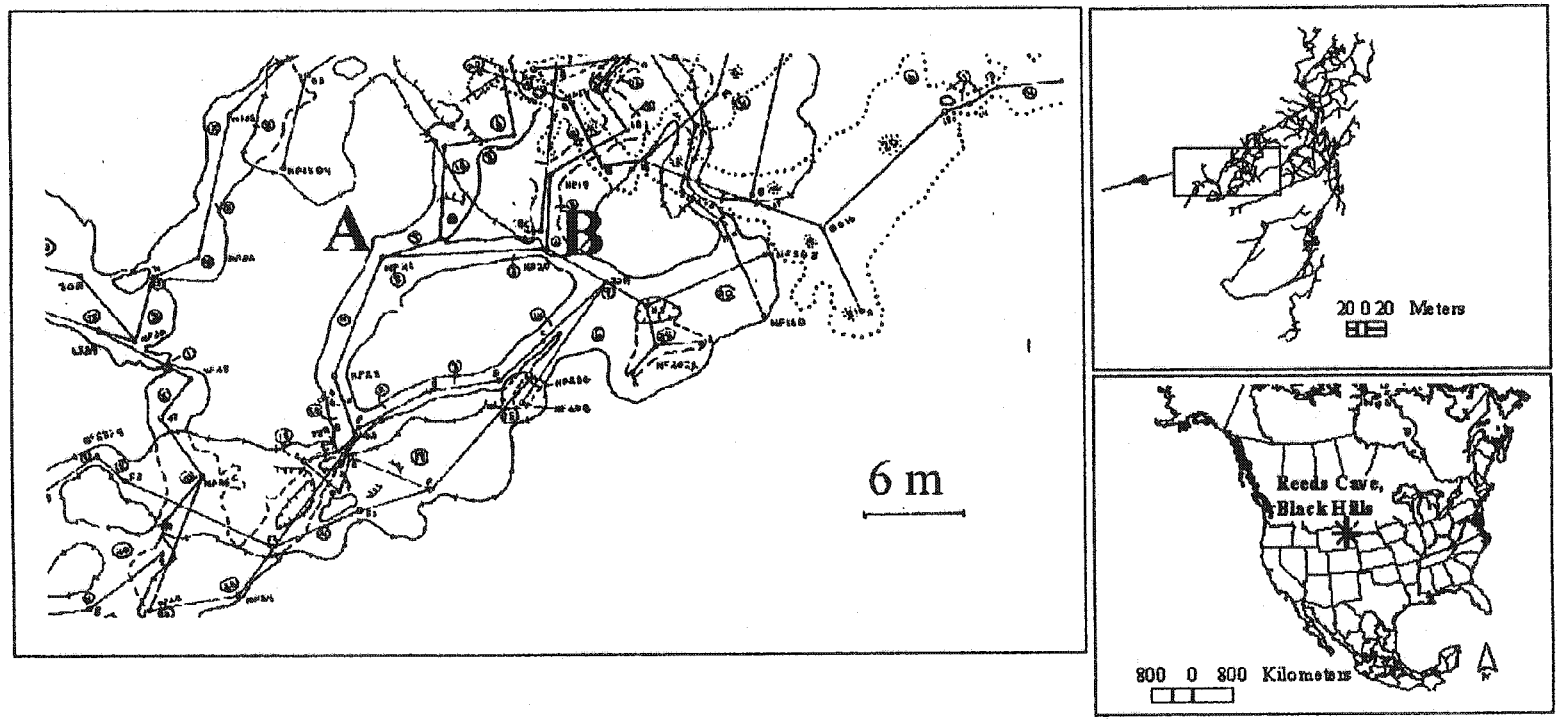

Figure 2.1. Location of Reed's Cave and position of samples 20000 (site A) and 99902 (site B).

evapotranspiration are reduced locally because infiltrating water rapidly reaches karstic voids with high humidity.

2.4. METHODS

Speleothem samples 99902 and 20000 were collected from two different sections in Reed's Cave (Figure 2.1). Sample 99902 was collected from the "New Formations Room" (site B), where calcite deposition is still occurring in some sections. Sample 20000 (site A) was collected from a crawlway to the northeast that appears to be without any modern drip waters. 20000 and the upper two-thirds of sample 99902 have the standard morphology of simple stalagmites, which accrete most new growth at the top and less accumulation from film flow down the sides (Figure 2.2) (Ford and Williams, 1989, 335-6). The lowest (i.e. earliest) portion of 99902 grew as a flowstone cover on a vertical face of limestone breccia (local breakdown in the cave), accreting only by film flow until it had sufficient protrusion to support the stalagmite growth upwards.

The speleothems were cut along their growth axes and examined for post-depositional alteration, which was absent. Sub-samples for dating were extracted using a 1.2 mm diameter carbide dental burr or a diamond wafering blade mounted on an Isomet low speed diamond saw. A U^{233}/U^{236} - Th^{229} double spike, calibrated in the McMaster Laboratory by J. Lundberg, was added to the sample after dissolution with dilute HNO_3 (Lundberg 1990). The U and Th fractions in the calcite were extracted using ferric hydroxide co-precipitation and anion column chemistry in a clean room with positive pressure.

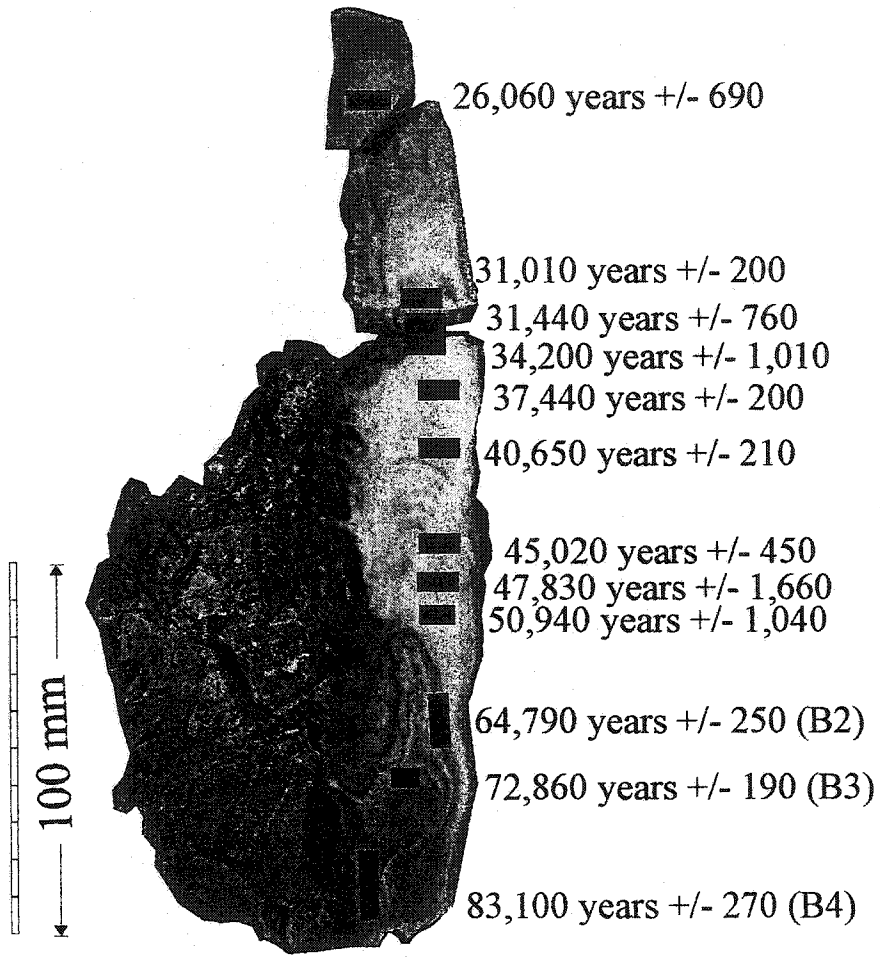

Figure 2.2 (a). Cross section photo of sample 99902 and uranium-series dating locations

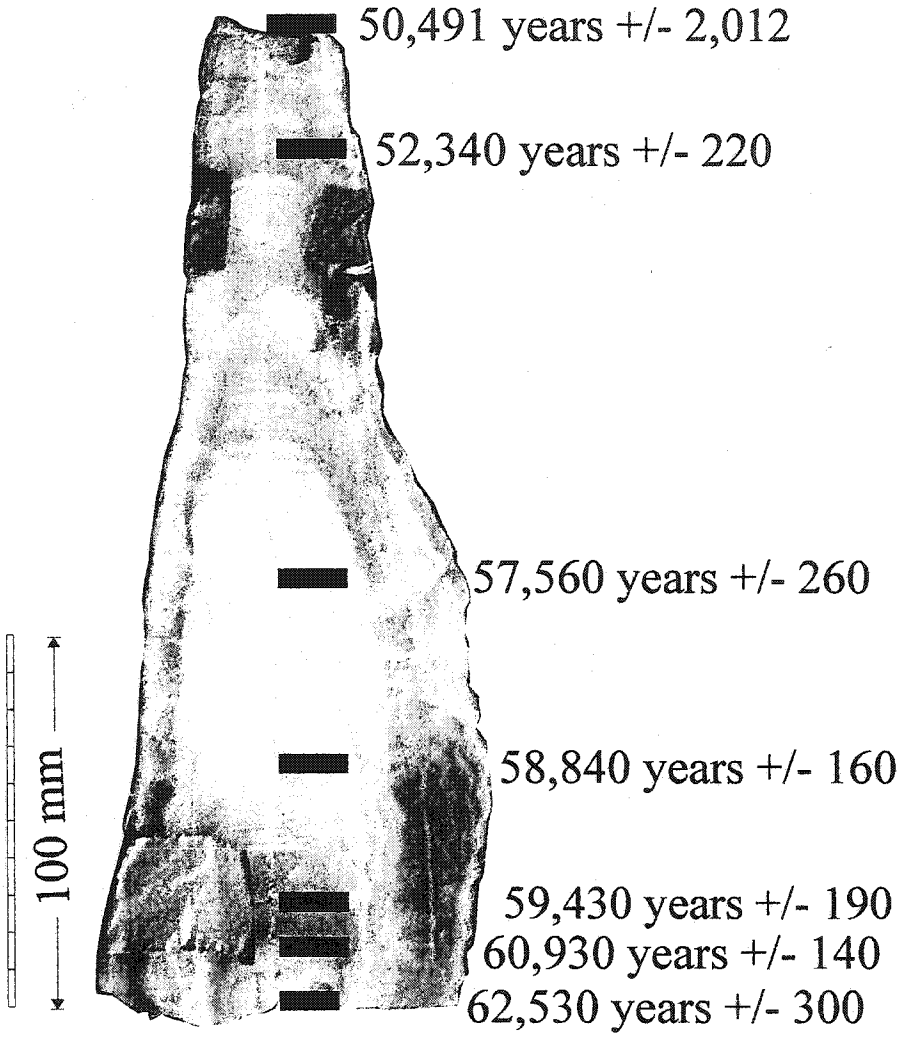

Figure 2.2 (b). Cross section photo of sample 20000 and uranium-series dating locations

For thermal ionization mass spectrometry (TIMS) on the McMaster VG 354 instrument, the uranium fraction was loaded in phosphoric acid on double rhenium-tantalum filament beads. Thorium fractions were loaded in phosphoric acid on double rhenium filament beads or with colloidal graphite on single rhenium filament beads. Mass spectrometric runs with the double filaments were done using the general peak jumping system with a Daly detector. The uranium samples were run in two stages for 2 to 3 hours with a side filament current of 2.0 to 2.4 amps. Double filament thorium analyses for samples with low detrital thorium were run in one stage for 2-3 hours with a side filament current of 2.2 to 2.6 amps. The two stage run was used for samples with high detrital thorium due to interference from high ^{232}Th. Detailed descriptions of these techniques are available from Lundberg (1990). Single filament thorium analyses were run for 2-3 hours with a higher side filament current of 4.0 to 5.0 amps, adapted from techniques described in Edwards et al. (1986). A dating program developed by J. Lundberg and S.-E. Lauritzen corrects for laboratory and machine error, propagates error on the ratios, calculates activity ratios and calculates the age with two sigma error (Lundberg 1990).

Samples for multi-collector inductive coupled plasma mass spectrometry (MC-ICP-MS) were run at the GEOTOP laboratory in Montreal, using a Micromass IsoProbe MC-ICP-MS in static multicollection mode with four Faraday collectors. The instrument settings were optimized using an ICP-MS-grade uranium solution. Typical settings for the ICP source are the following: forward Power- 1350 watts; cool gas- 13.50 L/min. Ar; intermediate gas- 1.030 L/min. Ar; nebulising gas- 0.700 L/min. Ar. Samples were

conditioned in 2% HNO_3 and introduced into the ICP source using an Aridus microconcentric nebuliser at an uptake rate of ~50µl/min. Data acquisition consisted of 50 second "on-peak-zero" measurement of gas and acid blank prior to aspiration of the sample. Upon aspiration, two half-mass unit baseline measurements were conducted for 15 seconds each within the mass range of 232.5 to 236.5 for data acquisition. Isotope ratios were measured for 50 scans at 10 seconds integration time. Following each analysis, washout used both 4% and 2% HNO_3 wash and rinse solutions, for a combined 10-15 minutes. For thorium samples, data acquisition consisted of 60 scans at 5 seconds integration time, using only three Faraday collectors. In addition, washout times were approximately 20-25 minutes. Ages are reported with an error of two standard deviations. Data reduction for calculation of errors and activity ratios was done using a spreadsheet developed by B. Ghaleb at the GEOTOP centre. A second spreadsheet with an imbedded program was used for age calculation.

Calcite samples for oxygen and carbon isotope analysis were drilled out using 0.8mm and 0.4 mm cobalt dental drill bits. The derived powders, approximately 100 micrograms each, were run on an Autocarb system attached to an Optima mass spectrometer at McMaster. Results are reported in ‰ against the NBS-19 standard relative to VPDB standard. The precision of analyses was 0.06 ‰ for both isotope ratios.

Dripwaters were collected as spot samples, with some of the slower dripping sites left overnight. Their $\delta^{18}O$ values were determined by equilibration of water with CO_2 at 25 °C for 24 hours. The clean CO_2 gas was run on the Optima mass spectrometer against

the CO_2 tank standard. Results are reported relative to VSMOW standard and with an error of 0.2 ‰.

The power spectra for the oxygen isotope records were obtained using the program SPECTRUM (Schulz and Statteger 1997). This program was created for unevenly spaced time series like speleothem data that exhibit distinctly different periods of growth. The Lomb-Scargle Fourier transform avoids unnecessary interpolation that may occur with the Blackman-Tukey method.

2.5. RELATIONSHIPS BETWEEN CLIMATE AND SPELEOTHEM RECORDS

Oxygen isotope variations in speleothem calcite can be used as a paleoclimate proxy if these deposits were formed in oxygen isotope equilibrium with formation waters (Schwarcz 1986). Equilibrium conditions occur when there is slow deposition of calcite from the drip water. Rapid degassing of CO_2 or evaporation of drip water causes kinetic fractionation effects that can obscure the climate signal. For this study, three growth layers in each speleothem were used for the equilibrium test, i.e. that ^{18}O is uniform along the layer (Hendy, 1971). No covariance in oxygen and carbon isotopes along the growth layers was found, indicating that there was equilibrium deposition. However, the growth layers in these speleothems are very difficult to differentiate along their outer portions (Figures 2.2a and 2.2b), with the consequence that individual values for $\delta^{18}O_{ct}$ may be averaging thousands of years of growth. Other indications of the suitability of a sample are comparisons with other proxy records including other speleothems.

If a speleothem grows in oxygen isotope equilibrium with drip waters then variations in $\delta^{18}O$ of the calcite ($\Delta\delta^{18}O_{ct}$) are governed by the equation:

$$\Delta\delta^{18}O_{ct} = [d(\alpha_{ct\text{-}w})/dT]\Delta T + [d(\delta^{18}O_{ppt})/dT]\Delta T + \Delta(\delta^{18}O_{sw}) \quad (1.1)$$

which relates changes in $\delta^{18}O_{ct}$ to the temperature dependent changes in fractionation between calcite and water ($\alpha_{ct\text{-}w}$) and in $\delta^{18}O$ of precipitation ($\delta^{18}O_{ppt}$) and to changes in global ice volume as reflected in seawater $\delta^{18}O_{sw}$. The three components of this equation are defined by relationships determined from experimental and empirical studies. The temperature dependence of the fractionation is

$$d(\alpha_{ct\text{-}w})/dt = -0.24\ ‰/°C \text{ at } 25°C \quad (1.2)$$

(O'Neil et al. 1969). The effect of temperature on the isotopic composition of meteoric water was calculated using the IAEA data set from many global precipitation stations. The global average for the temperature effect on precipitation is

$$d(\delta^{18}O_{ppt})/dT = 0.69\ ‰/°C \quad (1.3)$$

as determined by Dansgaard (1964) and Rozanski et al. (1993). The relationship varies with location and can be as low as 0.18 – 0.3 ‰/°C for some inland locations. From our measured values of $\delta^{18}O$ in dripwaters from different seasons and winter snow values and the corresponding measured temperatures, the local value $d(\delta^{18}O_{ppt})/dT = 0.39$ ‰/°C. Secular variation in this relationship in the past allows some flexibility in these values when applying the relationship to interpretation of paleoclimate records. An additional complicating factor is the source and movement of storm tracks over the continent at different times in the past. Future analyses of speleothem fluid inclusion water may

enable determination of this relationship from the pre-Holocene period at Reed's Cave (Serefiddin et al. 2001).

One final consideration when evaluating the $\delta^{18}O$ of calcite is the effect of the isotopic composition of seawater on global meteoric water composition. We can estimate that $\Delta(\delta^{18}O_{sw}) = 1.2$ ‰/°C for glacial to interglacial transition as a result of accumulation of lighter oxygen isotopes in ice sheets and the enrichment of heavy isotopes in seawater as temperature decreased (Lea et al. 2000, Fairbanks 1989). The composition of precipitation falling on the continents is directly affected by this factor because seawater is the principal source of the moisture.

The net result of these competing effects on $\delta^{18}O_{ct}$ may vary significantly between caves, with the result that the net effect of decreasing temperature at a site can be either an increase or decrease in $\delta^{18}O_{ct}$. The general sense of isotopic change in response to climate change at a site can be determined by comparison of ice-age deposits with modern speleothem forming at the same site. As we shall see, other effects can also lead to a difference in the temperature-dependence of $\delta^{18}O_{ct}$ at different locations in the same cave.

2.6. RESULTS

2.6.1. Uranium-series dating and growth rates

Uranium-series dates are presented in Table 2.1. Fourteen dates in stratigraphic order were used to develop the age model for sample 99902 (Figures 2.2a, 2.3). This

Table 2.1. Uranium-series dating ratios, concentrations and ages for Reed's Cave 99902 and 20000

Sample[a,c]	Sample wt (g)	^{238}U (ppm)	$\delta^{234}U$ measured[b]	$[^{230}Th/^{238}U]$ (activity)	$[^{230}Th/^{234}U]$ (activity)	$[^{230}Th/^{232}Th]$ (activity)	Age (ka)	2 σ (+)	2 σ (-)	Technique
99902_B4[c]	0.5958	1.3167	159.844	0.62916	0.54245	2087.44	**83.10**	0.27	0.27	ICP
99902_B3[c]	0.6741	1.6268	172.537	0.58079	0.49533	2185.33	**72.86**	0.19	0.19	ICP
99902_B2[c]	0.7200	0.8746	178.725	0.53611	0.45482	2213.01	**64.79**	0.25	0.25	ICP
99902_1	1.8492	0.5732	268.159	0.48124	0.37948	1675.00	**50.94**	1.04	1.03	TIMS
99902_10	0.1808	0.0991	176.100	0.48124	0.35930	1163.11	**47.83**	1.66	1.63	ICP
99902_20	0.5560	0.7448	209.555	0.41442	0.34262	1023.67	**45.02**	0.45	0.45	ICP
99902_46	0.6410	0.7970	226.205	0.36630	0.31504	1022.49	**40.65**	0.21	0.21	ICP
99902_70	0.5519	0.9935	234.165	0.36308	0.29419	2010.53	**37.44**	0.20	0.20	ICP
99902_74	0.2037	0.1554	225.900	0.33369	0.27220	1464.10	**34.20**	1.02	1.01	ICP
99902_80	0.2096	0.2206	217.100	0.30793	0.25300	2217.40	**31.44**	0.76	0.76	ICP
99902_85	3.3083	1.3082	268.833	0.31768	0.25037	2002.27	**31.01**	0.20	0.20	TIMS
99902_140	1.1491	1.6920	261.313	0.27075	0.21466	1881.98	**26.06**	0.69	0.69	TIMS
20000_2	0.2408	2.4358	162.267	0.50414	0.43389	4972.19	**62.53**	0.30	0.30	ICP
20000_15	0.5835	2.4737	161.905	0.50383	0.43349	6875.99	**60.93**	0.14	0.14	ICP
20000_25	0.6161	1.9661	159.061	0.49336	0.42565	11457.50	**59.43**	0.19	0.19	ICP
20000_65	0.8834	1.4755	157.352	0.48886	0.42240	9302.50	**58.84**	0.16	0.16	ICP
20000_115	0.5804	1.5902	162.683	0.48307	0.41548	9848.02	**57.56**	0.26	0.26	ICP
20000_230	0.7880	1.2389	167.333	0.45052	0.38594	5491.77	**52.34**	0.22	0.22	ICP
20000_270	0.1092	1.2230	142.000	0.42779	0.37460	5451.43	**50.49**	2.01	2.01	ICP

[a] Number following sample ID is location of sample in mm from base

[b] $\delta^{234}U = ([^{234}U/^{238}U] - 1)_{activity} \times 1000$

[c] See Figure 2.2 for sample location

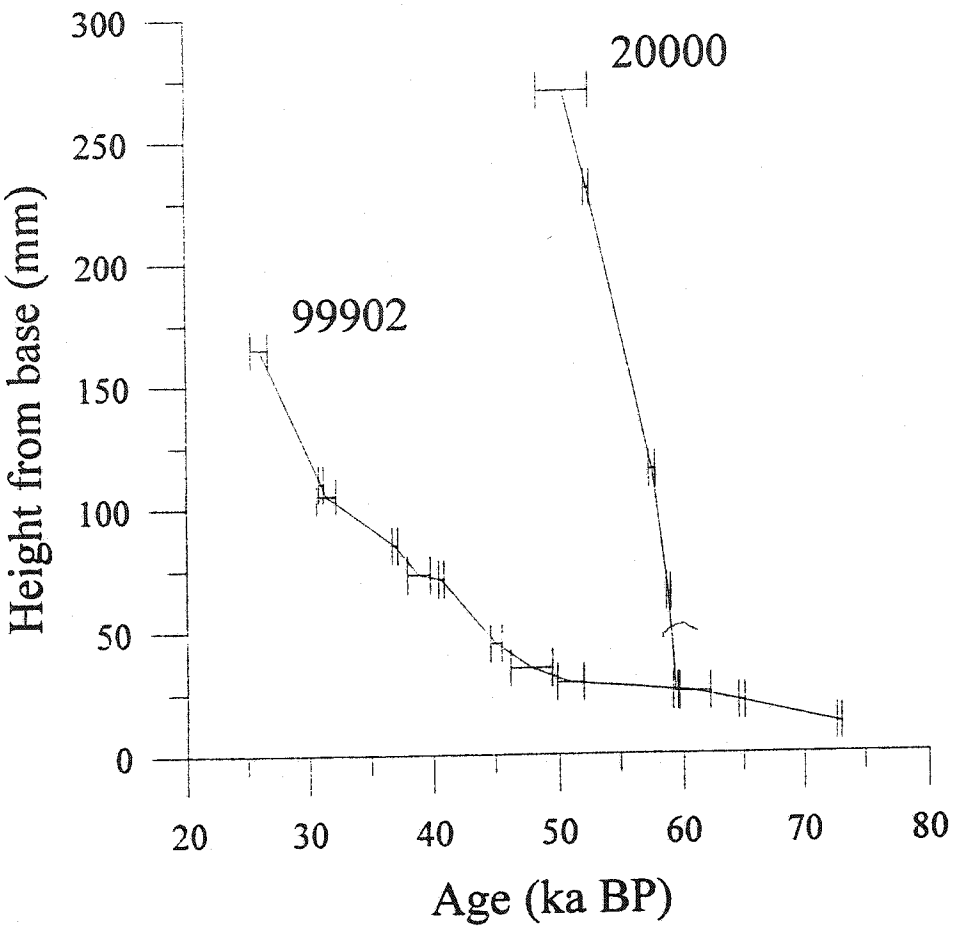

Figure 2.3. Age models for samples 99902 and 20000.

stalagmite grew from 86,000 to 24,000 years ago. In the early flowstone stage of accumulation from the 0 to 20 mm above base the average growth rate was less than 1 mm per thousand years. Switching to the stalagmite mode of growth at 50,000 years ago the rate increased considerably, being close to an average of 4.4 mm per thousand years until ~30,000 years ago. The rate was highest in the last section of growth, 80 to > 160 mm from the base, attaining a value of about 12 mm per thousand years between ~30,000 and 24,000 years ago. This could indicate an increase in catchment area for the dripwater and/or a period of increased precipitation just prior to the last glacial maximum at 20,000 years ago.

For 20000, seven ICP dates in stratigraphic order establish that it grew from 63,000 to 50,000 years ago (Figure 2.2b). The average growth rate ranges from 20 mm per thousand years to a maximum of 70 mm per thousand years (Figure 2.3). This is strong evidence that different drip sites within a cave can be responding to different drip water pathways or changes in catchment area, which, as will be shown, can result in variable isotope records

2.6.2. Oxygen isotopes

A useful tool for interpreting oxygen isotope variations is to determine how the $\delta^{18}O_{ct}$ changes with temperature. This can be done in two ways. First, we can compare $\delta^{18}O_{ct}$ formed in colder periods to the $\delta^{18}O_{ct}$ of modern (interglacial) calcite forming in the cave today. Second, we can observe the trend in $\delta^{18}O_{ct}$ with time during a transition from glacial to interglacial climate (as inferred by comparison with deep-sea cores or

other global records). From these comparisons we can estimate the sign of $d(\delta^{18}O_{ct})/dT$ which we will refer to as gamma (γ) (Schwarcz et al., in preparation).

Dripwaters in the cave range in $\delta^{18}O$ from -10 to -15 ‰. This is in agreement with measured values of approximately -10 to -14 ‰ for $\delta^{18}O$ of modern precipitation in this region (IAEA 2001). Using the O'Neil et al. (1969) temperature dependent fractionation equation, the average $\delta^{18}O$ for calcite-water pairs calculate to 9.8°C, which agrees well with measured modern average temperature.

Isotopic measurements of four actively growing speleothems (soda straw stalactites) have a modern range for $\delta^{18}O_{ct}$ from -9 ‰ to -13.6 ‰. The higher $\delta^{18}O_{ct}$ values are likely affected by evaporative fractionation because humidity in the cave may drop below 90%. The more depleted values at ~ -13 ‰ are more representative of modern $\delta^{18}O_{ct}$.

Speleothem 99902 was deposited during glacial MIS 5a, 4, 3 and the beginning of 2. The $\delta^{18}O_{ct}$ values for 99902 are in general higher than the range of modern stalactites, suggesting that $\gamma < 0$ for this deposit. In addition, $\delta^{18}O_{ct}$ values increase towards full glacial conditions, also confirming that $\gamma < 0$. This is in agreement with other speleothem records from eastern to central United States (Schwarcz et al., in preparation).

Sample 20000 has lower $\delta^{18}O_{ct}$ values than 99902 over their coeval period of growth, values which are not significantly different from the modern speleothems; this suggests that $\gamma = 0$. Towards the end of its record (the end of glacial MIS 4) $\delta^{18}O_{ct}$ increases with a shift towards warmer climate suggesting that $\gamma > 0$.

Speleothem 99902 grew in two major phases differing in growth rate and in the character of its isotopic variation (Figure 2.4). The temporal resolution for isotopic analyses averages 766 years from 82,000 to 50,000 years ago and 120 years from 50,000 years ago to the cessation of growth at 24,000 years ago. The full range of $\delta^{18}O_{ct}$ for 99902 is -12.2 to -8.5 ‰ with most of the variation occurring in the last 20,000 years of growth.

The first growth phase extended from 82,000 years to 50,000 years ago at a mean growth rate of 0.8 mm per thousand years, representing the slowest period of growth. The records of $\delta^{18}O$ and $\delta^{13}C$ are smoothed when compared to more oscillatory records of the subsequent phase. However, the amplitude of variation in the records is similar. There is a general trend of increasing $\delta^{18}O_{ct}$ values towards a maximum at around 55,000 years. This trend takes place during the transition from the end of MIS 5 to MIS 4, suggesting it represents a cooling in climate over this period. The most prominent feature of the early part of the record is the shift in $\delta^{18}O_{ct}$ that begins approximately 71,000 years ago, which is 1,000 to 3,000 years after the start of MIS 4. Minor peaks in $\delta^{18}O_{ct}$ suggest coldest intervals at 62,500, 56,000 and 49,500 years ago. In the transition from MIS 4 to MIS 3, there is a general decrease in $\delta^{18}O_{ct}$ coupled with an increase in growth rate and increase in the amplitude and frequency of oscillations in the isotopic records.

The second phase of growth lasted from 48,500 to 24,000 years ago,with major cold events at 30,250 years, 26,500 years and 24,000 years ago. The speleothem ceased growing approximately 3,000 years before the LGM, the oscillations of its $\delta^{18}O$ signal increasing in intensity as the drip sites became inactive due to colder temperatures above

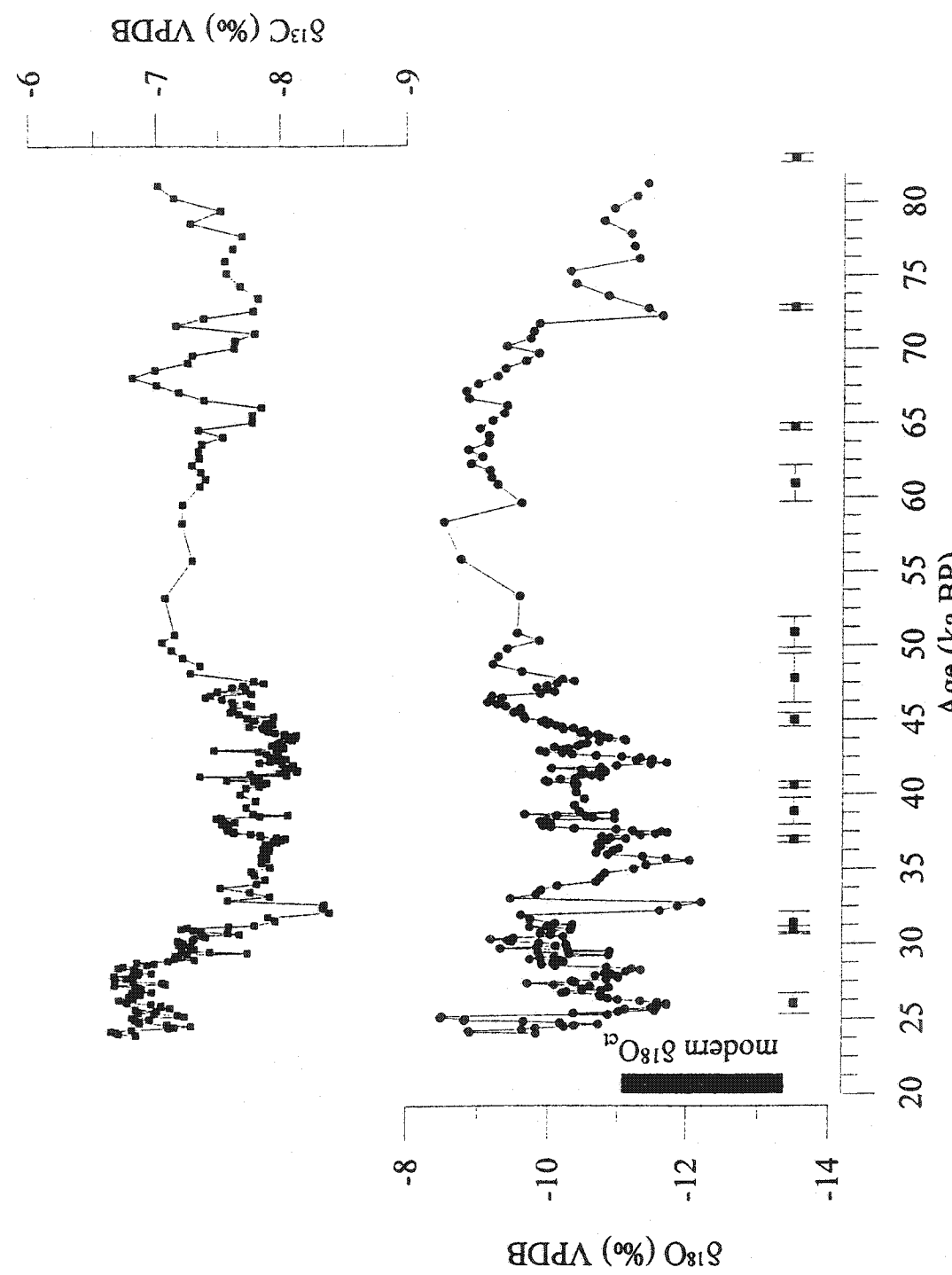

Figure 2.4. Oxygen and carbon isotope time series for sample 99902. Location of dates with error bars shown above x-axis.

the cave. This phase of growth covered most of MIS 3, which also displays the strongest millennial scale variation in the GISP2 oxygen isotope record from Greenland (Grootes and Stuiver 1993, Dansgaard et al. 1993). After a sharp cold event at ~ 47,500 years ago, major peak-trough cycles in $\delta^{18}O_{ct}$ with a mean shift of 2.0 ‰ in magnitude occur on average every 2,000 -3,000 years and last about 2,800 years.

The growth history of stalagmite 20000 (Figure 2.5) is partly coeval with that of 99902, spanning MIS 4 and the beginning of MIS 3. Although it grew only a few tens of meters away from 99902, the $\delta^{18}O_{ct}$ records of these two stalagmites are strikingly different. First, we have already noted that 20000 grew 350 times faster than 99902 over their period of concurrent growth, due to differing depositional modes as noted and probably to a higher rate of infiltration. Second, we see that there are significant differences in the average $\delta^{18}O_{ct}$ values for the coeval portions of each speleothem (Figure 2.6). $\delta^{18}O_{ct}$ of 20000 ranges from zero to about 3.5 ‰ lower than 99902. Third, we note that there are short (millennial to centennial) time-scale variations in both $\delta^{18}O$ and $\delta^{13}C$ in 20000 that are not seen in the record of 99902. To some extent, this difference might be due to our inability to analyse 99902 on a sufficiently fine time scale due to its much slower growth rate. The closest spaced samples of 99902 over this period show no variations in $\delta^{18}O$ or $\delta^{13}C$ larger than $\pm$ 0.1 ‰, but even these may be averaging higher frequency oscillations whose average values are uniform. Using a 0.4 mm drill each sample spans between 400 and 2,500 years of growth, whereas the cyclicity in the 20000 isotope record is on a time scale of between 10 to 150 years. The larger fluctuations in $\delta^{18}O_{ct}$ of 20000 could suggest that the residence time of its recharge water

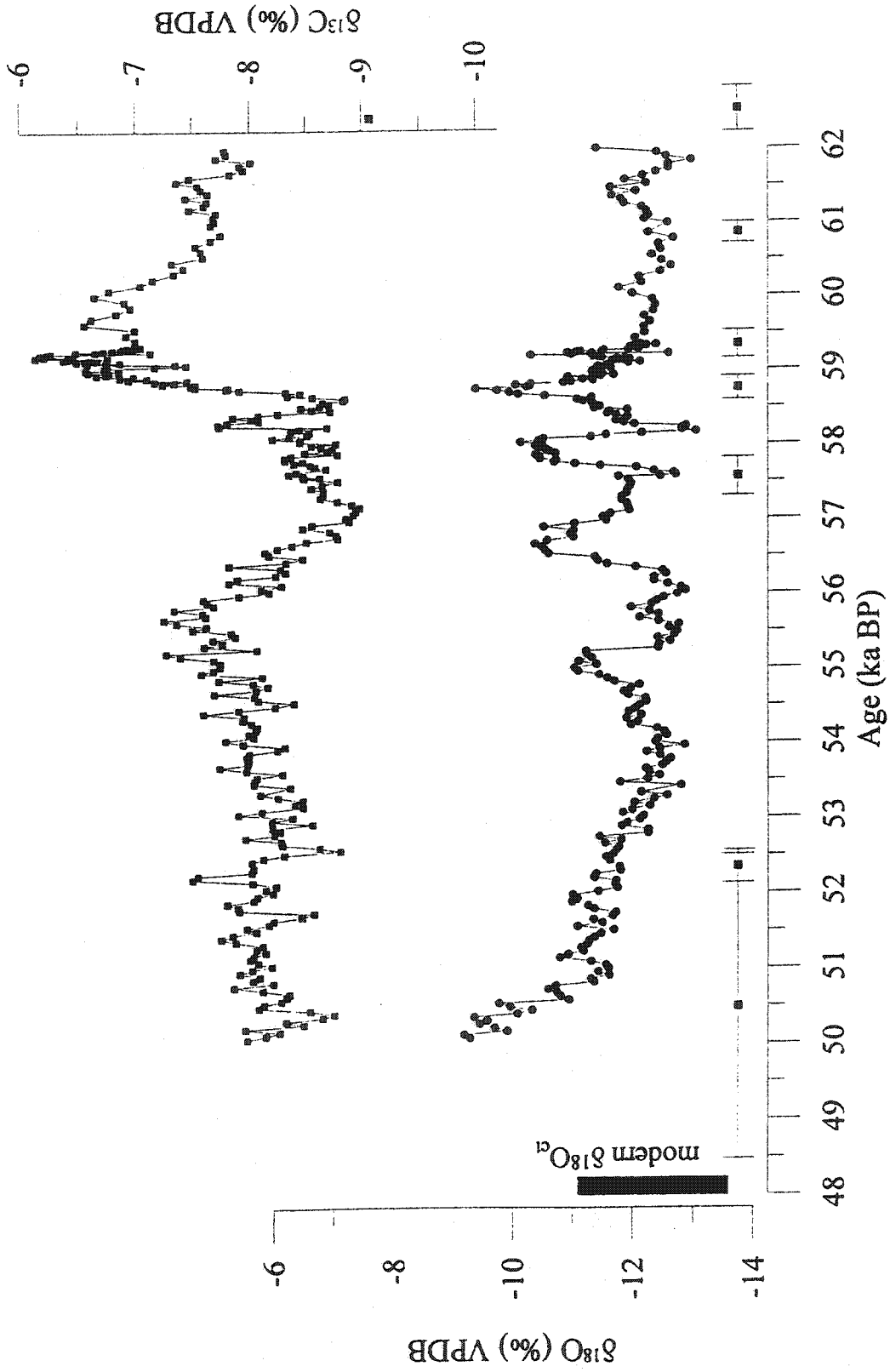

Figure 2.5. Oxygen and carbon isotope time series for sample 20000. Location of dates with error bars shown above x-axis.

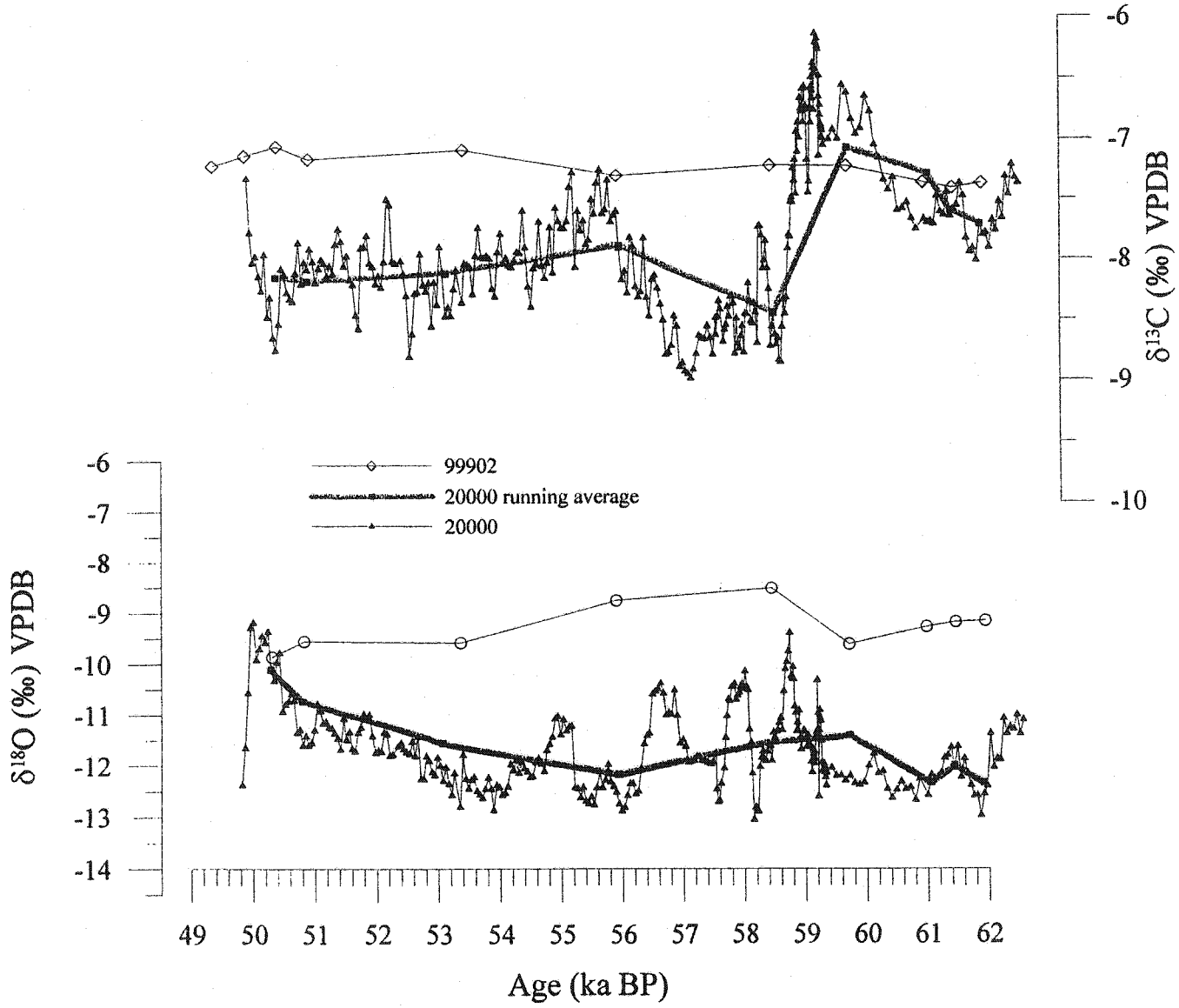

Figure 2.6. Oxygen and carbon isotope time series for coeval period of growth include running average for sample 20000.

may not have been very long and that water had very little time to equilibrate with the host rock.

The range of $\delta^{18}O$ variation for sample 20000 is 3.9‰, essentially identical in magnitude to the 3.7‰ found in 99902, but recording depleted peaks that extend through modern $\delta^{18}O_{ct}$ values. When the speleothem started growing at 62,000 years ago, $\delta^{18}O_{ct}$ values were in the most depleted part of the range until about 59,000 years ago. There were major peaks of ^{18}O enrichment at 59,250 years, 58,750 years, 58,000 years, 56,500 years and 55,000 years ago. These are closely spaced intervals, indicating that these records were capturing rapid environmental variation. The last portion of the record shows a gradual increase of $\delta^{18}O_{ct}$ values after 54,000 years ago.

Assuming that $\gamma > 0$, sample 20000 is displaying rapid cool to warm oscillations across the MIS 4 to MIS 3 transition and into stage 3. The close of its growth between 54,000 and 50,000 years ago was marked by a trend to higher $\delta^{18}O_{ct}$ values, indicative of warming climate; this is matched by a trend to more negative $\delta^{13}C$ values over the same interval.

2.6.3. Carbon isotopes

The carbon isotope records for samples 99902 and 20000 are less divergent than their oxygen isotope records. $\delta^{13}C$ of 20000 varies from zero to about 1 ‰ lower than that of 99902. However, the total range of $\delta^{13}C$ values is larger in 20000: 3.4 ‰ compared to 1.7‰ for 99902. For the period of coeval growth, $\delta^{13}C$ is almost constant

for sample 99902 at c. -7 ‰ whereas $\delta^{13}C$ varies in 20000 in short-term, low-amplitude oscillations similar to those seen in $\delta^{18}O_{ct}$. The 20000 $\delta^{13}C$ displays a striking offset of about -1 ‰ at 59,000 years ago. This negative excursion probably reflects higher soil productivity, which could result from warmer temperatures.

2.7. DISCUSSION

2.7.1. Intrasite isotopic differences

When we compare the two oxygen isotope records over the limited period when both speleothems were being deposited, we see a significant difference in values of $\delta^{18}O$ (Figure 2.6): the average $\delta^{18}O_{ct}$ value of 99902 is 1.4 ‰ greater than that of 20000. The carbon isotopes are offset as well, but the average $\delta^{13}C$ values of the two samples only differ by 0.4 ‰ (Figure 2.6). The different appearances of the isotope records for the two stalagmites can be explained in part by the difference in growth rates and morphology. The reduced variability in the early part of 99902 record is partly due to the slower deposition rate from reduced calcium ion excess and our inability to resolve the high-frequency variations in $\delta^{18}O$ and $\delta^{13}C$ values for these compact growth layers. These two speleothems were deposited less than 15 meters of one another far inside the cave, thus will have experienced the same temperature histories. Therefore, their differences in isotopic composition must be due to differences in the composition of the drip waters from which they grew.

The higher growth rate for 20000 may indicate a lesser degree of water-rock interaction and very little time for homogenization of infiltration water. This alone cannot account for the difference in average $\delta^{18}O$ of the feed waters to the two sites. Seasonality of water recharge can have a large impact on the average $\delta^{18}O$ at a particular drip site, due to the large seasonal variation in $\delta^{18}O_{ppt}$ of up to 15 ‰, which is expected to occur at sites in this climatic zone (Rozanski et al. 1993). The lower average $\delta^{18}O$ of sample 20000 may be because drip water was biased to winter precipitation, e.g. as snowmelt waters, while recharge to 99902 was not (Figure 2.7). Based on its much higher growth rate, we may assume that the drip rate at the site of formation of 20000 was higher and therefore variations in the isotopic composition of infiltration water due to seasonal bias may have been retained in the drip waters forming the speleothem calcite. By contrast, slower drips at the site of 99902 may represent a more homogeneous average of summer and winter infiltration. Evidence of intra-cave isotopic variability in Holocene speleothems from Norway is suggested to result from differences in percolation pathways and surface effects on these waters (Linge et al. 2001). Additionally, the enrichment in the early growth of sample 99902 may be due to evaporative effects from reduced humidity in the cave. A long-term, detailed investigation of intra-cave dripwater variability is needed before these theories can be confirmed.

Independent evidence for the existence of intra-cave, intersite differences in $\delta^{18}O$ of drip waters lies in our measurements of drips currently entering the cave, which differ between drip sites by as much as 5 ‰. It is conceivable that such intersite differences could have existed during the Pleistocene as well. The reason for these differences in

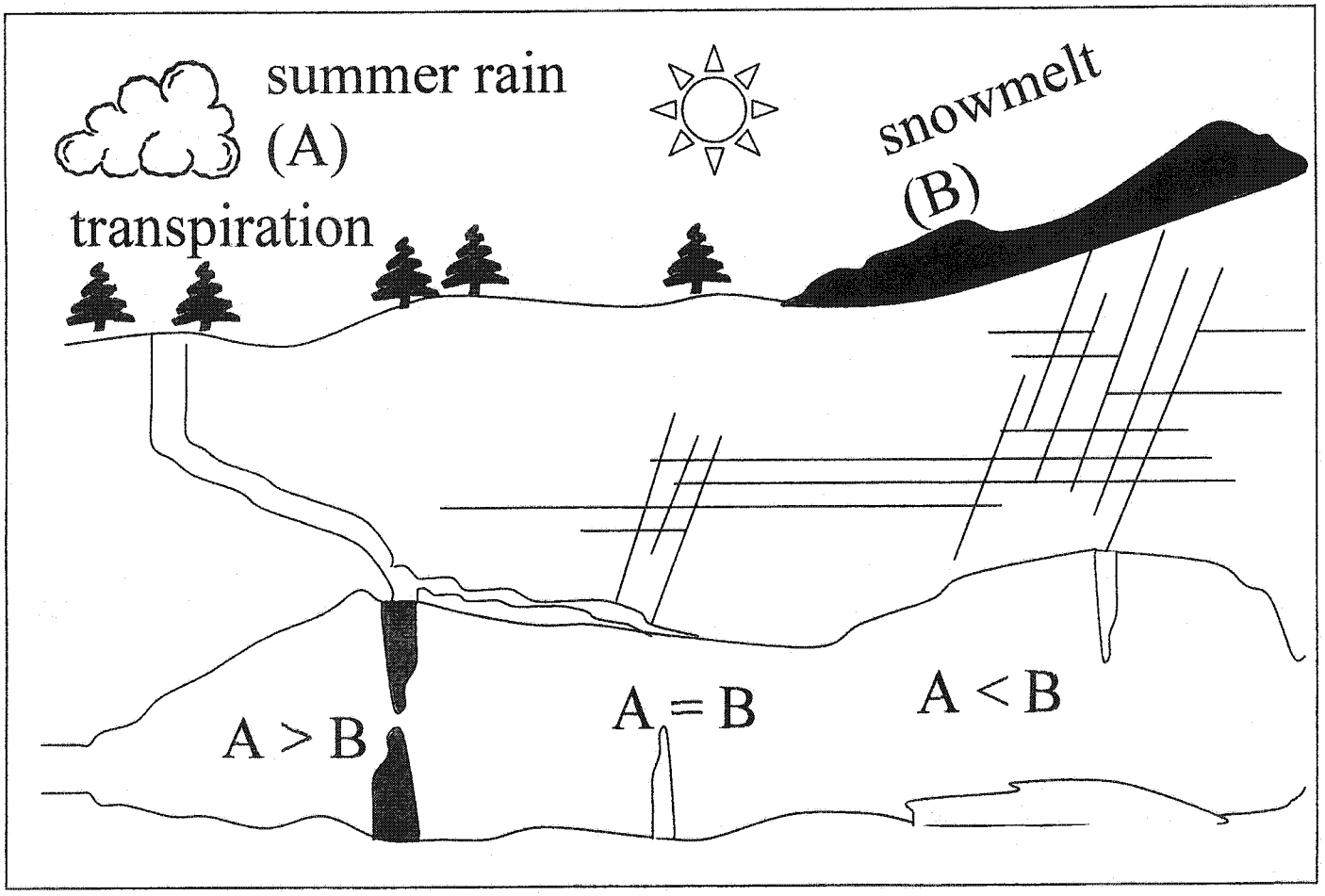

Figure 2.7. Effects of seasonal bias and hydrology on dripwater.

mean $\delta^{18}O$ of drip water are not well understood, and presumably relate to subtle differences in the routes followed by recharge water from the surface to cave drip sites. Terrain and vegetation differences above the cave could have led to differences in the proportion of winter versus summer precipitation entering the cave. An alternative explanation is that modern drip paths have been highly disturbed by quarrying activities. Soil has been removed from the quarry surface and reduced on the flanks in preparation for extension of the quarry. The impact may have widened variability in the isotopic composition of the drips. The true modern range of $\delta^{18}O$ in the dripwater may be less than 5 ‰ and weighted towards more depleted values of -12 to -13.5 ‰.

The smoother record of 99902 over the interval of coeval growth with 20000 may indicate that feed water to 99902 was spending a long time in the recharge zone, permitting long-term homogenization. Higher variability of the record for 20000 as well as its much faster growth rate are consistent with rapid infiltration times at this site. The high frequency variation of $\delta^{18}O_{ct}$ prior to the gradual increase at 54,000 years ago is similar to fluctuations seen over the same interval in Soreq Cave stalagmites (Figure 2.8). There is a negative shift of 3‰ in $\delta^{13}C$ at 59,000 years ago that is synchronous with warming in the marine record and at Crevice Cave (Figure 2.9b) (Martinson et al. 1987, Dorale et al. 1998).

After 50,000 years ago, the isotopic record for sample 99902 shows variability similar to that of sample 20000. This reinforces the idea that growth rate is largely responsible for the differences in the two records over their coeval period of growth. The measured growth rate for 99902 also increases by over a degree of magnitude to more

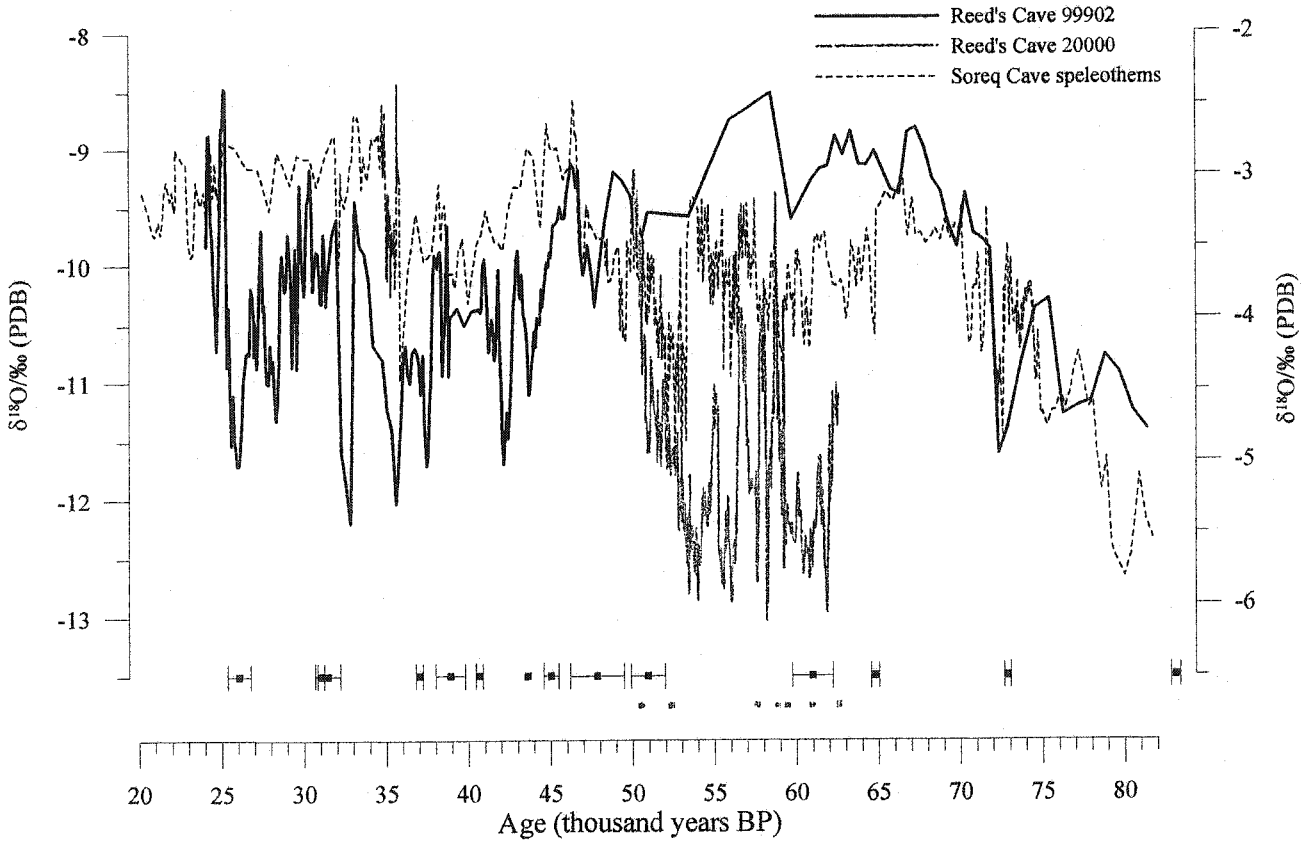

Figure 2.8. $\delta^{18}O_{ct}$ records from Soreq Cave (Bar-Matthews et al. 1999) plotted with the Reed's Cave $\delta^{18}O_{ct}$ records. Note how both Soreq Cave and Reed's Cave 20000 record high growth rates during the coeval period of growth. Error bars are shown for Reed's Cave samples at bottom of graph.

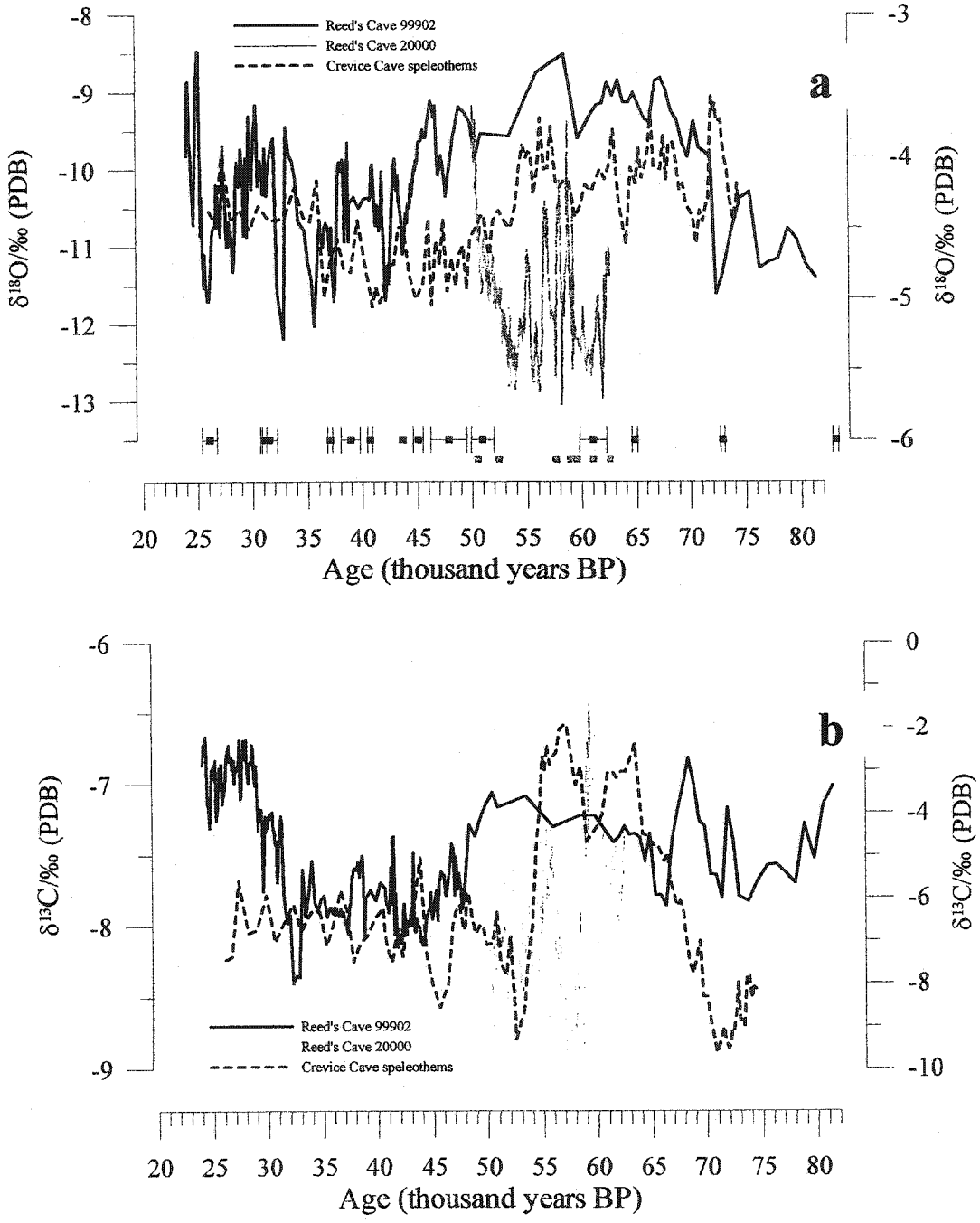

Figure 2.9. (a) Times series records of 99902 and 20000 $\delta^{18}O$ compared with record from Crevice Cave stalagmites (Dorale et al. 1998). (b) Times series records of 99902 and 20000 $\delta^{13}C$ compared with record from Crevice Cave stalagmites (Dorale et al. 1998)

closely resemble that of 20000. In addition, the range of $\delta^{18}O_{ct}$ increases to -8.5 to -12.2 ‰, not unlike the -9.0 to 13.0 ‰ range for 20000.

2.7.2. Comparison to other proxies

There are few terrestrial climate proxy records for the pre-LGM Wisconsin glacial period in North America, particularly in regions that were covered by or close to the margins of the Laurentide Ice Sheet (LIS). There is little evidence of Dansgaard-Oeschger oscillations in the mid-continental regions (Leuschner and Sirocko 2000). Lake cores in the vicinity of the Black Hills are limited almost entirely to the Holocene period, as are published records of speleothem deposits from neighboring states. The glacier advances in western North America can be correlated with Heinrich events 2 and 4 (Clark and Bartlein 1995), which also appear to be well expressed as positive excursions in the 99902 oxygen isotope record.

An important record from Crevice Cave, Missouri (Dorale et al. 1998) overlaps periods of growth in both of the Reed's Cave samples and is one of the few other continental records of interstadial events in North America. The Crevice Cave $\delta^{18}O_{ct}$ record shows inverse correlation with the variations in speleothem 20000 from 62,000 to 48,000 years ago (Figure 2.9). Specifically, interstadial events between 56,000 and 60,000 years are present in both records. There is also a corresponding depletion in $\delta^{18}O_{ct}$ in the transition from MIS 4 to 3 starting at 57,000 years ago in the Crevice Cave samples and Reed's Cave sample 99902.

The $\delta^{18}O_{ct}$ record for speleothems of Soreq Cave, Israel have features similar to some seen in the Reed's Cave records during the Wisconsin glacial period (Figure 2.9). An ~2.5 ‰ enrichment of ^{18}O during late MIS 5a and into MIS 4 occurs from 80,000 to 65,000 years ago in both Soreq Cave and sample 99902. High frequency and amplitude oscillations in $\delta^{18}O_{ct}$ are seen in both Soreq Cave and sample 20000. Positive excursions in the Soreq Cave $\delta^{18}O_{ct}$ record that may represent Heinrich events 5 and 2 at 46 ka and 25 ka respectively are well expressed in the $\delta^{18}O_{ct}$ record for sample 99902. The ~ 6 ‰ offset in the $\delta^{18}O_{ct}$ values between Soreq and Reed's Cave may be attributed to greater aridity in the Soreq Cave region. There is also considerable influence on the isotopic composition of feed waters from the Mediterranean Sea, which would produce localized effects not seen in the Black Hills. The general agreement between the Soreq Cave $\delta^{18}O_{ct}$ record and the longer record in sample 99902 is evidence that distant speleothems can be recording the same relative changes in global temperature.

Short-lived peaks of colder climate in the 99902 oxygen isotope record also correspond well with $\delta^{18}O$ variations in the GISP2 ice core record (Figure 2.10). Heinrich events 4 and 2 (H4 and H2) may be matched with with cold peaks in the 99902 oxygen isotope time series at 41,000 and 24,000 years years ago respectively, coinciding with the major late Pleistocene glacier advances in western North America (Clark and Bartlein 1995). At the time of Heinrich events 5 and 2 (H5 and H2) we see an enrichment of ^{18}O in sample 99902 (Figure 2.10). The lack of sensitivity in the 99902 $\delta^{18}O_{ct}$ before 47,000 years ago explains the absence of any of the earlier well-defined Heinrich events. Negative excursions in sample 20000 at 56,000 years, 57,500 years, 58,000 years, 58,500

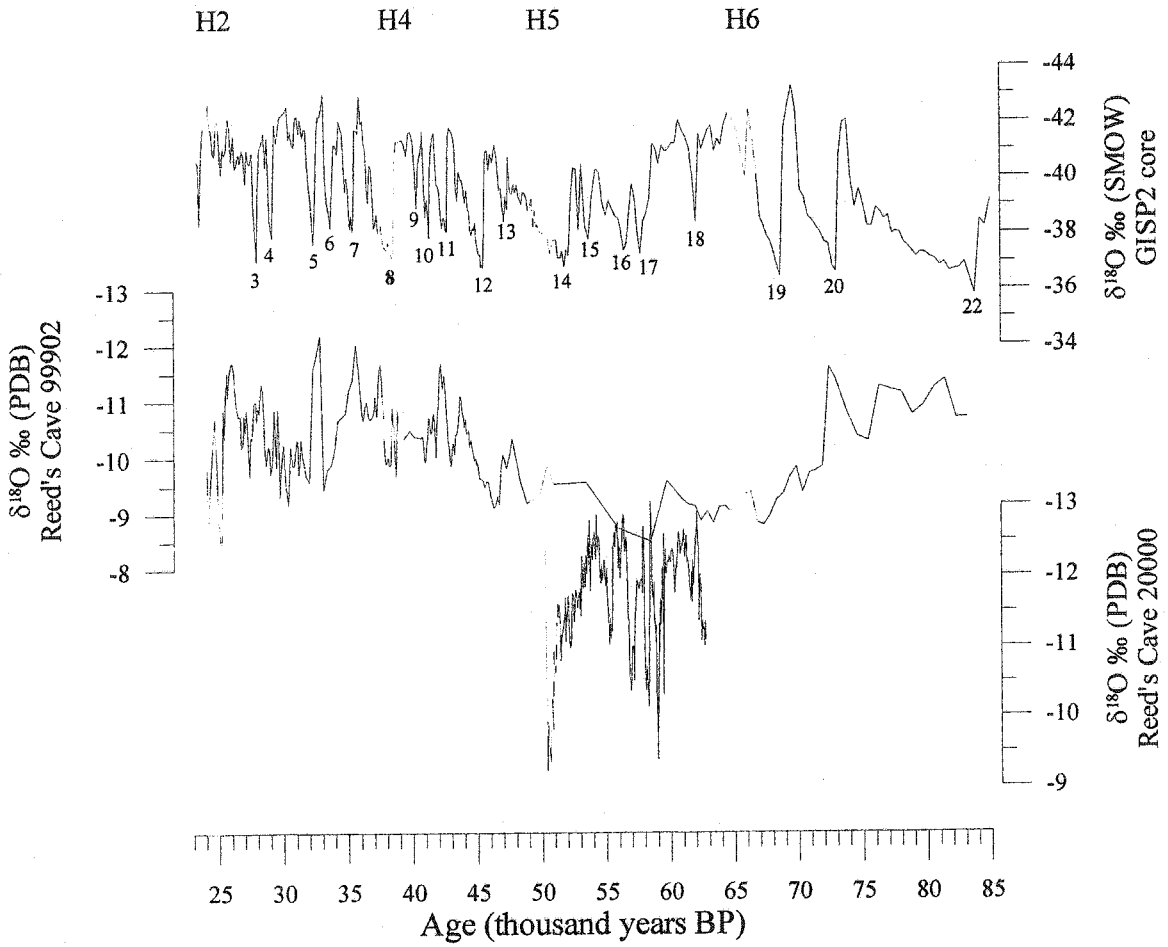

Figure 2.10. Times series records of 99902 and 20000 $\delta^{18}O$. The shaded bars indicate timing of Heinrich events in DSDP 609 (Bond et al. 1992). Numbered peaks in 99902 indicate locations of D-O interstadial events from Dansgaard et al (1993).

years, and 59,000 years ago following Heinrich event 6 are similar to coeval events in the GISP2 ice core $\delta^{18}O$ record (Figure 2.10). The tightly spaced events between 59,000 and 55,000 years suggest an atmospheric response to a forcing mechanism that reveals itself on a very short time scale.

The difficulty of interpreting carbon isotope records is attributed to the complex interactions such as soil respiration and carbonate dissolution in the aquifer systems overlying the cave (Baker et al. 1997). The most striking feature in the 99902 $\delta^{13}C$ record is the change from generally positive to negative correlation with $\delta^{18}O$ variation (Figure 2.4). It appears that although the oxygen isotopes are recording short-term climate, the carbon isotope record is more loosely coupled to climate change. The primary cause of $\delta^{13}C$ variation is likely changes in surface vegetation density and distribution and the concordant changes in soil CO_2 abundance and isotopic composition. This could be recording a shift from C_3 to C_4 vegetation, but it is difficult to explain with only a ~1‰ change in $\delta^{13}C$ in sample 99902. The $\delta^{13}C$ for 20000 is relatively stable except for the abrupt 3‰ depletion at 59,000 years ago that corresponds to a similar but chronologically offset depletion in the Crevice Cave carbon isotope record (Figure 2.9b). This warm interval is reflected in the oxygen isotope records in both 99902 and 20000.

2.7.3. Power-spectrum analysis of the isotope records

Spectral analysis of paleoclimate time series can reveal periodicity in proxy records. Deep sea sediment records from the North Atlantic (Bond et al. 1999, Bond et al. 1997, Bond et al. 1992) and Greenland ice core records (Dansgaard et al. 1993) show

strong millennial scale cyclicity in addition to the well-established Milankovitch cycles. The possible global extent of these signals has been established from records in ocean sediments in the Santa Barbara Basin (eastern Pacific Ocean), the Indian Ocean, in continental paleovegetation proxies from the Pacific Northwest, and in the Vostok ice cores (Alley et al. 1999, Pisias et al. 2001, Herbert et al. 2001, Whitlock and Grigg 2000, Anderson et al. 2000). Comparison to periodicity in other speleothem records can help us determine if these are local and/or proxy specific cycles or if they are truly recording the Dansgaard-Oeschger events.

The power spectra from the two speleothems are in closer agreement than the oxygen isotope time series (Figure 2.11). The spectra show similar peaks although their power varies. There is a 7,650 year cycle in the full time series for stalagmite 99902, which agrees very well with average spacing of 7,980 years for Heinrich events 0 to 5 using the median of several reported ages compiled by Anderson et al. (2000). Shorter 1,500 and 1,600 year cycles are present in both Reed's Cave speleothems but do not show a strong power relative to the other peaks in 99902 when computed within its full time series. Better resolution of these cycles is seen when the 8,000 year, 20,000 year and 41,000 year peaks are removed (Figure 2.11).

Because there is temporal variability in the speleothem oxygen isotope record and in both growth rate and climate over time, spectra were obtained for the different phases of growth in the two speleothems. Power spectra for the full oxygen isotope time series for 99902 and 20000 have peaks at the 1,000 - 2,000 year periodicity, but they are below the 95% significance level. For the periods 50,000 years ago to 24,000 years ago and

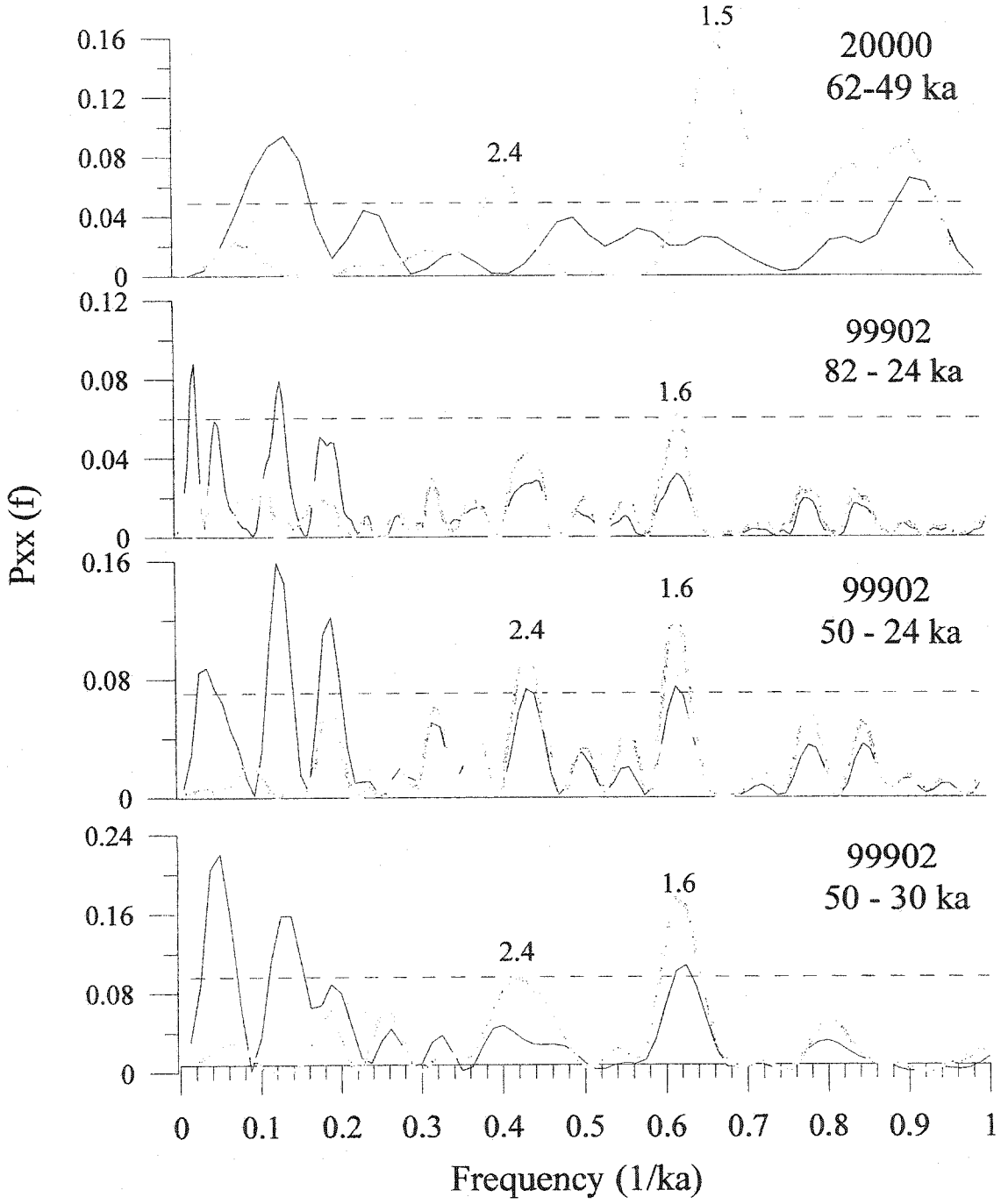

Figure 2.11. Spectral results for times series analysis of samples 99902 and 20000 oxygen isotopes. Solid black line represents unfiltered time series for each time window. Thick grey line represents filtered time series with cycles >= 8,000 years removed.

50,000 years ago to 30,000 years ago in speleothem 99902, there is significant periodicity at both 8,000 years and 1,600 years (Figure 2.11), while the faster growth rate of 20000 allows us to observe cyclicity with a period of about 1,000 years; even higher frequency oscillations are evident in the $\delta^{13}C$ record of 20000.

This millennial-scale cyclicity supports the notion that there were periods of higher instability in climate during the last glacial cycle. Spectral analysis of the Reed's Cave speleothems provides additional evidence that the cave is responding to a mechanism that is affecting climate on a hemispheric and likely a global scale.

2.8. CONCLUSIONS

This paper presents well-dated records of $\delta^{18}O_{ct}$ for speleothems for central North America during the Wisconsin glacial period. We investigated coeval speleothems that had offsets in growth; they show that different drip sites in a cave may not behave similarly. The agreement of the two Reed's Cave speleothems with interstadial events in ice core records, Heinrich events and timing of interglacial/glacial transitions in deep sea sediment records and $\delta^{18}O_{ct}$ and $\delta^{13}C$ variations in other speleothems confirms that some global climate signals are being recorded. Major shifts in climate from interglacial to glacial conditions in the mid-continent are displayed in both Reed's Cave and Crevice Cave, Missouri, but the local conditions have significant influence on the small scale variations in the $\delta^{18}O_{ct}$ record. The absolute ages for the $\delta^{18}O_{ct}$ record in Reed's Cave

speleothem provides an independent chronology for Heinrich events and D-O oscillations that are present in these records.

The two partially coeval speleothems from this cave display strikingly different isotopic records, showing that different drip sites in a cave may respond differently to climate change. Differing speleothem morphology may also exert control on variable isotopic composition between the coeval records. During the period of simultaneous deposition, the temperature response ($d(\delta^{18}O_{ct})/dT$) of the two speleothems has opposite signs, probably as a result of seasonal bias in the recharge of drip water to one of the samples.

Correlation of periodicity found in the speleothem oxygen isotope records with periodicity in Greenland ice cores supports the proposal that millennial-scale variation is initiated in the North Atlantic but transmission of this signal is highly complicated. The mixed oceanic-atmospheric conveyance results in asynchronous timing of these events in different proxies, but their common periodicity indicates a similar forcing mechanism. The more precise chronology of this record provides a more reliable timeline for events and periodicities. The Reed's Cave speleothems suggest that there is very little lag between the North Atlantic and climate responses in central North America. The ages for Heinrich events as revealed by North Atlantic and European proxy records appear to be occurring at the same time, but it is not likely that the effects of iceberg discharges on ocean circulation directly affect temperatures and precipitation in the mid-continent. Rather, it is more likely that these reflect rapid changes in the size and extent of the g

Laurentide ice sheet, which would have affected atmospheric circulation quickly and could have produced corresponding high frequency signals in the speleothem records.

2.9. ACKNOWLEDGEMENTS

The authors are grateful to the Natural Sciences and Engineering Research Council (Canada) for their support of this research, partly through a Special Project grant ("Climate System History and Dynamics") to R. Peltier, and partly through operating grants to HPS and DCF. We are grateful to Martin Knyf and Nicki Robinson for assistance in isotopic analyses. We appreciate the considerable efforts of Joyce Lundberg in the preparation and calibration of the U-Th spike used in uranium-series dating. We thank A. Simonetti and B. Ghaleb (University of Quebec at Montreal: GEOTOP) for their assistance in carrying out multi-collector ICP-MS analyses of some samples. Jason Morrison assisted us in developing power-spectrum analyses of the data.

2.10. REFERENCES

Alley, R.B., Clark, P.U., Keigwin, L.D. and Webb, R.S. (1999) Making Sense of Millennial-Scale Climate Change. *Mechanisms of global climate change at millennial time scales, Geophysical Monograph 112*, 385-394.

Anderson, R. S., Betancourt, J. L., Mead, J. I., Hevly, R .H. and Adam, D. P. (2000). Middle- and late-Wisconsin paleobotanic and paleoclimatic records from the southern Colorado Plateau, USA. *Palaeogeography, Palaeoclimatology, Palaeoecology* **155**, 31-57.

Bakalowicz, M., Ford, D. C., Miller, T. E., Palmer, A. N. and Palmer, M. V. (1987). Thermal genesis of dissolution caves in the Black Hills, South Dakota. *Geological Society of America Bulletin* **99**, 729-738.

Baker, A., Ito, E., Smart, P. L. and McEwan, R. F. (1997). Elevated and variable values of ^{13}C in speleothems in a British cave system. *Chemical Geology* **136**, 263-270.

Bar-Matthews, M., Ayalon, M., Kaufman, A. and Wasserburg, G.J. (1999). The Eastern Mediterranean paleoclimate as a reflection of regional events: Soreq Cave, Israel. *Earth and Planetary Science Letters* **166**, 85-95.

Bond, G.C., Showers,W., Elliot, M., Evans, M., Lotti, R., Hajdas, I., Bonani, G., Johnson, S., Webb, R.S., Keigwin, L. D. (1999). The North Atlantic's 1-2 kyr climate rhythm; relation to Heinrich events, Dansgaard/Oescher cycles and the Little Ice Age. *Mechanisms of global climate change at millennial time scales, Geophysical Monograph 112*, 35-58.

Bond, G., Showers, W., Cheseby, M., Lotti, R, Almasi, P. deMenocal, P., Priore, P., Cullen, R., Hajdas, I. and Bonani, G. (1997). A Pervasive Millennial-Scale Cycle in North Atlantic Holocene and Glacial Climates. *Science* **278**, 1257-1266.

Bond, G. C., H. Heinrich, W. Broecker, L. Labeyrie, J. McManus, J. Andrews, S. Huon, R. Jantschik, S. Clasen, C. Simet, K. Tedesco, M. Klas, G. Bonani, G. and S. Ivy. (1992). Evidence for massive discharges of icebergs into the North Atlantic ocean during the last glacial period. *Nature* **360**, 245-249.

Bradley, R. S. 1999. Paleoclimatology : Reconstructing Climates of the Quaternary. San Diego: Academic Press.

Clark, P.U. and Bartlein, P.J. (1995). Correlation of late Pleistocene glaciation in the western United States with North Atlantic Heinrich events. *Geology* **23** (6), 483-486.

Dansgaard, W. (1964). Stable isotopes in precipitation. *Tellus* 16: 438-468.

Dansgaard, W., Johnsen, S. J., Clausen, H. B., Dahl-Jensen, D., Gunderstrup, N. S., Hammer, C. U., Hvidberg, C. S., Steffensen, J. P., Sveinbjörnsdottir, A. E, Jouzel, J. and Bond, G. (1993). Evidence for general instability of past climate from a 250-kyr ice-core record. *Nature* **364**, 218-220.

Dorale, J. A. (2000). A high-resolution record of climate and vegetation change from Crevice Cave, Missouri during the last interglacial-glacial cycle. Unpublished PhD thesis, University of Minnesota, Minneapolis, Minnesota.

Dorale, J. A., Edwards, R. L., Ito, E. and González, L. A. (1998). Climate and Vegetation History of the Midcontinent from 75 to 25 ka: A Speleothem Record from Crevice Cave, Missouri, USA. *Science* **282**, 1871-1874.

Edwards, R. L., Chen, J. H. and Wasserburg, G. J. (1986). ^{238}U-^{234}U-^{230}Th-^{232}Th systematics and the precise measurement of time over the past 500,000 years. *Earth and Planetary Science Letters* **81**, 175-192.

Fairbanks, R. G. (1989). A 17,000 year glacio-eustatic sea level record: influence of glacial melting rates on the Younger Dryas event and deep ocean circulation. *Nature* **342**, 637-642.

Frumkin, A., Ford, D. C. and Schwarcz, H. P. (1999). Continental oxygen isotopic record of the last 170,000 years in Jerusalem. *Quaternary Research* 51: 317-327.

Gascoyne, M. (1992). Palaeoclimate determination from cave calcite deposits. *Quaternary Science Reviews* **11**: 609-632.

Grootes, P.M., Stuiver, M., White, J.W.C., Johnsen, S. J., and Jouzel, J. (1993). Comparison of oxygen isotope records from the GISP2 and GRIP Greenland ice cores. *Nature* **366**, 552-554.

Hendy, C. H. (1971). The isotopic geochemistry of speleothems - I. The calculation of the effects of different modes of formation on the isotopic composition of speleothems and their applicability as palaeoclimatic indicators. *Geochim. Cosmochim. Acta* **35**, 801-824.

Herbert, T. D., Schuffert, J. D., Andreasen, D., Heusser, L., Lyle, M, Mix, A., Ravelo, A. C., Stott, L. D. and Herguera, J. C. (2001). Collapse of the California Current During Glacial Maxima Linked to Climate Change on Land. *Science* **293**, 71-76.

IAEA (2001). *GNIP Maps and Animations*, International Atomic Energy Agency, Vienna. Accessible at *http://isohis.iaea.org*

Lea, D.W., Pak, D.K. and Spero, H.J. (2000). Climate Impact of Late Quaternary Equatorial Pacific Sea Surface Temperature Variations. *Science* **289**, 1719-1724.

Leuschner, D.C. and Sirocko, F. (2000). The low-latitude monsoon climate during Dansgaard-Oeschger cycles and Heinrich events. *Quaternary Science Reviews* **19**, 243-254.

Linge, H., Lauritzen, S.-E., Lundberg, J., and Berstad, I.M. (2001). Stable isotope stratigraphy of Holocene speleothems: examples from a cave system in Rana, northern Norway. *Palaeogeography, Palaeoclimatology, Palaeoecology* **167**, 209-224.

Lundberg, J. (1990). Dating of carbonates by mass spectrometry: a technical manual. Department of Geography, McMaster University, Hamilton, Ontario, Technical Memorandum 90-2.

Martinson, D. G., Pisias, N. G., Hays, J. D., Imbrie, J., Moore, T. C. and Shackleton, N. J. (1987). Age Dating and the Orbital Theory of the Ice Ages: Development of a High-Resolution 0 to 300,000-Year Chronostratigraphy. *Quaternary Research* **27**, 1-29.

McDermott, F., Frisia, S., Huang, Y., Longinelli, A., Spiro, B., Heaton, T. H. E., Hawkesworth, C. J., Borsato, A., Keppens, E., Fairchild, I. J., Van der Borg, K., Verheyden, S., and Selmo, E. (1999). Holocene climate variability in Europe: Evidence from ^{18}O, textural and extension-rate variations in three speleothems. *Quaternary Science Reviews* **18** (8-9),1021-1038.

O'Neil, J. R., Clayton, R. N. and Mayeda, T. K. (1969). Oxygen isotope fractionation in divalent metal carbonates. J. Chem. Phys. **51**, 5547-5558.

Palmer, A.N. and Palmer, M.V. (1989). Geologic history of the Black Hills caves, South Dakota. *National Speleological Society of America Bulletin* **51**, 72-99.

Pisias, N.G., Mix, A. and Heusser, L. (2001). Millennial scale climate variability of the Northeast Pacific Ocean and Northwest North America based on Radiolaria and pollen. *Quaternary Science Reviews* **20** (14): 1561-1576.

Rozanski, K., Araguás- Araguás, L., and Gonfiantini, R. (1993). Isotopic patterns in modern global precipitation. In *Climate Change in Continental Isotopic Records, Geophysical Monograph 78*. American Geophysical Union, Washington: 1-36.

Schulz, M. and Stattegger, K. (1997). Spectral analysis of unevenly spaced paleoclimatic time series. *Computers and Geosciences* **23**, 929-945.

Schwarcz, H. P. (1986). Geochronology and isotope geochemistry in speleothems. In *Handbook of Environmental Isotope Geochemistry* (P. Fritz and J. Fontes, eds.), 271-303. Amsterdam: Elsevier Publishers.

Schwarcz, H.P., Serefiddin, F., and Ford, D.C. Proxy records of paleoclimate from oxygen isotopic variations in speleothems: What's the sense? Submitted to *Earth and Planetary Science Letters*.

Schwarcz, H. P., Harmon, R. S., Thompson, P. and Ford, D. C. (1976). Stable isotope studies of fluid inclusions in speleothems and their paleoclimatic significance. *Geochim. Cosmochim. Acta* **40**: 637-665.

Serefiddin, F., Ford, D.C. and Schwarcz, H. P. 2001. Isotopic composition of paleoprecipitation from fluid inclusion in speleothem calcite. *Abstracts with Programs - Geological Society of America* Vol. 33, no. 6 (2001): 24.

Whitlock, C., Sarna-Wojcicki, A.M., Bartlein, P.J. and Nickman, R.J. (2000). Environmental history and tephrostratigraphy at Carp Lake, southwestern Columbia Basin, Washington, USA. *Palaeogeography, Palaeoclimatology, Palaeoecology* **155**, 7 - 29.

CHAPTER THREE. TERRESTRIAL RECORDS OF CLIMATE CHANGE IN THE MID-CONTINENT OF NORTH AMERICA FROM 530,000 TO 150,000 YEARS AGO

3.1. INTRODUCTION

Terrestrial proxy records can test climate models that attempt to predict changes in temperature, atmospheric circulation and global ice cover. Deep-sea sediment and ice core records provide us with long records extending back over hundreds of thousands of years (Martinson et al. 1987 and Dansgaard et al. 1993), but the dating of these records is problematic and the resolution of climatic events is commonly poor. Deep sea cores and ice cores do not contain suitable material for absolute dating techniques. Terrestrial records show great promise in this respect; significant work has been done using loess, pollen, paleosols and speleothems. Speleothems, secondary cave calcite deposits, are ideal because they are formed in the very stable cave environment and can be dated using absolute radiometric techniques (Schwarcz 1986). The Devil's Hole thermal water calcite $\delta^{18}O_{ct}$ record is a continuous proxy record of climate that extends back 500 ka BP, but the smoothing of the isotope record masks short-term variability (Winograd et al. 1997). The oxygen and carbon isotopic composition of speleothem calcite gives high resolution records of isotopic change related to changes in temperature, meteoric precipitation and vegetation patterns (Gascoyne et al. 1980, Dorale et al. 1992, and Frumkin et al. 1999, Wang et al. 2001). Temperature dependent fractionation and climatically influenced

isotopic variations in precipitation serve as control $\delta^{18}O_{ct}$ ($\delta^{18}O$ of calcite). With the significant advances in uranium-series techniques that can extend reliable ages of speleothems back to 700 ka BP, it is now possible to present records back to marine isotope stage (MIS) 13.

Marine isotope stage 11 (~420 to 360 ka BP) has been studied as an important analog for the current interglacial period. It has been suggested that MIS 11 is the warmest and/or longest interglacial period in the past 500 ka (Poore and Dowsett 2001, Kindler and Hearty 2000, Murray et al. 2000, Hearty et al. 1999, Scherer et al. 1998, Oppo et al. 1998, Rousseau et al. 1992, Imbrie et al. 1993). However, MIS 11 does not show the largest amplitude of insolation in the last 5 million years (Mix et al. 1995, Pisias et al. 1995 and Shackleton et al. 1995). There is some disagreement on the timing and duration of this interglacial period due to conflicting records from marine sediment records (Bauch et al. 2000, Hodell et al. 2000, King and Howard 2000). Additional evidence from speleothem records could give more precise chronology on the duration and structure of MIS 11.

Spectral analysis of the various proxies in deep-sea cores shows cycles of 100 ka, 41 ka and ~23 ka from Milankovitch (orbital) forcing. Speleothems records with absolute uranium-series ages not only give precise timing for major interglacial/glacial transitions but also confirm the presence of the Milankovitch and millennial-scale cycles in the mid-Pleistocene. There is very little evidence of millennial cycles prior to the last glacial period. Harmonic analysis also reveals that the intervals between interglacial and glacial extremes show the most variability (Oppo et al. 1998). The 5 to 10 ka cyclicity is

similar to the late Pleistocene millennial scale Dansgaard-Oeschger oscillations and Heinrich events. It is believed these fluctuations are related to the timing of freshwater and iceberg discharges into the North Atlantic which influenced SSTs and NADW formation (Oppo et al. 1998).

This paper presents results from uranium-series dating and stable isotope analysis of three speleothems deposited in Reed's Cave, South Dakota from 530 ka BP to 150 ka BP. An earlier study considered deposits from this cave dating from the last glacial cycle (84 -25 ka; Serefiddin et al., submitted, Chapter 2). The three mid-Pleistocene isotope time series are compared to determine intrasite variability and the presence of a global climate signal. The isotope records are examined to determine if there is variability in $d(\delta^{18}O_{ct})/dT$ over time. Spectral analysis of the $\delta^{18}O_{ct}$ records reveal orbitally forced cycles in the terrestrial climate record. The results provide a unique record of climate change in the mid-continent that can be compared to marine, ice core and Chinese loess records to investigate the linkages between different components of the climate system.

3.2. PALEOCLIMATE RECONSTRUCTION USING SPELEOTHEMS

Stable isotope analysis of speleothems has now been applied in a substantial number of paleoclimate reconstructions (Gascoyne 1992, Dorale et al. 1992, Lauritzen 1995,Frumkin et al. 1999, Wang et al. 2001). Speleothems from Missouri, Israel and Norway show that interstadial climate events such as Heinrich events and Dansgaard-Oeschger oscillations can be readily resolved (Lauritzen 1996, Bar-Matthews et al. 1999, Dorale 2000).

If a speleothem is deposited in oxygen isotopic equilibrium in a cave then its isotopic composition is controlled by climate:

$$\Delta\delta^{18}O_{ct} = [(d\alpha_{ct\text{-}w})/dT]\Delta T + [d(\delta^{18}O_{ppt})/dT]\Delta T + \Delta(\delta^{18}O_{sw}) \quad (1)$$

This expression combines the effects of the temperature dependent fractionation ($(d\alpha_{c\text{-}w})/dT$), isotopic changes in meteoric precipitation ($d(\delta^{18}O_{ppt})/dT$) which control $\delta^{18}O$ of drip water, and ice-volume effects of change in the isotopic composition of seawater ($\Delta(\delta^{18}O_{sw})$). The dripwater function can also be affected by seasonality in $\delta^{18}O_{ppt}$ combined with seasonal bias in recharge of drip waters feeding a particular site (Serefiddin et al., submitted, Chapter 2). $\delta^{18}O_{ct}$ would change according to long-term changes in the amount of precipitation falling seasonally.

The determination of absolute paleotemperatures may not be possible given the many complicating factors in $\delta^{18}O_{ct}$ variation. Nevertheless, records of both $\delta^{18}O_{ct}$ and $\delta^{13}C_{ct}$ appear to act as paleoclimate proxy recorders as inferred from correlations with ice core, marine sediment and other proxy records. However, in addition to correlating general trends in isotope data with climate shifts, the higher resolution speleothem records can add detail to those of deep sea and ice cores, which are smoothed because of bioturbation and ice flow dynamics.

In using isotopic records from speleothems as paleoclimate proxies, it is important, however, to consider the sign of $\gamma = d(\delta^{18}O_{ct})/dT$ for the specific deposit (Schwarcz *et al.*

in preparation). If $\gamma > 0$, then $\delta^{18}O_{ct}$ increases with increasing temperature, and vice versa. This can be calibrated by comparing modern or interglacial-age $\delta^{18}O_{ct}$ values with glacial age $\delta^{18}O_{ct}$ values at the same site: for $\gamma > 0$, modern and interglacial calcite should be enriched in ^{18}O.

In general, when using speleothems to reconstruct paleoclimate we are restricted by the harsh realities of sampling. It is impossible, in general, to know *a priori* the age of a speleothem except that actively growing deposits must include some zero-age material. Therefore, it is not possible to select samples to provide continuous records for a given time range. Also, conservation rules limit the number, size and location of samples that be collected. Reed's Cave is, however, being destroyed by quarrying operations, and sampling was not restricted. We obtained samples spanning all but a small part of the potentially datable part of the Pleistocene. Curiously none of our samples dated to the last glacial/interglacial cycle (marine isotope stage [MIS] 6, 5a-e).

3.3. SAMPLES AND LOCATION

Reed's Cave (43° 34' 12" N, 103° 38' 36" W, 1400 m asl) lies in the Black Hills of South Dakota, near the center of the continent and far from oceanic influence on precipitation (Figure 3.1). Western South Dakota is at the convergence of the Pacific, Arctic and Gulf of Mexico air masses (Bryson 1966). Reed's Cave is a multi-level maze cave developed in Mississippian Pahasapa limestone. The average annual temperature is 8 °C and there the average annual precipitation is 783 mm with 476 mm from rain and

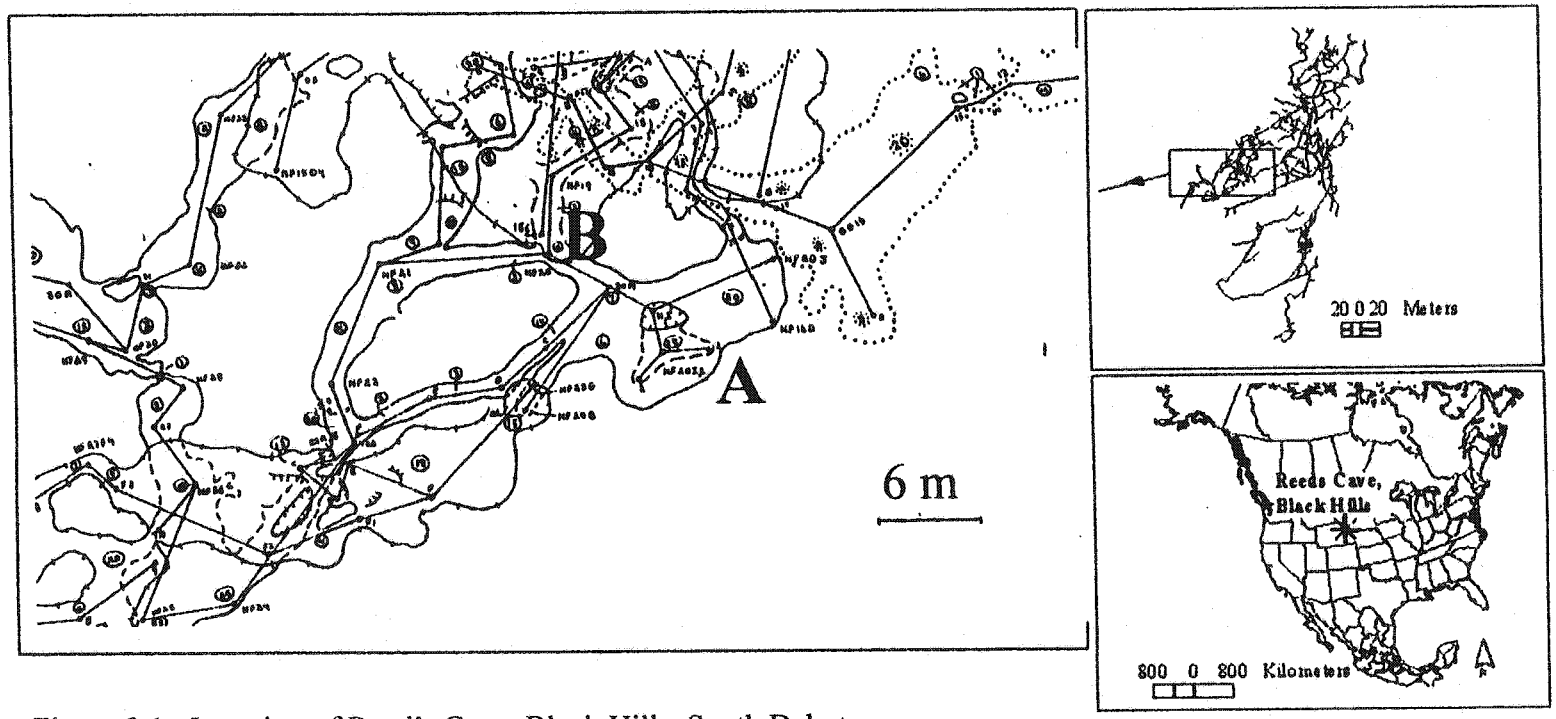

Figure 3.1. Location of Reed's Cave, Black Hills, South Dakota. Samples 99901 and 20001 collected from site A and sample 99900 collected from site B.

307 mm (water equivalent) from snow. Adjacent areas support vegetation of a mixed prairie and hardwood forest. The surface above the cave is the site of quarrying that has been active for the past 20 years. Modern dripwater composition and hydrology is not representative of conditions prior to the quarry activity, thus speleothem depositions have changed as well. Measurements of modern calcite are used with caution in the determination of the sign of gamma.

Three speleothems that have base dates in the 500-200 ka BP range were selected to investigate the structure and timing of mid-Pleistocene interglacials and glacials, with an emphasis on MIS 11. The samples were collected from the same chamber in the cave and two speleothems (99901 and 20001) were growing within 1 meter of each other (Figure 3.1). The third sample (99900), growing no more than 10 meters away, would not experience a significant difference in the cave environment but may have formation waters that originated in slightly different locations or followed a different pathway through the aquifer.

3.4. METHODS

The three speleothems were prepared for uranium-series disequilibrium dating in the McMaster University laboratories. Sample aliquots were extracted by two methods. Some samples were sliced using a diamond wafering blade on a low speed saw. The remainder of the samples were removed using a cobalt dental burr to grind out the required amount of powder. Sample sizes ranged from 150 mg to 5 g, depending on age and uranium concentration. Uranium and thorium species were extracted by column

chemistry by methods described in Lundberg (1990). The uranium and thorium were analyzed by thermal ionization mass spectrometry at the McMaster laboratory (Li et al. 1989) and by multi-collector ICP-MS at GEOTOP at University of Quebec at Montreal (Cheng et al. 2001).

Samples for stable isotope analysis for oxygen and carbon isotope analysis were drilled up the growth axis at 0.5 mm and 1 mm intervals using a 1/64" cobalt dental drill. Two growth layers were selected from samples 99901 and 20001 and three growth layers from 99900 for equilibrium tests (Hendy 1971). The powders were run on an Optima mass spectrometer with Autocarb attachment. The samples were run against the NBS-19 standard and reported versus VPDB.

Spectral analysis of isotopes data was done using time series program based on a combination of Lomb-Scargle Fourier transform and the Welch-Overlapped-Segment-Averaging method. The data was processed using SPECTRUM software (Schulz and Statteger 1997).

3.5. RESULTS

3.5.1. Uranium-series dates

Uranium-series results are presented in Table 3.1. The chronology for the isotope records was established using four dates for samples 99900, and three dates each for samples 99901 and 20001. Growth rates were assumed constant between dated intervals for creating age models. Results for the Reed's Cave samples include both TIMS and

Table 3.1. Uranium-series dating ratios, concentrations and ages for Reed's Cave 99900, 99901 and 20001

Sample ID[a,c]	Sample wt (g)	^{238}U (ppm)	$\delta^{234}U_{measured}$[b]	$[^{230}Th/^{238}U]$ (activity)	$[^{230}Th/^{234}U]$ (activity)	$[^{230}Th/^{232}Th]$ (activity)	Age corrected (kya)	2 s (+)	2 s (-)	Technique
99900_3 (F4)		2.86	42.10		1.05070		**528.0**	45.0	34.0	ICP
99900_20(F3)		2.86	61.20		1.06980		**527.0**	46.0	34.0	ICP
99900_106(F1)		2.55	74.10		1.06200		**367.0**	11.0	10.0	ICP
99900_131R	1.171	2.59	80.50	0.90762	0.84000	1158.5	**190.2**	1.0	1.0	ICP
99901_1	2.490	5.21	64.77	1.073854	1.00853	51158.0	**458.7**	35.4	26.8	TIMS
99901_75	2.056	3.18	61.23	1.057668	0.99664	1963.0	**405.1**	58.4	38.1	TIMS
99901_130	1.174	2.81	66.93	1.049551	0.98371	8356.6	**357.8**	31.0	24.2	TIMS
20001_20	0.575	1.84	66.38	1.076035	1.00905	919.9	**458.5**	36.8	27.7	TIMS
20001_50	1.089	3.03	57.52	1.053777	0.99646	21023.4	**409.2**	48.7	33.9	TIMS
20001_top	1.101	2.36	112.87	1.000552	0.89907	955.7	**226.9**	6.3	6.0	TIMS

[a] Number following sample ID is location of sample in mm from base

[b] $\delta^{234}U = ([^{234}U/^{238}U] - 1)_{activity} \times 1000$

[c] See Figure 3.2 for sample location

multi-collector ICP-MS analyses (Table 3.1). The error is expressed as the two sigma values. Uranium concentrations are very high, ranging from 1.8 to 5.2 ppm. In general the older dates have large uncertainties as they approach the limit of the U series dating method. There is indication of some leaching in growth layers due to the high $^{234}U/^{238}U$ activities for many samples that were analyzed but did not provide dates (Table 3.2). The ratios indicate that the samples are beyond the dating limit of our technique. The samples that did produce dates may be representing intervals of increased growth in which leaching did not occur. This may also be coinciding with interglacial periods.

All three samples, but 99900, in particular, appear to have periods of little or no growth during the colder or drier intervals. These intervals may be indicated by lighter banding that has been representative of interrupted growth in other speleothem samples (Ford and Williams 1989). There are two TIMS and two ICP-MS dates with mean errors of 26 ka and 6 ka respectively (Figure 3.2a). There is an additional TIMS age at 131 mm from base that agrees with the ICP-MS date of higher precision. Sample 99901 has three TIMS dates and appears to have minor hiatus at 40 mm from base following the MIS 12 glacial maxima at 430 ka BP (Figure 3.2b). The mean error for the TIMS dates is 36 ka. There are three TIMS dates for sample 20001 with a mean error of 27 ka (Figure 3.2c). From visual inspection the growth appears to be uninterrupted but three light colored growth layers at approximately 15 mm from base (475 ka BP), 58 mm from base (380 ka BP) and 90 mm from base (277 ka BP) may represent extremely slow periods of growth or brief hiatuses. Growth rates for all speleothems are given, showing a much higher growth rate for sample 99901 (Figure 3.3).

Table 3.2. Uranium-series dating ratios and concentration data for Reed's Cave 99900, 99901 and 20001

Sample	Sample wt (g)	Spike wt (g)	^{238}U (ppm)	$[^{234}U/^{238}U]$ (activity)	$[^{230}Th/^{234}U]$ (activity)	$[^{230}Th/^{232}Th]$ (activity)	Technique
99900_1	2.1360	0.3898	3.015	1.0412	0.9981	434.00	TIMS
99900_3 (F4)			2.861		1.0507		ICP
99900_14	0.9363	0.4241	3.855	1.0364	1.0303	691.00	TIMS
99900_20(F3)			2.860		1.0774		ICP
99900_29	0.3183	0.2943	2.484	1.0212	1.0508	5386.06	ICP
99900_35.5	0.5909	0.3346	3.330	1.0507	1.0394	2628.54	TIMS
99900_49	0.2984	0.3801	1.833	1.0040	1.0673	531.15	ICP
99900_49G	0.2563	0.3120	2.110	1.0870	0.9955	523.00	TIMS
99900_54T	0.6396	0.2675	1.394	1.0474	1.0236	1559.30	TIMS
99900_54IC	0.3006	0.2631	1.398	1.0151	1.0413	1615.39	ICP
99900_55	3.0788	0.3835	1.807	1.0654	0.9928	3347.00	TIMS
99900_66	1.1401	0.3655	1.438	1.0641	1.0178	4175.00	TIMS
99900_70(F2)			0.827		1.0698		ICP
99900_73	0.7585	0.3675	1.354	1.0325	1.0302	5140.15	ICP
99900_103	0.8783	0.3705	2.666	1.0289	1.0260	12221.37	ICP
99900_106(F1)			2.550		1.0620		ICP
99900_108R	0.2310	0.3838	4.026	1.0351	1.0137	4814.21	ICP
99900_118	0.1087	0.3063	2.186	1.0391	1.0291	831.98	ICP
99900_131R	1.1710	0.3137	2.593	1.0805	0.8400	1158.55	ICP
99900_131	1.0452	0.3460	3.305	1.0991	0.8506	1876.23	TIMS
99901_1	2.4901	0.3971	5.212	1.0648	1.0085	51158.00	TIMS
99901_10	0.2109	0.2135	4.439	1.0387	1.0433	20502.86	ICP
99901_20	0.2050	0.1806	4.726	1.0419	1.0389	27042.27	ICP
99901_38	0.2631	0.2147	5.172	1.0593	1.0480	36488.96	ICP
99901_43	0.2168	0.3077	6.543	0.7199	1.0261	16518.15	ICP
99901_53	0.2725	0.2135	3.001	1.0642	1.0367	12038.57	ICP
99901_75	2.0560	0.4118	3.176	1.0612	0.9966	1963.00	TIMS
99901_75R	0.2235	0.2057	2.574	1.0461	1.0182	7378.97	ICP
99901_92	0.2270	0.1745	2.582	1.0350	1.0248	9310.39	ICP
99901_104	0.2063	0.2946	3.385	1.0350	1.0165	12320.57	ICP

Table 3.2. Uranium-series dating ratios and concentration data for Reed's Cave 99900, 99901 and 20001

Sample	Sample wt (g)	Spike wt (g)	^{238}U (ppm)	$[^{234}U/^{238}U]$ (activity)	$[^{230}Th/^{234}U]$ (activity)	$[^{230}Th/^{232}Th]$ (activity)	Technique
99901_110	0.2100	0.1910	3.509	1.0319	1.0237	11954.02	ICP
99901_120	0.2169	0.2031	3.157	1.0289	1.0199	11672.90	ICP
99901_130	1.1742	0.3245	2.811	1.0669	0.9837	8356.62	TIMS
20001_B	0.9987	0.3912	1.827	1.0721	0.9849	725.29	TIMS
20001_0	0.2849	0.2058	1.819	1.0344	1.0398	1141.86	ICP
20001_10	0.2393	0.2101	1.700	1.0312	1.0320	4360.89	ICP
20001_20	0.5747	0.2723	1.838	1.0664	1.0091	919.93	TIMS
20001_38	0.3187	0.1977	3.051	1.0376	1.0247	28318.65	ICP
20001_50	1.0885	0.2801	3.035	1.0575	0.9965	21023.38	TIMS
20001_58	0.2777	0.1933	3.430	1.0445	1.0205	16803.26	ICP
20001_70	0.2565	0.1966	3.519	1.0296	1.0390	9593.92	ICP
20001_80	0.2050	0.1806	2.132	1.0251	1.0240	22642.21	ICP
20001_100	0.2433	0.1915	3.880	1.0165	0.9663	29022.00	ICP
20001_top	1.1010	0.3768	2.357	1.1129	0.8991	955.71	TIMS

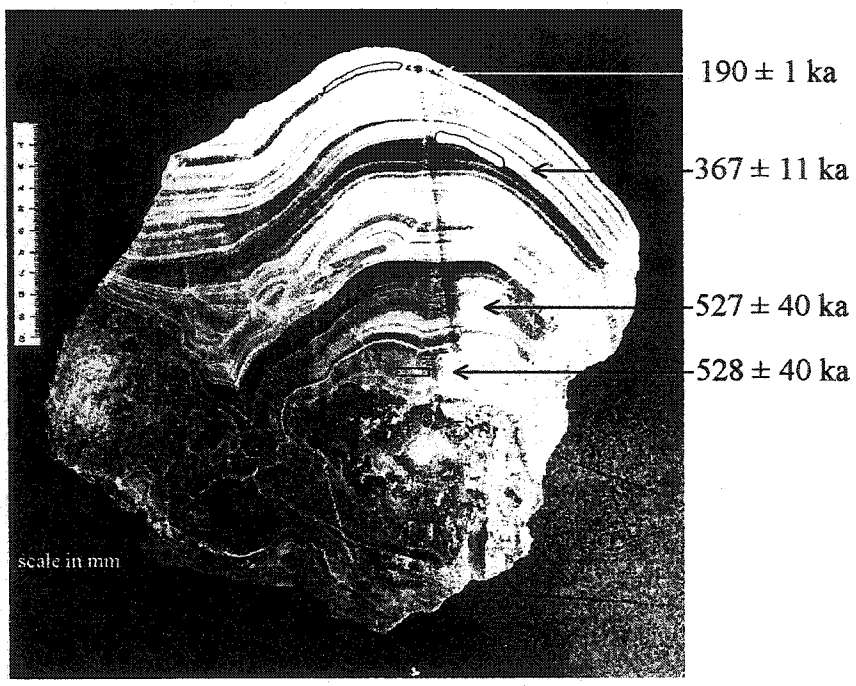

Figure 3.2. (a) Cross section of sample 99900 with location of ages.

(b)

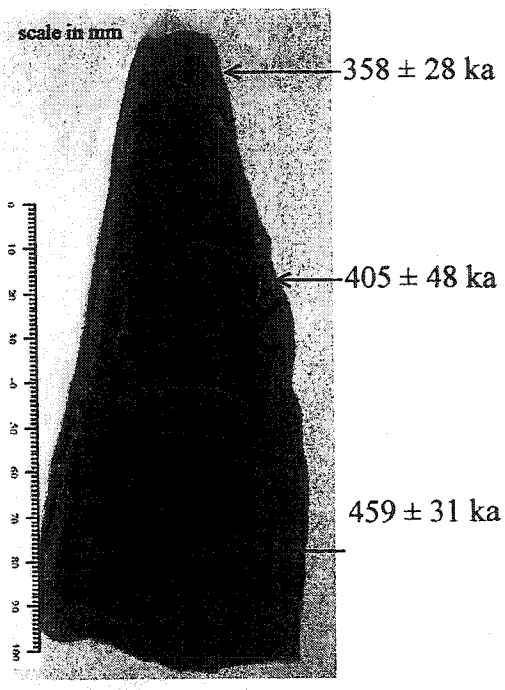

(c)

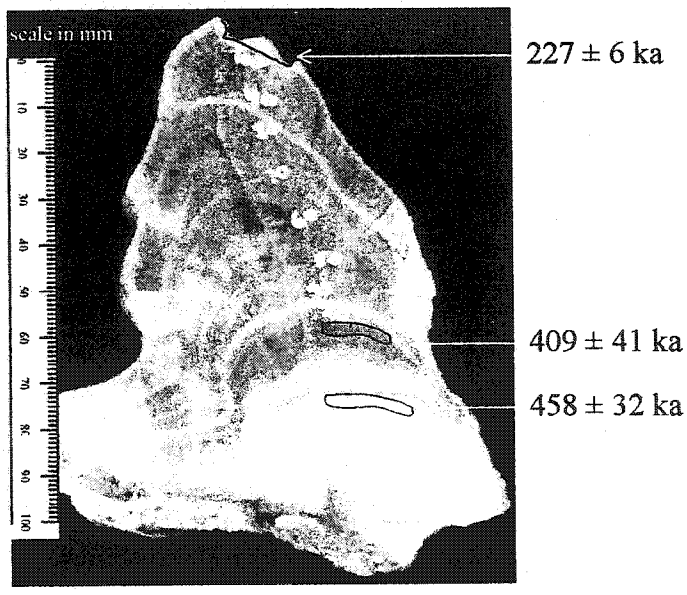

Figure 3.2. Cross section of (b) sample 99901 and (c) 20001 with location of ages.

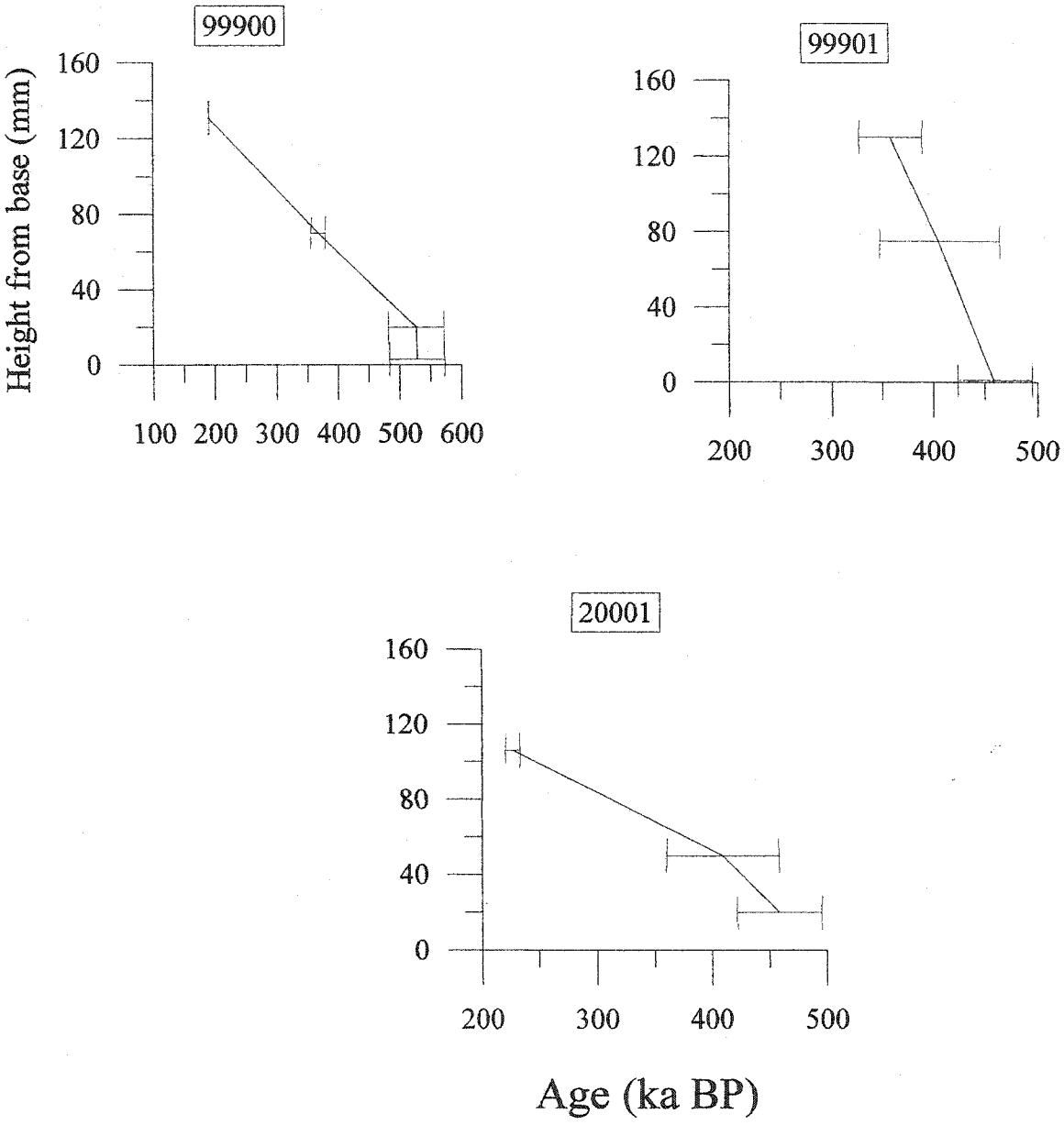

Figure 3.3. Age models for samples 99900, 99901 and 20001.

Lighter growth layers in the samples are believed to represent periods of attenuated growth rates (Ford and Williams 1989, Hill and Forti 1997). Reduced infiltration rates above the cave can reduce drip rates in the cave, cause lowered humidity in the cave, and possibly cause evaporative fractionation in these layers during deposition. However, we did not observe isotopic fractionation in any of our samples. Lowered humidity could occur during glacial periods when there is a reduction in subsurface infiltration due to ice cover or permafrost development. The Laurentide ice sheet did not extend to this part of South Dakota and there is no evidence of permafrost. A hiatus may also occur during particularly warm periods when rainfall is limited.

3.5.2. Stable isotope analysis

Isotopic variation in speleothem can be used as a paleoclimate proxy if the calcite is deposited in isotopic equilibrium with its dripwater The speleothems were tested for equilibrium deposition conditions to ensure that kinetic fractionation effects have not obscured the climate signal. The conditions for equilibrium (Hendy ,1971), are that, within a single growth layer, there is no variation in $\delta^{18}O_{ct}$, and no covariance of $\delta^{18}O_{ct}$ and $\delta^{13}C$. At least 3 growth layers were examined in each of the three speleothems used in this study.

The oxygen isotope variation in a speleothem is controlled by: a) temperature dependent fractionation of the calcite-water system; b) original composition of precipitation infiltrating as feedwater; and c) $\delta^{18}O$ of seawater during time of deposition.

Depending on the relative influence of each variable, $\delta^{18}O_{ct}$ may increase or decrease (or remain constant) with increasing temperature. We define a variable $\gamma = d(\delta^{18}O_{ct})/dT$ to express the climatic dependence of $\delta^{18}O_{ct}$ (Schwarcz et al. in preparation).

3.5.3. Oxygen isotope variations in the samples

Sample 99900, which grew over the interval from 525 ka to c.150 ka, has a range in $\delta^{18}O$ of 4.9 ‰ over its full growth interval (Figure 3.4). Most of this variation is in the first half of its growth history, whereas the $\delta^{18}O_{ct}$ record of the upper half is relatively featureless, suggesting that γ has changed markedly from its value near the base.

Sample 99901 (Figure 3.5) grew from 460 ka to 360 ka, overlapping the early growth period of 99900. Its $\delta^{18}O_{ct}$ record varies over a range of 4.4 ‰ and resembles that of 99900, but is inverted, implying that the sign of γ is opposite for these two deposits. The MIS 11/12 transition at 421 ka BP is marked by a rapid decrease in the $\delta^{18}O_{ct}$ value that indicates a rapid warming following the glacial maximum. A sharp transition from pinkish to white calcite in the speleothem suggests the presence of an extreme climatic event that may be driving the negative excursion in the $\delta^{18}O_{ct}$ value (Figure 3.2b). The timing of this transition is in question due to poor age control for 99901 in this interval. There are significant negative excursions in $\delta^{18}O_{ct}$ at 430 ka BP and 395 ka BP that correspond to color transitions in the calcite from a darker, translucent color to white. $\delta^{18}O_{ct}$ decreases during the MIS 12/11 transition by about 4 ‰, about 60% of the full interglacial-glacial isotopic change.

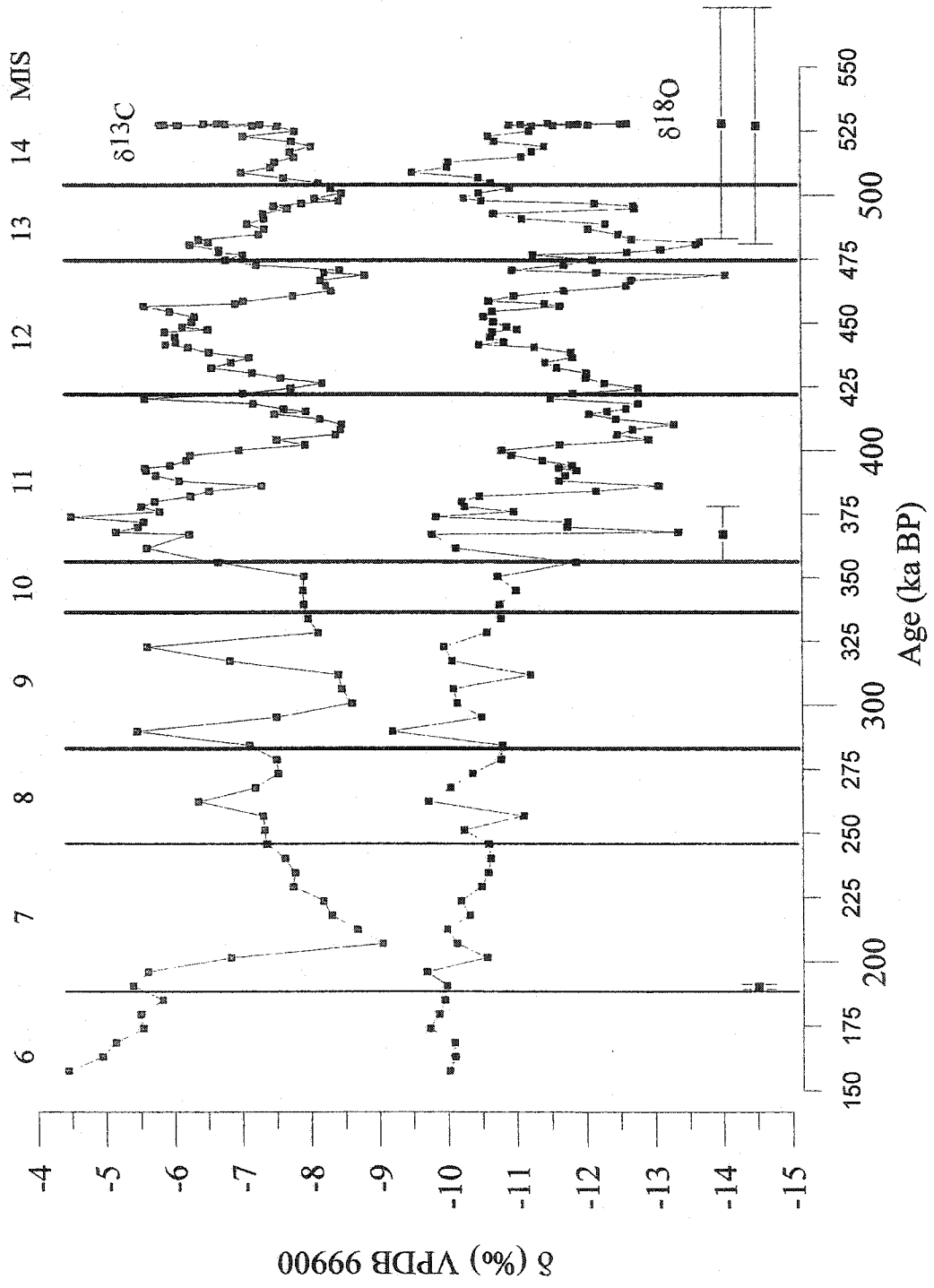

Figure 3.4. Oxygen and carbon isotope time series for sample 99900. Ages with errors shown above x-axis.

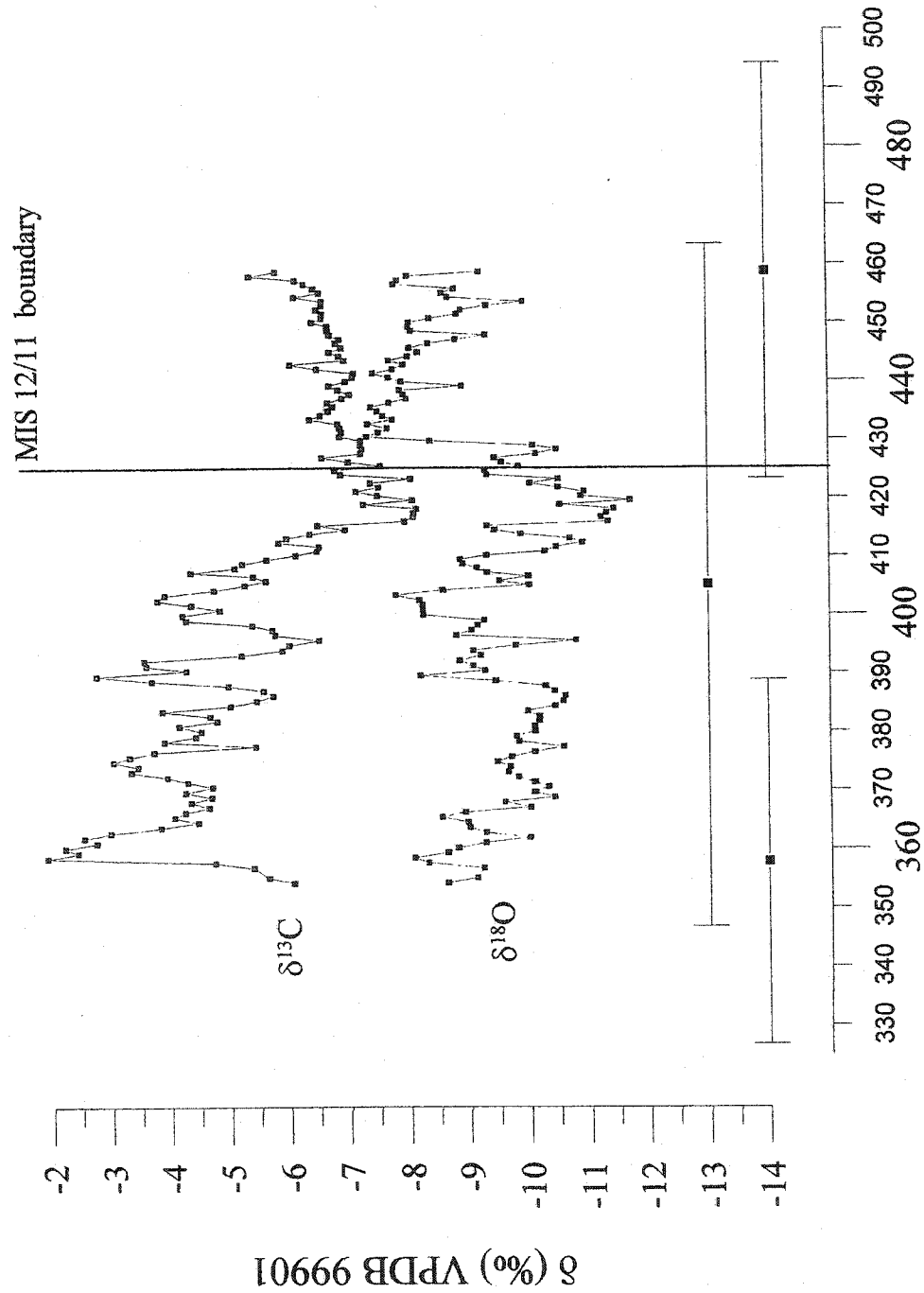

Figure 3.5. Oxygen and carbon isotope time series for sample 99901. Ages with errors shown above x-axis.

Sample 20001, which grew from c. 490 ka to 225 ka, has a 5 ‰ range in $\delta^{18}O_{ct}$; most of this variation occurs after 300 ka, whereas between 450 and 350 ky, the oxygen isotope record for 20001 is smoothed. The local mechanisms controlling $\delta^{18}O_{ct}$ values appear to be canceling out to give $\gamma \approx 0$ (Figure 3.6). After 300 ka BP the isotopes show a much greater magnitude of variation. There is a depletion of ^{18}O of ~4 ‰ at 275 ka BP that is synchronous with the start of MIS 8, suggesting that $\gamma > 0$ for this section of the speleothem.

A comparison of the results between the three speleothems shows a very complex relationship. Between 450 and 340 ka, the mean $\delta^{18}O_{ct}$ value for 99900 is 1.8 ‰ more depleted than the averages for 99901 and 20001. This 3.5 ‰ average offset between these records represents 70% of the full range of the oxygen isotope record for 99900. A similar offset of up to 4 ‰ is seen between two Wisconsin age speleothems from Reed's Cave (Serefiddin et al. submitted, Chapter 2). After 340 ka, 20001 and 99900 exhibit similar average $\delta^{18}O_{ct}$ values. Each of the records has comparable ranges of $\delta^{18}O_{ct}$ values of 4 to 5 ‰. Both 20001 and 99000 have long periods of growth (at different times) during which $\delta^{18}O_{ct}$ variation is very small (c. 1 ‰).

3.5.4 Spectral analyses

Spectral analysis was done for the three samples to determine periodicity in the oxygen isotope data. The harmonic analysis results for samples 99900 and 20001 are

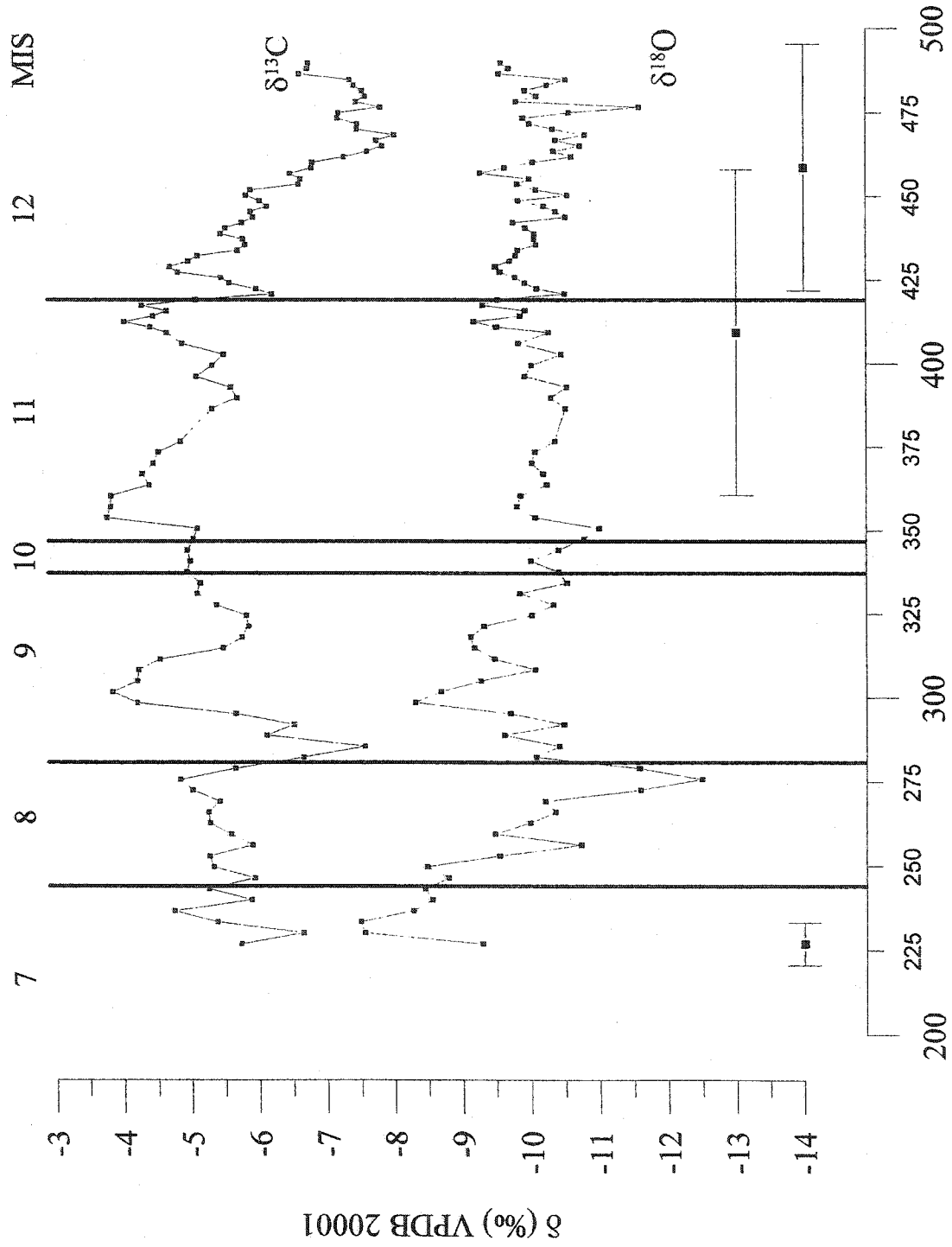

Figure 3.6. Oxygen and carbon isotope time series for sample 20001. Ages with errors shown above x-axis.

suspect because the hiatuses that are likely present in the speleothems would affect the time series. The spectrum for sample 99901 appears to give valid periodicity because it is less likely that the isotope record was interrupted by any hiatuses. The strongest and only significant peak (95% confidence level) for the spectrum records the 41 ka periodicity from the obliquity cycle (Figure 3.7). This is the strongest cycle in the SPECMAP record also (Bradley, 1999). However, the 99901 record is only 100,000 y long, so that the significance of a 41,000 y cycle in this record is suspect.

3.6. DISCUSSION

3.6.1. Oxygen isotopic records of coeval samples: Variations in climate response

The periods of growth for these three samples differ, but comparisons can be made between samples over coeval periods of deposition. Between 430 and 390 ka BP in 99900 and 99901 show similar oscillations in $\delta^{18}O_{ct}$ but of opposite polarity (Figure 3.8): γ is negative for 99900 and positive for 99901. During the same period 20001 shows much less variation in $\delta^{18}O_{ct}$ (amplitude < 2 ‰) implying that $\gamma \approx 0$. Leading into this interval there appears to be a hiatus or large reduction in growth rate in 99901. The 3.5‰ depletion that occurs just before 430 ka BP may be interrupted by a hiatus and suggests the cooling may be started in sample 99901 about 50 ka earlier, similar to an event in the SPECMAP record (Figure 3.9). The most extreme values during interglacial MIS 11 are at around 405 ka BP, which agrees well with SPECMAP (Figure 3.9).

The reversed polarities of these two records implies that the factors controlling $\delta^{18}O_{ct}$

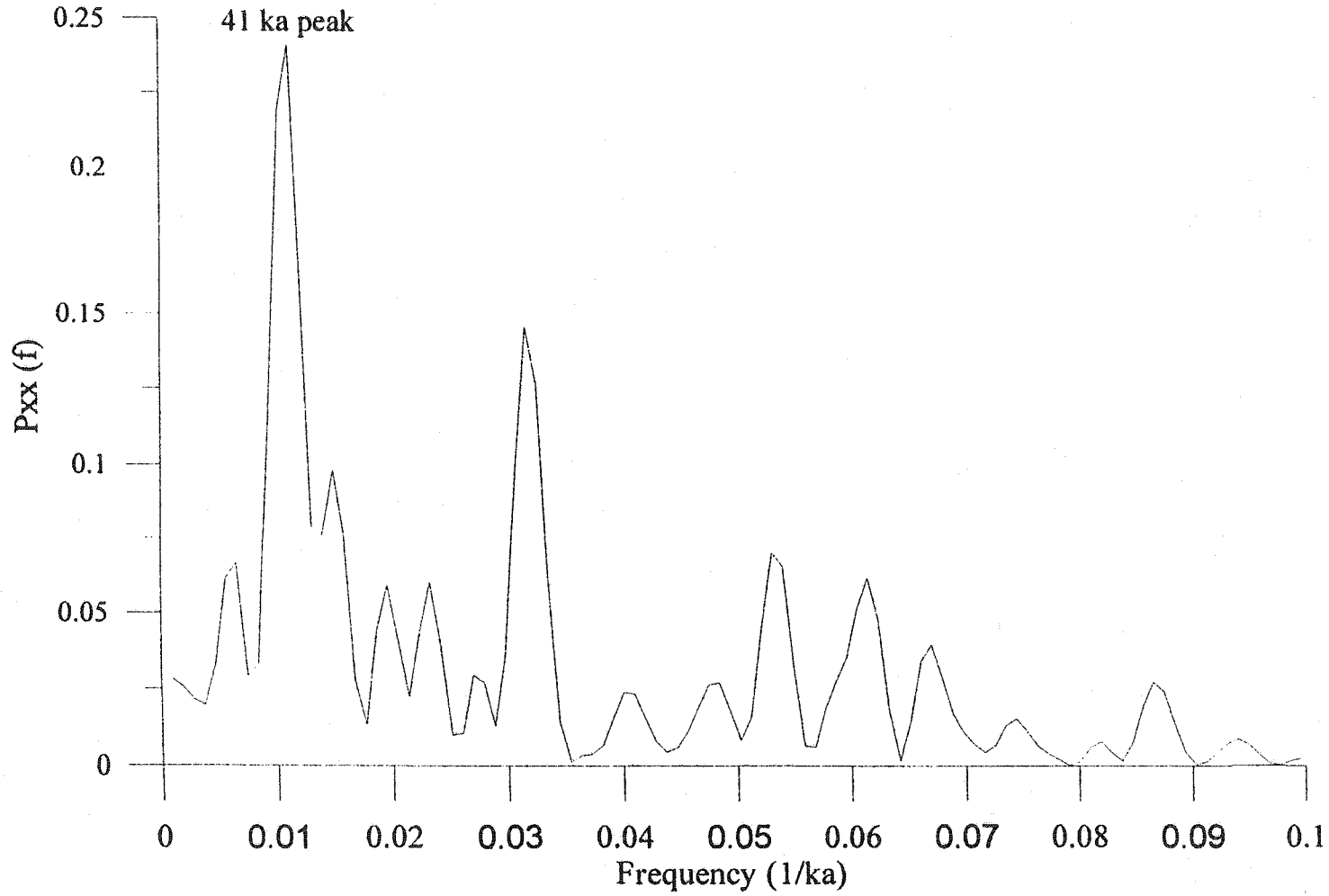

Figure 3.7. Results of spectral analysis for sample 99901.

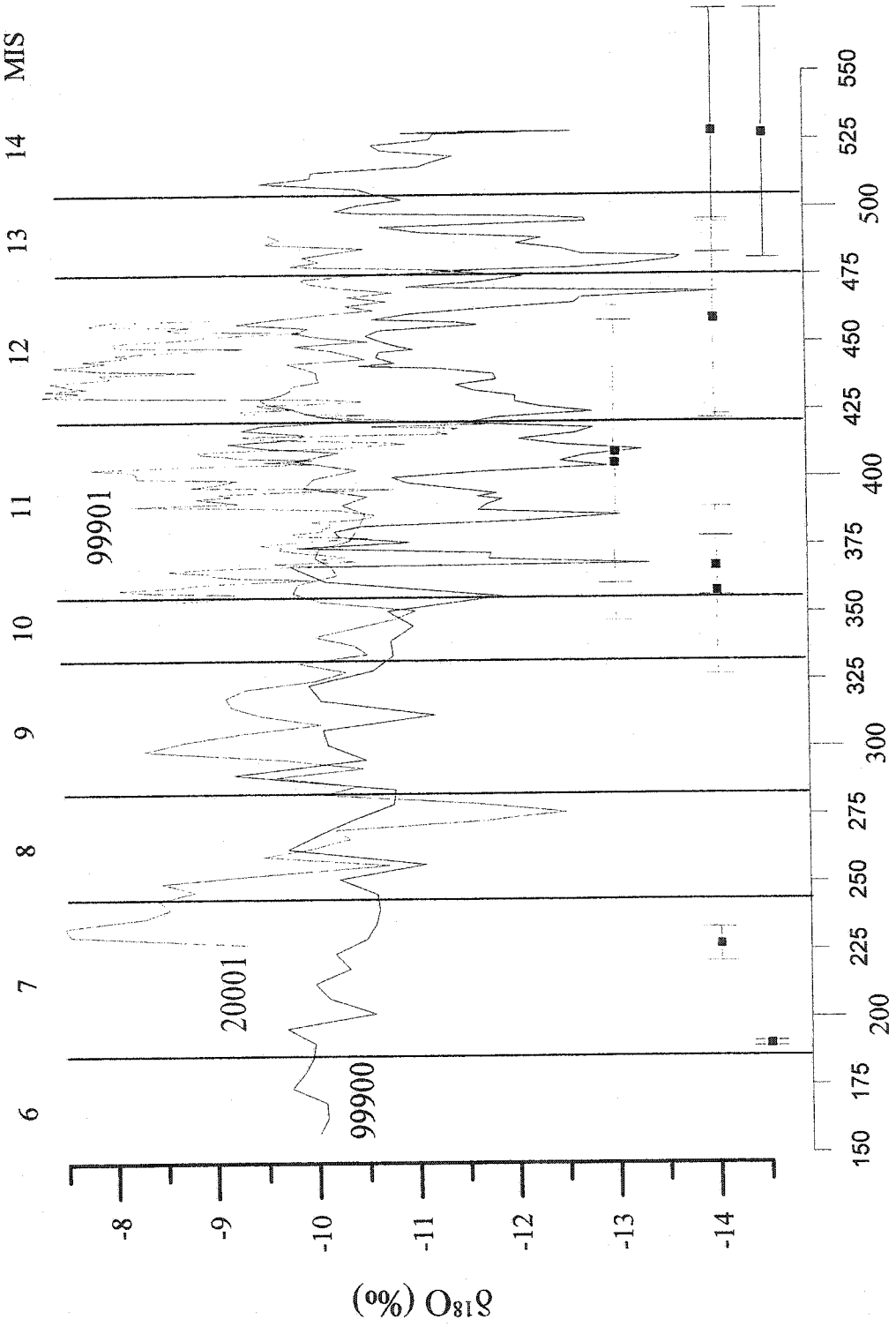

Figure 3.8. Oxygen isotope time series for samples 99900, 99901 and 20001.

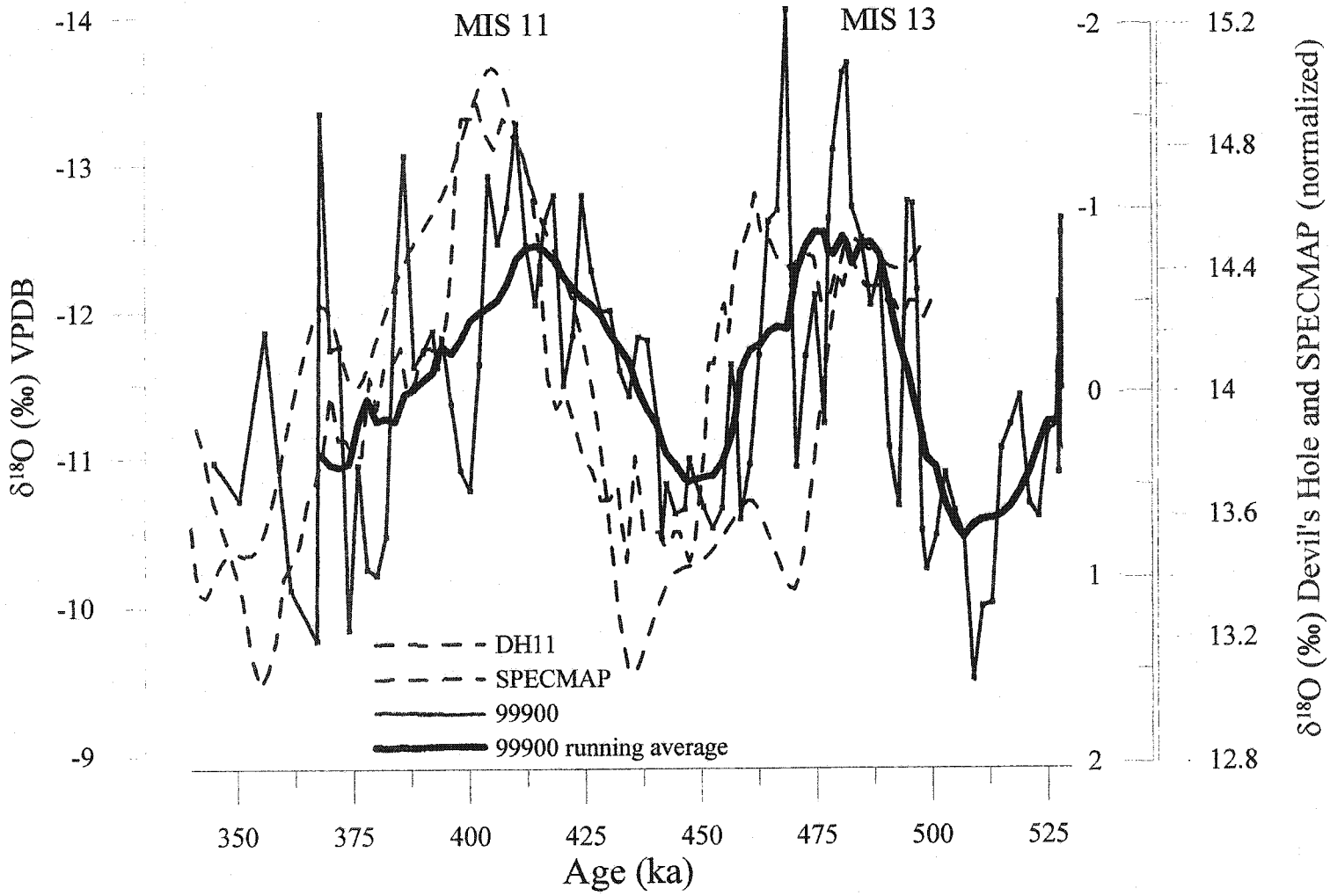

Figure 3.9. Oxygen isotope time series during MIS 11 and MIS 13 for sample 99000, SPECMAP, and Devil's Hole (DH11). DH11 scale is reported to SMOW scale and scale for SPECMAP is inverted for comparison.

at the sites of these two stalagmites (a few meters apart in the cave) are quite different. In an earlier paper (Serefiddin et al., submitted, Chapter 2) we have speculated that differences in the seasonality of the input of recharge water could account for offsets in $\delta^{18}O$ between two sites. Specifically, if recharge at one site was dominated by spring melting of winter snows, then $\delta^{18}O_{ct}$ would be significantly lower at that site. Here, however, we see a further variant in which not only the average $\delta^{18}O$ of calcite, but its response to climate change has been reversed between two drip sites. This could reflect a stronger dependence of $\delta^{18}O_{ct}$ on the T-effect on precipitation for 99901 ($\gamma > 0$) and a stronger dependence on the T-effect on fractionation between calcite and water for 99900 ($\gamma < 0$). The average $\delta^{18}O_{ct}$ values of 99900 are depleted in ^{18}O versus sample 20001 and 99901 by approximately 2.5 to 4 ‰ (respectively), suggesting that the drip waters may have contained a higher percentage of winter precipitation (Serefiddin et al. submitted, Chapter 2). A balance between the precipitation and calcite-water fractionation effects may explain the flat signal during the earlier part of the record for 20001, giving $\gamma \approx 0$. The records of 99900 and 99901 are offset by ~ 6 ‰ (Fig. 3.8) during the MIS 13 and 11 interglacial; this difference is reduced almost entirely during the MIS 12 glacial period. The timing of the MIS 12 maxima in 99900 and minima in 99901 agree well within the 2σ error of their ages. The MIS 13 maximum is more pronounced in 99901 and could be absent or delayed in 99900.

The time interval between 350 and 250 ka BP shows similar $\delta^{18}O_{ct}$ values centered at -10 ‰ for samples 99900 and 20001 (Figure 3.10). Sample 99900 has a subdued record suggesting $\gamma \approx 0$, whereas 20001 shows more distinct maxima and minima at MIS 9 and

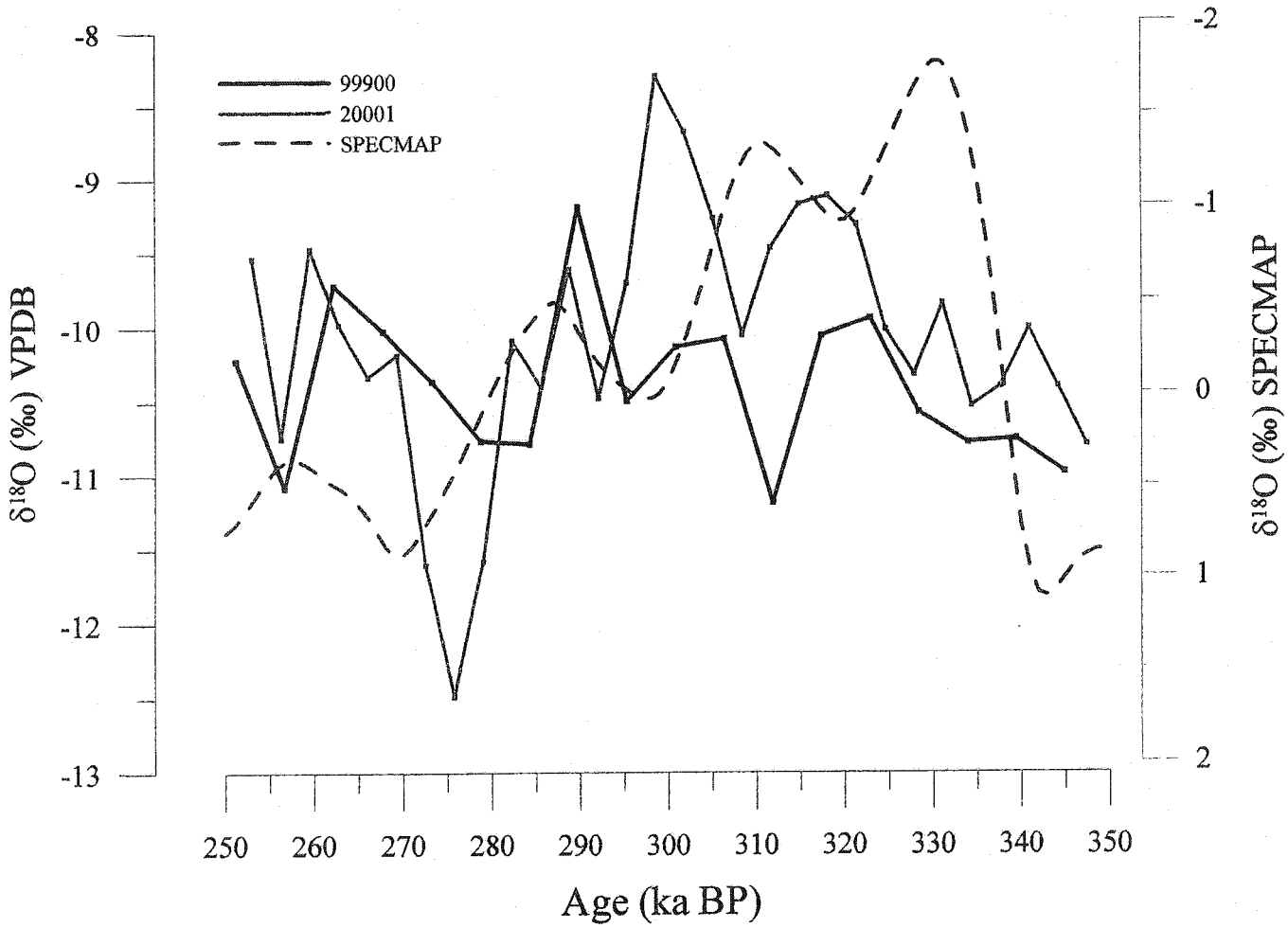

Figure 3.10. Oxygen isotope time series for samples 99900, 20001 and SPECMAP from 350 to 250 ka BP (Martinson et al. 1987).

8 respectively, consistent with $\gamma > 0$. Therefore the response of $\delta^{18}O_{ct}$ in sample 20001 is closely linked to the T-dependence of the isotopic composition of infiltrating waters. There is also evidence for a reduction in growth rate or long hiatus in 99900 at around 360 ka based on the presence of many light colored layers that can form due to evaporative effects from reduced infiltration and drip rates. The apparently weaker response to climate of the $\delta^{18}O_{ct}$ signal in 99900 after 360 ka BP may be due to changes in hydrology and drip rates. The growth rate for 99900 was very low after this date and sampling resolution may not have captured short-term oscillations in the record.

In summary, we see that the $\delta^{18}O_{ct}$ records of each of these three closely-spaced, and partly coeval samples are quite different. In general, they differ in two distinct respects: a) the average $\delta^{18}O$ values of one of the records (99901) is significantly offset (lower $\delta^{18}O$ values) than the averages of 99900 or 20001; b) the climate response of the three speleothems is different, and also varies within each speleothem through its depositional history.

The first of these effects we attribute to systematic differences in the proportion of spring snow-melt *vs* summer rain in the drip water feeding each speleothem; 99901 is dominated by winter precipitation, while 99900 and 20001 may be receiving feedwaters that represent an unbiased average of annual precipitation. The maximum offset between 99901 and 99900 approaches 6 ‰, which is a significant fraction of the current difference between winter and summer precipitation in this region of c. 15 ‰ [Rozanski et al, 1993].

The origin of changes in γ is less easily understood. It is especially difficult to understand how two coeval speleothems in the same passage of one cave can have γ values with opposite signs. We surmise that this also reflects some difference in the way in which winter *vs* summer precipitation contributes to the feedwater of each site, but in such a way that shifts from glacial to interglacial climate affect this difference in opposite ways. One obvious feature is that samples with $\gamma < 0$ must have drip waters with attentuated temperature dependence; this could reflect a dominance of recharge from one season only, as long as $\delta^{18}O$ of precipitation in that season had not changed markedly between glacial and interglacial stages.

3.6.2. Marine isotope stages 11 and 13

MIS 11, which spans an interval from 420 to 365 ka BP (Hayes et al. 1976) is a single well-defined peak in SPECMAP. In two of the Reed's Cave speleothems (99900 and 99901), this interglacial cycle is recognizable but marked by a complex series of shorter cycles with a period of about 10 ka (Figure 3.11). These rapid climate events are also present in European pollen records (Tzedakis et al. 1997). The major variations in the record at this time support theories of major climatic instability/disturbance. Scherer et al. (1998) suggest that there was a major ice sheet collapse during MIS 11, also consistent with the exceptionally high peak in the SPECMAP record of this interglacial. We might therefore expect a larger corresponding signal in the Reed's Cave speleothem records from MIS 11. The evidence of a sustained or more intense warming during this

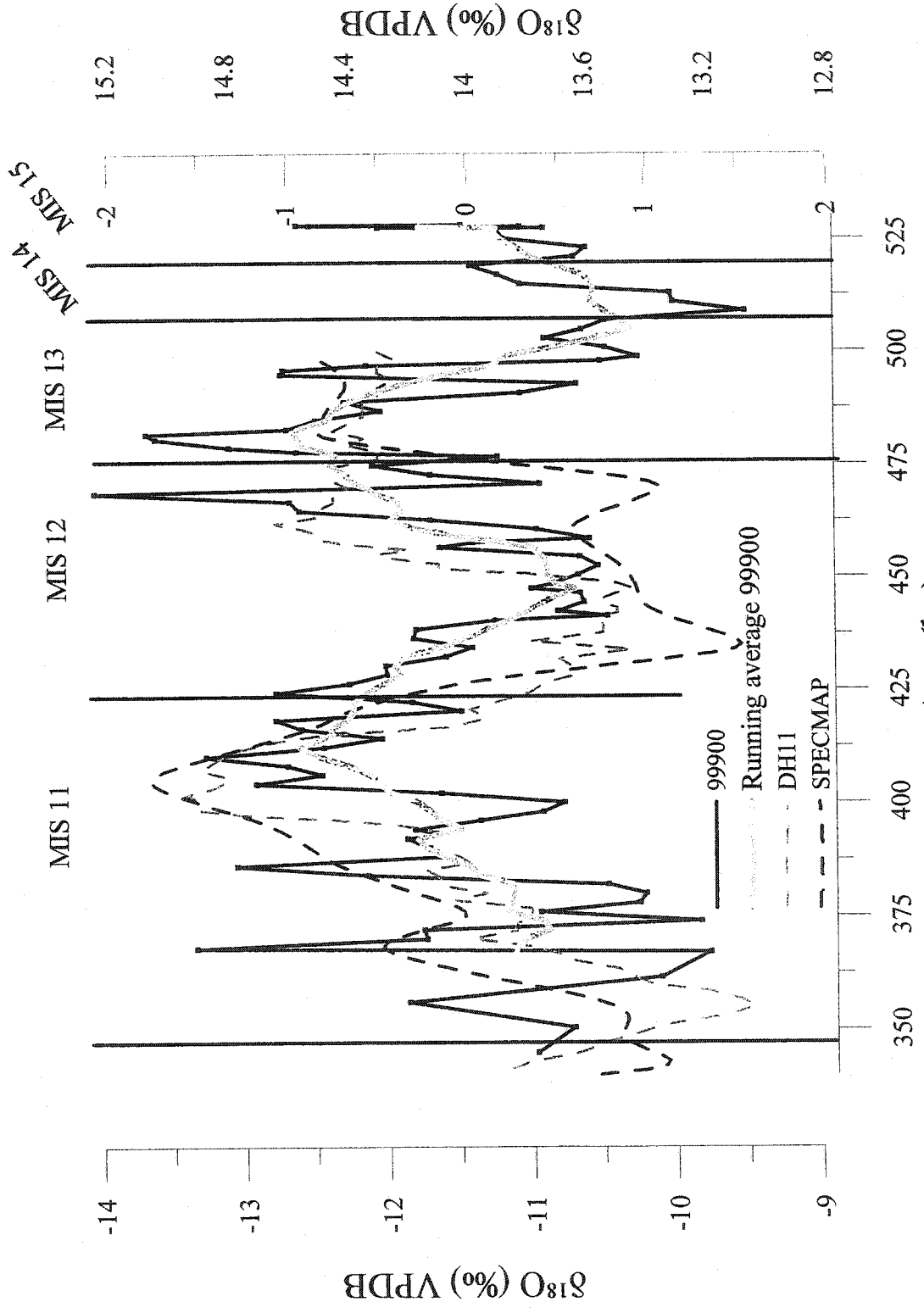

Figure 3.11. Oxygen isotope time series for sample 99900 and SPECMAP from MIS 15 to MIS 11.

time is not strikingly evident. The $\delta^{18}O_{ct}$ variations in samples 99900 and 99901 suggest an extended interval of warming that began at ~ 440 ka BP and lasted until approximately 370 ka BP. However a single well-defined peak in sample 99900 corresponding to MIS 11 contains large oscillations in $\delta^{18}O_{ct}$ values. The overall (average) decrease in $\delta^{18}O_{ct}$ confirms that terrestrial records are showing a period of warm climate at this time. The high variability in the oxygen isotope records for 99900 and 99901 are similar to high amplitude oscillations in European pollen sequences during MIS 11 (Tzedakis et al. 1997). It is evident that terrestrial records such as these show much more short-term variability than is seen in the marine $\delta^{18}O$ record; this may be in response to local fluctuations in continental climate on a millennial time scale.

Considering the record of MIS 13, Sample 99900 shows three peaks of enrichment in ^{18}O (Figure 3.11), which resemble three peaks of soil development with Chinese loess record (Vidic et al. in press). The climate signal for MIS 13 appears to be slightly warmer than for MIS 11 based on the greater enrichment in ^{18}O, which is the opposite of the trend in the marine isotopic records. This difference is shown more clearly in a graph of the moving average of $\delta^{18}O_{ct}$ of sample 99900 (Figure 3.11).

Thus, for both MIS 11 and 13, we see that, while the average response of $\delta^{18}O_{ct}$ for the Reed's Cave speleothems resembles that of the marine isotopic record, the speleothems also display higher-frequency cycles whose amplitude is a large fraction of the total glacial/interglacial difference.

3.6.3. Comparison to other proxy records

A comparison to limited speleothem results from the mid-Pleistocene shows synchronous response to climate. The Jewel Cave speleothem, JC 11, started growing prior to 700 ka BP and records similar magnitude of isotopic variation for the MIS 13, 11 and 9 interglacials (Ford et al., in preparation). The MIS 11 interval shows transitional events between the glacial and interglacial extremes of similar duration and magnitude (over 50% of interglacial/glacial $\delta^{18}O_{ct}$ change) to events in 99900. A speleothem record from Norway shows similar growth characteristics to those found in the Reed's Cave speleothems (Lundberg and Lauritzen 1999). The main periods of growth for the Norwegian speleothem LP-6 are placed at 502 ka BP and 420-380 ka BP. Reed's Cave sample 99900 grew from ~530 ka BP to 340 ka BP and 99901 grew from before 450 ka BP to 340 ka BP, after which there is likely a long period of growth cessation or multiple, shorter hiatuses. Very few other terrestrial deposits with absolute radiometric dates exist, with the exception of loess deposits dated by thermoluminescence (Little et al. 2002). The Russian and Chinese loess records have lower resolution than the speleothem $\delta^{18}O_{ct}$ and the timing of MIS 11 in particular is not synchronous with the SPECMAP stratigraphy (Vidic et al., in press, Little et al. 2002).

The Reed's Cave data shows a pacing of climate events similar to that seen in marine isotopic records, but they are more sensitive to local conditions and short-term events. Comparing all three speleothems to the SPECMAP marine $\delta^{18}O_{ct}$ records shows the more sensitive response of the $\delta^{18}O_{ct}$ records to local environmental and climate conditions at a higher time resolution (Figure 3.12). Sample 99900 shows significant local climate

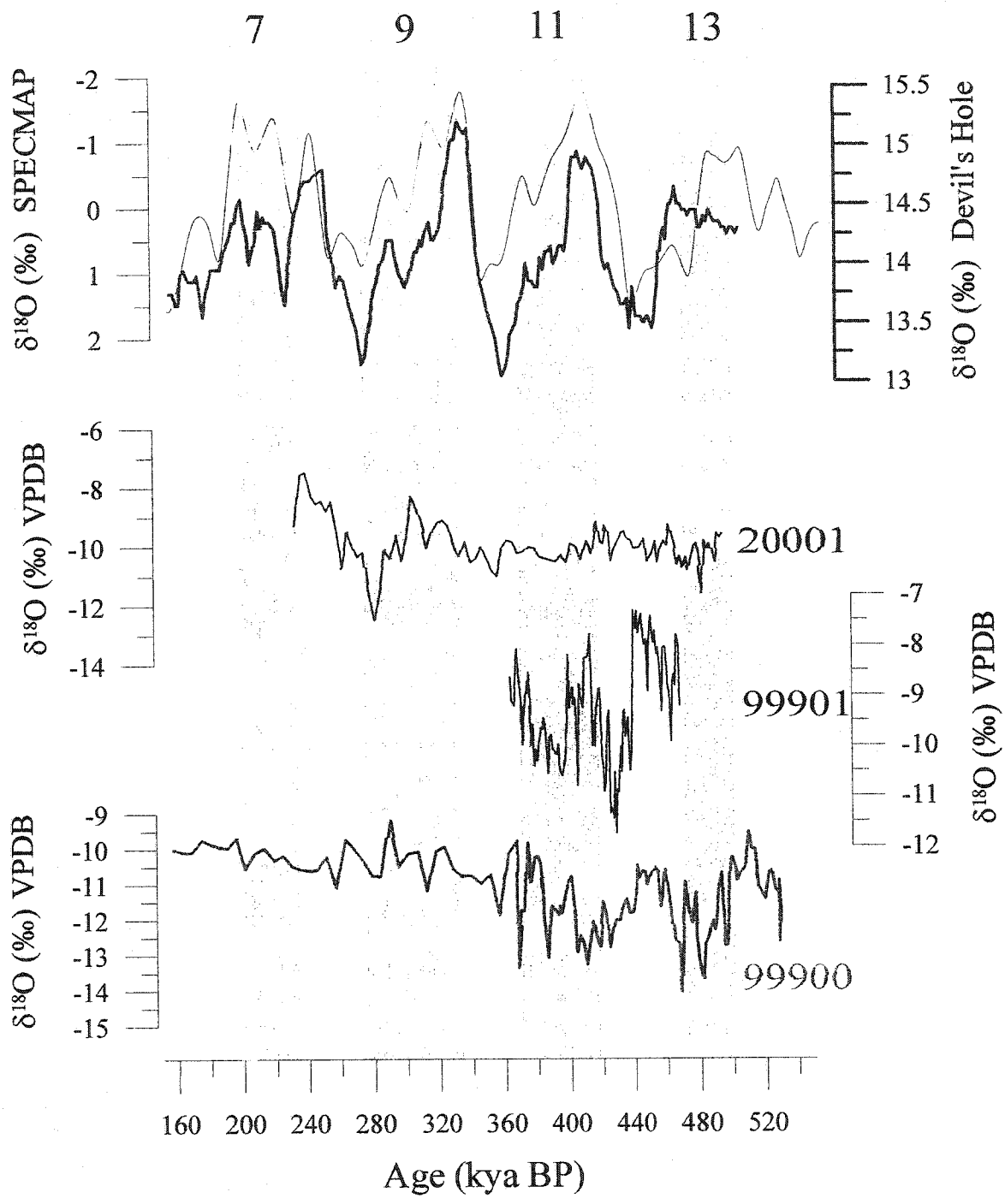

Figure 3.12. Oxygen isotope time series for samples 99900, 99901, 20001, SPECMAP and Devil's Hole (DH11).

events that interrupt the smoother 100-ka cycle that appear to be in the record but cannot be verified by spectral analysis. The 41 k periodicity in the SPECMAP record appears in the Reed's Cave speleothem record for sample 99901 (Figure 3.7). Also, the general agreement between moving average curves and SPECMAP records indicates that the 100 ka periodicity is also present in this record. More precise estimates of the duration of $\delta^{18}O_{ct}$ oscillations between the glacial and interglacial extremes cannot be determined without increased precision of dating and higher resolution isotope sampling.

3.7. CONCLUSION

Coeval records for three speleothems deposited in the mid-Pleistocene show that there can be different responses of $\delta^{18}O_{ct}$ to climate within one cave. A similar result was obtained for two Wisconsin age speleothems in Reed's Cave (Serefiddin et al., submitted, Chapter 2). This is likely due to heterogeneity in the overlying environment and the hydrology at time of deposition. Most striking is the strong negative correlation in samples 99900 and 99901 indicating the opposite climatic responses of $\delta^{18}O_{ct}$ in these two deposits. As well, we see differences in the average $\delta^{18}O_{ct}$ for coeval speleothems deposited in close proximity. This confirms that seasonality and local environmental conditions are a significant factor in the $\delta^{18}O_{ct}$ of speleothem calcite. These two stalagmites were deposited at adjacent locations in the cave, but with very different hydrology and sources. The catchment area for the source waters of the two speleothems may have been different as well, as seen in their reverse signs for gamma.

The climate record in the three speleothems shows a robust isotope response to the warming during MIS 13 and 11. The high resolution records show a very sensitive response in the central continent. The convergence of the Pacific, Arctic and Gulf of Mexico circulation systems in the center of the continent results in a dynamic response to global changes in climate. The isotopic variation can be magnified if there is a concurrent change in isotopic composition as well as shift in the source of storm tracks. Eventually δD data on fluid inclusions (Serefiddin et al., 2002) could be used to identify changes in source areas and for the calculation of paleotemperatures.

Without absolute paleotemperatures, it may not be possible to show the extent of warming during past interglacials. However, these isotope records show that MIS 13 and 11, at least were long but unstable periods of warmth as suggested by some researchers. There appears to be a somewhat greater magnitude of warming or climate reorganization during MIS 13 than MIS 11, contrary to the evidence from the marine record. It is most important to consider, however, that these isotope records are recording regional temperature change, so higher regional temperatures here may not reflect the global temperature change.

3.8. REFERENCES

Bar-Matthews, M., A. Ayalon, A. Kaufman, and G. J. Wasserburg. (1999). The eastern Mediterranean paleoclimate as a reflection of regional events; Soreq Cave, Israel. *Earth and Planetary Science Letters* **166**: 85-95.

Bauch, H. A., H. Erlenkeuser, J. P. Helmke, U. Struck, and J. W. Farrell. (2000). A paleoclimatic evaluation of marine oxygen isotope stage 11 in the high-northern Atlantic (Nordic seas). Marine isotope stage 11 (MIS 11); new insights for a warm future. *Global and Planetary Change* **24**: 27-39.

Bond, G. C., H. Heinrich, W. S. Broecker, L. D. Labeyrie, J. McManus, J. Andrews, S. Huon, R. Jantschik, S. Clasen, C. Simet, K. Tedesco, M. Klas, G. Bonani, and S. Ivy. (1992). Evidence for massive discharges of icebergs into the North Atlantic ocean during the last glacial period. *Nature (London)* **360**: 245-249.

Bradley, R. S. (1999). *Paleoclimatology: Reconstructing Climates of the Quaternary*. 2nd ed. San Diego: Academic Press. 1-613 p.

Bryson, R. A. (1966). Air masses, streamlines, and the boreal forest. *Geographical Bulletin* **8**: 228-269.

Dansgaard, W., Johnsen, S. J., Clausen, H. B., Dahl-Jensen, D., Gunderstrup, N. S., Hammer, C. U., Hvidberg, C. S., Steffensen, J. P., Sveinbjörnsdottir, A. E, Jouzel, J. and Bond, G. (1993). Evidence for general instability of past climate from a 250-kyr ice-core record. *Nature* **364**: 218-220.

Dorale, J. A. (2000). A high-resolution record of climate and vegetation change from Crevice Cave, Missouri during the last interglacial-glacial cycle. Unpublished PhD thesis, University of Minnesota, Minneapolis, Minnesota.

Dorale, J. A., L. A. Gonzalez, M. K. Reagan, D. A. Pickett, M. T. Murrell, and R. G. Baker. (1992). A high-resolution record of Holocene climate change in speleothem calcite from Cold Water Cave, Northeast Iowa. *Science* **258**: 1626-1630.

Frumkin, A., D. C. Ford, and H. P. Schwarcz. (1999). Continental oxygen isotopic record of the last 170,000 years in Jerusalem. *Quaternary Research* **51**: 317-327.

Gascoyne, M. (1992). Paleoclimate determination from cave calcite deposits. *Quaternary Science Reviews* **11**: 609-632.

Harmon, R. S., Gascoyne, M., and Schwarcz, H.(1999). Speleothem paleoclimatology; the present as a guide to the past. Geological Society of America (GSA), 1999 annual meeting, Denver, CO.

Hearty, P. J., P. Kindler, H. Cheng, and R. L. Edwards. (1999). A +20 m middle Pleistocene sea-level highstand (Bermuda and the Bahamas) due to partial collapse of Antarctic ice. *Geology (Boulder)* **27**: 375-378.

Hendy, C. H. (1971). The isotopic geochemistry of speleothem, 1. The calculation of the effects of different modes of formation on the isotopic composition of speleothems and their applicability as paleoclimatic indicators. *Geochimica et Cosmochimica Acta* **35**: 801-824.

Hodell, D. A., C. D. Charles, U. S. Ninnemann, and J. W. Farrell. (2000). Comparison of interglacial stages in the South Atlantic sector of the southern ocean for the past 450 kyr; implications for marine isotope stage (MIS) 11. *Global and Planetary Change* **24**: 7-26.

Imbrie, J. ; Berger, A. ; Boyle, E. A. ;Clemens, S. C. ; Duffy, A. ; Howard, W. R. ; Kukla, G. ; Kutzbach, J. ; Martinson, D. G. ; McIntyre, A. ; Mix, A. C. ; Molfino, B. ; Morley, J. J. ; Peterson, L. C. ; Pisias, N. G. ; Prell, W. L. ; Raymo, M. E. ; Shackleton, N. J. ; Toggweiler, J. R. (1993). On the structure and origin of major glaciation cycles; 2, The 100,000-year cycle. *Paleoceanography* **8(6)**: 698-735.

Kindler, P., P. J. Hearty, and J. W. Farrell. (2000). Elevated marine terraces from Eleuthera (Bahamas) and Bermuda; sedimentological, petrographic and geochronological evidence for important deglaciation events during the middle Pleistocene. *Global and Planetary Change* **24**: 41-58.

King, A. L. and W. R. Howard. (2000). Middle Pleistocene sea-surface temperature change in the Southwest Pacific Ocean on orbital and suborbital time scales. *Geology (Boulder)* **28**: 659-662.

Lauritzen, S. E. (1995). High-Resolution Paleotemperature Proxy Record for the Last Interglaciation Based on Norwegian Speleothems. *Quaternary Research* **43**: 133-146.

Li, W. -X., Lundberg, J., Dickin, A. P., Ford, D. C., Schwarcz, H. P., McNutt, R. and Williams, D. (1989). High-precision mass-spectrometric uranium-series dating of cave deposits and implications for palaeoclimate studies. *Nature (London)* **339**: 534-536.

Little, E. C., O. L. Lian, A. A. Velichko, T. D. Morozova, V. P. Nechaev, K. G. Dlussky, and Rutter.N.W. (2002). Quaternary stratigraphy and optical dating of loess from the east European Plain (Russia). *Quaternary Science Reviews* **21**: 1745-1762.

Lundberg, J. (1990). U-series dating of carbonates by mass spectrometry with examples of speleothem, coral and shell. Unpublished PhD thesis, McMaster University, Hamilton, Ontario.

Lundberg, J. and Lauritzen, S.-E. (1999). Isotope stages 11-13 from a North Norwegian speleothem; paleoclimate, vegetation, and fire traces. Geological Society of America (GSA), 1999 annual meeting, Denver, Colorado.

Martinson, D.G., Pisias, N.G., Hays, J.D., Imbrie, J., Moore, T.C. and Shackleton, N.J. (1987). Age Dating and the Orbital Theory of the Ice Ages: Development of a High-Resolution 0 to 300,000-Year Chronostratigraphy. *Quaternary Research* **27**: 1-29.

Mix, A. C., N. G. Pisias, W. Rugh, J. Wilson, A. Morey, T. K. Hagelberg, L. A. Mayer, T. R. Janecek, J. G. Baldauf, S. F. Bloomer, K. A. Dadey, K. C. Emeis, J. Farrell, J. A. Flores, E. M. Galimov, T. K. Hagelberg, P. Holler, S. A. Hovan, M. Iwai, A. E. S. Kemp, D. C. Kim, G. Klinkhammer, M. Leinen, S. Levi, M. A. Levitan, M. W. Lyle, A. K. MacKillop, L. M. Meynadier, A. C. Mix, T. C. Moore, Jr., I. Raffi, C. Ravelo, D. Schneider, N. J. Shackleton, J. P. Valet, E. Vincent, S. K. Stewart, and editor. (1995). Benthic foraminifer stable isotope record from Site 849 (0-5 Ma); local and global climate changes. Proceedings of the Ocean Drilling Program; scientific results; eastern Equatorial Pacific, covering Leg 138 of the cruises of the drilling essel JOIDES Resolution: 371-412.

Murray, R. W., C. Knowlton, M. Leinen, A. C. Mix, C. H. Polsky, J. W. Farrell, and editor. (2000). Export production and terrigenous matter in the central Equatorial Pacific Ocean during interglacial oxygen isotope stage 11. *Global and Planetary Change* **24**: 59-78.

Oppo, D. W., J. F. McManus, and J. L. Cullen. (1998). Abrupt climate events 500,000 to 340,000 years ago; evidence from subpolar North Atlantic sediments. *Science* **279**: 1335-1338.

Pisias, N. G., L. A. Mayer, T. R. Janecek, J. G. Baldauf, S. F. Bloomer, K. A. Dadey, K. C. Emeis, J. Farrell, J. A. Flores, E. M. Galimov, T. K. Hagelberg, P. Holler, S. A. Hovan, M. Iwai, A. E. S. Kemp, D. C. Kim, G. Klinkhammer, M. Leinen, S. Levi, M. A. Levitan, M. W. Lyle, A. K. MacKillop, L. M. Meynadier, A. C. Mix, T. C. Moore, Jr., I. Raffi, C. Ravelo, D. Schneider, N. J. Shackleton, J. P. Valet, E. Vincent, and S. K. Stewart. (1995). Proceedings of the Ocean Drilling Program; scientific results; eastern Equatorial Pacific, covering Leg 138 of the cruises of the drilling vessel JOIDES Resolution, Balboa, Panama, to San Diego, California, Sites 844-854, 1 May-4 July 1991. Proceedings of the Ocean Drilling Program, Scientific Results 138.

Poore, R. Z. and H. J. Dowsett. (2001). Pleistocene reduction of polar ice caps; evidence from Cariaco Basin marine sediments. *Geology (Boulder)* **29**: 71-74.

Rousseau, D. D., J. J. Puissegur, and F. Lecolle. (1992). West-European terrestrial molluscs assemblages of isotopic stage 11 (middle Pleistocene); climatic implications. *Palaeogeography, Palaeoclimatology, Palaeoecology* **92**: 15-29.

Scherer, R. P., a. Aldahan, S. Tulacyzk, G. Possnert, H. Engelhardt, and B. Kamb. (1998). Pleistocene collapse of the West Antarctic Ice Sheet. *Science* **281**: 82-85.

Schwarcz, H. P. (1986). Geochronology and isotope geochemistry in speleothems. In *Handbook of Environmental Isotope Geochemistry* (P. Fritz and J. Fontes, eds.), 271-303. Amsterdam: Elsevier Publishers.

Schwarcz, H. P., Harmon, R. S., Thompson, P. and Ford, D. C. (1976). Stable isotope studies of fluid inclusions in speleothems and their paleoclimatic significance. *Geochim. Cosmochim. Acta* **40**: 637-665.

Shackleton, N. J., M. A. Hall, D. Pate, L. A. Mayer, T. R. Janecek, J. G. Baldauf, S. F. Bloomer, K. A. Dadey, K. C. Emeis, J. Farrell, J. A. Flores, E. M. Galimov, T. K. Hagelberg, P. Holler, S. A. Hovan, M. Iwai, A. E. S. Kemp, D. C. Kim, G. Klinkhammer, M. Leinen, S. Levi, M. A. Levitan, M. W. Lyle, A. K. MacKillop, L. M. Meynadier, A. C. Mix, T. C. Moore, Jr., I. Raffi, C. Ravelo, D. Schneider, N. J. Shackleton, J. P. Valet, E. Vincent, S. K. Stewart, and editor. (1995). Pliocene stable isotope stratigraphy of Site 846. Proceedings of the Ocean Drilling Program; scientific results; eastern Equatorial Pacific, covering Leg 138 of the cruises of the drilling vessel JOIDES Resolution: 337-355.

Tzedakis, P. C., V. Andrieu, J. L. de Beaulieu, S. Crowhurst, M. Follieri, H. Hooghiemstra, D. Magri, M. Reille, L. Sadori, N. J. Shackleton, and T. A. Wijmstra. (1997). Comparison of terrestrial and marine records of changing climate of the last 500,000 years. *Earth and Planetary Science Letters* **150**: 171-176.

Tzedakis, P. C., V. Andrieu-Ponel, J. L. de Beaulieu, H. J. B. Birks, S. Crowhurst, M. Follieri, H. Hooghiemstra, D. Magri, M. Reille, L. Sadori, N. J. Shackleton, T. A. Wijmstra, and G. N. Thomas. (2001). Establishing a terrestrial chronological framework as a basis for biostratigraphical comparisons. *Quaternary Science Reviews* **20**: 1583-1592.

Viau, A.E., Gajewski, K., Fines, P., Atkinson, D.E. and Sawada, M.C. (2002). Widespread evidence of 1500 yr climatic variability in North America during the past 14,000 yr. *Geology* **30**:455-458

Vidic, N. J., Verosub, K. L., and Singer, M. J. *In Press*. The Chinese Loess Perspective on Marine Isotope Stage 11 as an Extreme Interglacial. AGU monograph series.

Winograd, I. J., Landwehr, J. M., Ludwig, K. R., Coplen, T. B., and Riggs, A. C. (1997). Duration and Structure of the Past Four Interglacials. *Quaternary Research* **48**: 141-154.

CHAPTER FOUR. RECORDS OF CLIMATE CHANGE IN CENTRAL AND WESTERN NORTH AMERICA FROM δD VARIATIONS IN SPELEOTHEM FLUID INCLUSIONS

4.1. INTRODUCTION

Speleothem isotope variations have been used as proxies for warming and cooling periods, moisture availability, monsoon activity and shifts in overlying vegetation regimes (Dorale et al. 1992, Gascoyne 1992, Hellstrom et al. 1998, Frumkin et al. 1999, Wang et al. 2001, Neff et al. 2001). The application of uranium-series disequilibrium dating gives these proxies high-precision chronological control (Schwarcz 1986, Dorale 2000). The interpretation of oxygen and carbon isotopic variations in speleothems remains rather problematic because local and regional environmental conditions can alter the global climate signal (Linge et al. 2001, Serefiddin et al. 2002, Schwarcz et al. submitted). The ratio of stable isotopes of hydrogen (δD) of fluid inclusions in speleothem calcite can be used to investigate changes in precipitation and calculate paleotemperatures as an additional proxy to refine climate models.

The objective of this research is to develop high resolution paleotemperature reconstructions for late Pleistocene North America. Modern dripwater and Holocene fluid inclusion samples will be compared to the speleothem records from the Wisconsin glacial period. Samples across North America will be used to cover a wide range of geographic, climatic and topographic regions. The results of this research can give quantitative information about temperature, air mass positions and give us a better

understanding of how ice sheet dynamics affects climate. A high resolution record of temperature change for the Black Hills of South Dakota will give insight on the extent of cooling in the mid-continent during the glacial period.

4.1.1. Previous fluid inclusion research with speleothems

During crystal growth speleothems can trap and preserve some of the original seepage water as fluid inclusions, providing a source of information on the past isotopic composition of precipitation. Fluid inclusions often comprise as much as 0.1 to > 1.0 wt % of a speleothem (Schwarcz et al. 1976). Pioneering research in the 1970's on speleothems found that δD of fluid inclusions were equivalent to surface precipitation waters (Schwarcz et al. 1976, Schwarcz and Yonge 1983, Yonge et al. 1985). Rozanski and Dulinski (1987) found similar results but their sample size was too large to give good high resolution data. Later researchers found a 20-30‰ offset in δD values when the water was removed by heating at temperatures over 800°C versus extraction at lower temperatures (Yonge 1982, Goede et al. 1986, 1990, Matthews et al. 2000). This offset was believed to be a result of fractionation occurring during the heating and extraction process. This offset could also be due to an additional component of highly fractionated water that is bound to the calcite lattice (Yonge 1982, Schwarcz, pers. comms.) Recent improvements on the extraction technique at the University of East Anglia gave results that attribute the offset to amount of water being extracted, but can be avoided if sufficient water is collected (Dennis et al. 2001). Thermal desorption of released water

from the crushed calcite at 150°C gives almost complete recovery of extracted water and showed negligible offset, so the water released in the high temperature experiments may be related to additional, structurally bound water.

4.1.2. Previous isotopic studies of meteoric water

The oxygen and hydrogen isotopes of precipitation show a strong relationship to temperature, amount of precipitation, distance from the ocean as well as relative influence of different North American air masses (Welker 2000, Rozanski et al. 1993 and 1992, and Gat 1980). In the Black Hills region the δD in precipitation varies seasonally from -70 to -102 ‰ while $\delta^{18}O$ varies from -10 to -14 ‰ (IAEA 2001). An important characteristic of North American air masses is the signature of source areas. Air masses derived from the Pacific Northwest have an oxygen isotopic composition of ~ -3 ‰ compared to -7 ‰ for Gulf of Mexico air masses. As the air masses move inland there can be a depletion up to 8 ‰ (Welker 2000). During the winter months, there is a trough in $\delta^{18}O$ isolines that represents more depleted meteoric waters in the Black Hills (Bryson 1966). This indicates an additional air mass with its source in the Arctic. The depletion can be as high as 15 ‰ (IAEA 2001). Modern studies of meteoric waters found a seasonal difference as high as 25 ‰ in the higher elevations of the Rocky Mountains (Welker 2000). Dansgaard (1964) and Rozanski et al (1993) calculated the global average seasonal temperature dependence of $\delta^{18}O$ in precipitation to be 0.69 ‰/°C.

However, this temperature dependence varies regionally; the value is as low as 0.1 - 0.3 ‰/C° for inland areas.

Corresponding temperature and regionally dependent shifts would occur in δD, as governed by the meteoric water line relationship to be $\delta D = 8\ \delta^{18}O + 10$ (Craig 1961, Dansgaard 1969). This is the global average for the relationship between deuterium and oxygen isotopes in precipitation. The slope and D-excess ($d_0 = 8\ \delta^{18}O - \delta D$) can change with location and over time (Rozanski et al. 1993, Merlivat and Jouzel 1979). This relationship is used to calculate $\delta^{18}O$ values from the measured δD in fluid inclusions. The δD of fluid inclusions can be used to show if these relationships remained constant throughout the Quaternary or if they differed during the glacial times as indicated by earlier studies (Schwarcz and Yonge 1983, Jouzel et al. 1982).

4.1.3. Paleotemperature reconstructions using fluid inclusions

When calcite forms in oxygen isotopic equilibrium with water, we can calculate the temperature of formation from the isotopic fractionation, $\alpha_{c\text{-}w}$, between calcite and water, where $\alpha_{c\text{-}w} = (^{18}O/^{16}O)\text{calcite}/(^{18}O/^{16}O)_{water}$. The calculation of paleotemperatures using the O'Neil *et al.* (1969) calcite-water fractionation equation

$$1000 \ln \alpha_{c\text{-}w} = 2.78 \times 10^{-6} \times T^{-2} - 2.89 \qquad (4.1)$$

requires knowledge of the $\delta^{18}O$ of the drip water from which the speleothem was precipitated. We assume that this is equal to the initial $\delta^{18}O$ of fluid inclusions trapped in the speleothem. Although these fluid inclusions can be analyzed for both $\delta^{18}O$ and δD,

$\delta^{18}O$ is not used because the isotopes of the calcite and the water may have exchanged following deposition of the speleothem. Instead, we calculate the initial $\delta^{18}O$ value of the trapped water from its measured δD, using the appropriate meteoric water line for the period in which the sample grew.

Estimation of absolute paleotemperatures using oxygen isotope variation in calcite alone has had some success (Goede et al. 1986, 1990; Dorale et al. 1992, Dorale et al. 1998, Gascoyne 1992, Lauritzen and Lundberg 1999). Early attempts at calculations using $\delta^{18}O_w$ calculated from δD of fluid inclusions gave negative temperatures, which is impossible because speleothems cannot form in freezing conditions when water cannot infiltrate the subsurface (Harmon et al. 1979). This suggested that the meteoric water line relationship was likely different in the past glacial periods. In a more recent study, Genty et al. (2002) measured δD in large fluid-filled voids in a speleothem and calculated a -1.3 °C temperature difference from modern for a growth layer in a French speleothem dated at 100 ka. The $\delta^{18}O$ of fluid inclusion water was calculated using the measured δD and local meteoric water line relationship $\delta D = 8\delta^{18}O + 7.7$ (Genty et al. 2002). The growth layer grew during marine isotope substage 5c, a period in the interglacial that appears to have been slightly cooler than present (Martinson et al. 1987 and Jouzel et al. 1987). Late Holocene records from Great Britain show isotopic composition of fluid inclusion waters that are not significantly different from modern drips (Dennis et al. 2001).

4.2. METHODS

The speleothems were dated using uranium-series disequilibrium dating techniques (Schwarcz 1986, Dorale 2000). Crushed or powered calcite samples ranging from 200 mg for multi-collector inductive coupled plasma mass spectrometry (MC-ICPMS) analysis to 2 g for thermal ionization mass spectrometry (TIMS) were prepared by anion exchange chemistry in the McMaster clean laboratory, with the addition of a $^{229}Th/^{236}U$ spike calibrate by J. Lundberg, Carleton University. The extracted uranium and thorium components are run by single and double filament technique on a VG 354 TIMS at McMaster or on the VG MC-ICPMS at GEOTOP in Montreal. For thermal ionization mass spectrometry (TIMS), uranium and thorium are loaded on rhenium and tantalum filaments and analyzed in a VG354 mass spectrometer; the ratios of $^{234}U/^{238}U$ and $^{230}Th/^{234}U$ are used to determine the age. The precision of measurements averages 1%. For analysis of U and Th by MC-ICPMS, the elements are introduced into the instrument dissolved in 1% nitric acid. The advantage of MC/ICP-MS is faster throughput and higher precision (< 0.5%).

The extraction of fluid inclusions employs equipment developed at the University of East Anglia Isotope Lab (Dennis et al. 2001). The crushing cell consists of the crushing chamber and a piston that is moved using an electromagnet (Figure 4.1). The base and tower of the cell are fitted with heaters for the removal of water before the sample is crushed to remove any atmospheric water vapor that may be present.

Slices of calcite were taken along growth layers with a maximum thickness of 5mm using a low speed Isomet diamond wafer saw. At least two samples were cut from

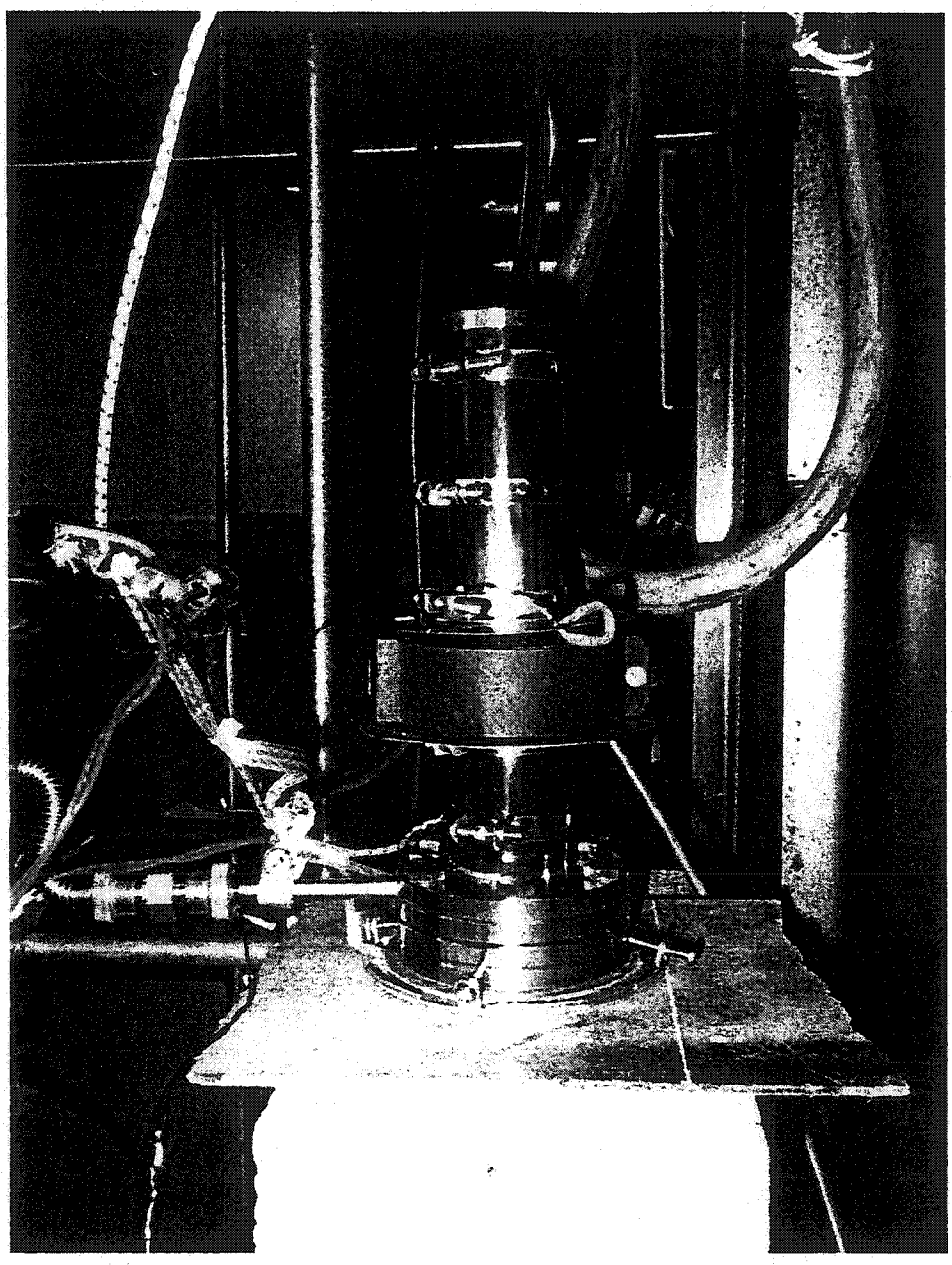

Figure 4.1. Crushing cell for extraction of fluid inclusion water.

each growth layer for repeat analyses. A portion of the slice weighing approximately 500 - 1000 milligrams is loaded into the cell and evacuated to a high vacuum. After the sample had been evacuated and heated at 100 °C for 15 minutes, it was gently crushed for 15 minutes by repetitive motion of the piston. During this time the crushing cell was closed off from the high vacuum pumps and opened to the U-trap (Figure 4.2). A dewar of liquid nitrogen was placed under the U-trap to collect the water and CO_2 released during crushing. After crushing, the cell was heated to 150 °C under vacuum to remove all adsorbed water. After heating is complete the U-trap temperature is increased to –120 °C to release any CO_2 which is pumped away. The cold trap is then warmed to room temperature and water is trapped in a pyrex tube together with 50 mg of zinc shavings ("Indiana Zn"). The water is later reduced by reaction with zinc at 500 °C for 1 h and the hydrogen gas is analyzed on a SIRA II mass spectrometer against H_2 from a laboratory standard (DTAP). The absolute δD values are calculated using the VSMOW and VSLAP reference waters for calibration. The precision of measurements of the standard is 0.11 ‰. A portion of the crushed calcite was reserved for analysis of $\delta^{18}O_{ct}$.

The volume of water in each calcite sample was estimated from the intensity of the major beam (^2H signal). Capillaries containing known masses of water were used to create a calibration curve. Samples that gave an intensity of less than 5.0×10^{-5} indicated less than 0.5 µl of water; these data were not used because they were most likely fractionated during extraction (Dennis et al. 2001).

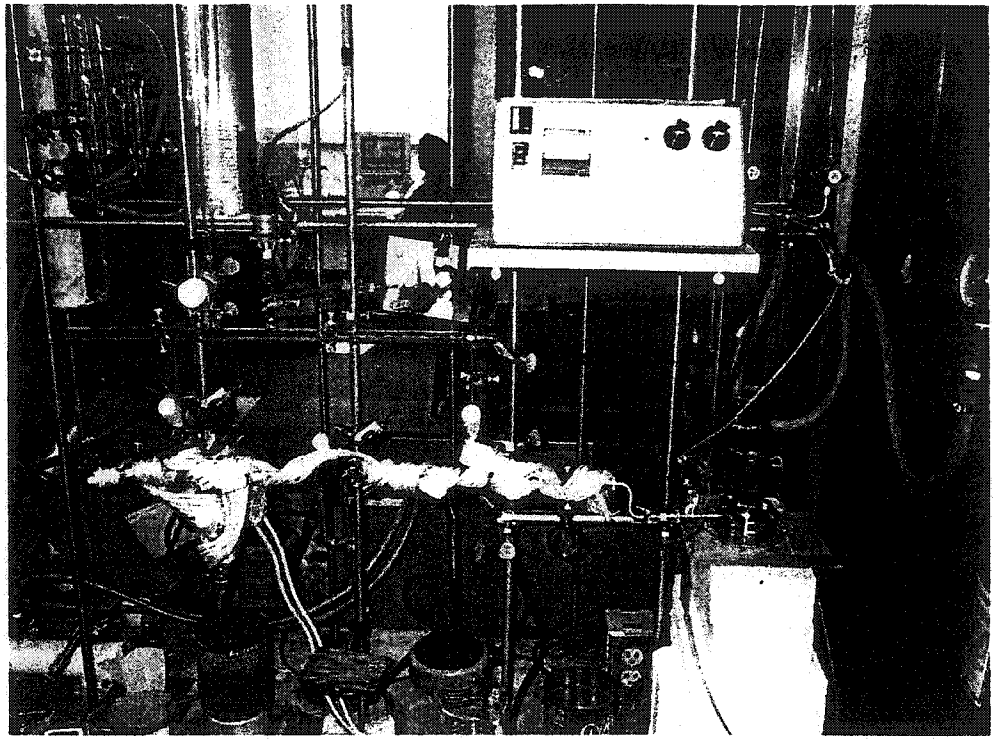

Figure 4.2. Vacuum line for collection of fluid inclusion water.

4.2.1. Samples

Samples were prepared for fluid inclusion analysis to evaluate δD and temperature variability during the Wisconsin glacial period from Reed's Cave, South Dakota and throughout multiple sites in western North America for the Holocene period (Figure 4.3). Additional samples from Austria and Israel were analyzed to investigate different climate regimes. In an attempt to produce high resolution records, sample size was reduced to ~1 g or less.

Speleothems 99902 (RC2) and 20000 (RC20) are two samples from Reed's Cave, South Dakota that partly grew at the same time, from 62 to 49 ka BP. These speleothems have partly divergent $\delta^{18}O_{ct}$ records but each appears to be recording climate, (Serefiddin et al. 2002). The analysis of the δD and paleotemperature calculations can test whether similar temperatures are being recorded by these two speleothems. Time resolution for each measurement ranges from 200 years during fast growth to 6300 years during slow growth for sample 99902. The faster growing speleothem 20000 has a time resolution ranging from 50 years to 690 years.

Last and modern interglacial speleothems from Rat's Nest Cave, Southern Canadian Rockies and Vanishing River Cave, Santa Cruz were analyzed to investigate temperature gradients in western North America. The two caves are from geographically distinct areas and should show differences in the paleotemperatures. Speleothem VR-1 from Santa Cruz grew from 8.5 to 0.5 ka BP in at sea level in a marine Mediterranean climate zone. The translucent, brown calcite has dissolution pockets containing clay

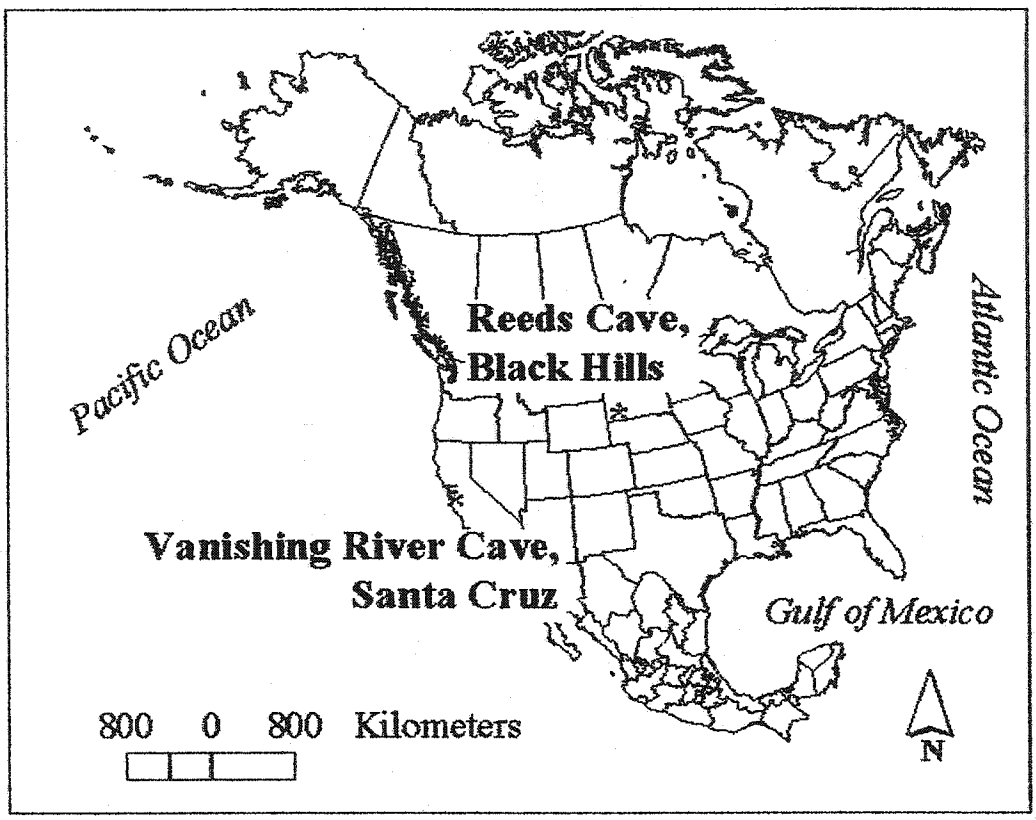

Figure 4.3. Site map showing location of Reed's Cave in the Black Hills of South Dakota and Vanishing River Cave in Santa Cruz on central California Coast.

detritus. These areas were avoided when preparing the samples. The oxygen isotope record shows very little variation (Holden et al, unpublished). The sample size averaged 5mm thick and averaged 300 years of growth. A minimum of two samples were taken from each growth layer, with a third cut if there was enough sample available. Eight samples from Rat's Nest Cave sample 881020 were taken for fluid inclusion extraction. Rat's Nest Cave is located in the southern Canadian Rockies at an elevation of 2000 m in a subalpine/alpine climate zone. The calcite in sample 881020 is an opaque, white color with palisade crystals. Inspection of individual crystals reveals a more translucent color, which indicates low fluid inclusion content. The ages for speleothem 881020 are not well constrained so no estimate was made for temporal resolution.

4.3. RESULTS

4.3.1. Tests of the procedure

Calibration of the crushing cell and vacuum line was done by measurements of DTAP standard water in glass capillaries alone and with Iceland spar following the procedure of Dennis et al. (2001). The reproducibility of samples was tested by analyzing replicates of the laboratory standard water, DTAP, in capillaries, together with 500 to 1000 mg pieces of Iceland Spar (MEXIS). Fourteen MEXIS samples were prepared but 3 samples produced transducer readings that indicated they were fractionated during transfer due to incomplete recovery or desorption (Table 4.1). The 11 remaining samples gave an average δD value of -61 ± 9‰ with a range of -49 to

Table 4.1. Results of standards analyses.

Sample ID	δD (‰) VSMOW	intensity	Measured water volume (μL)
Laboratory standard water			
DTAP*	-57.58		
Standard water filled capillary			
CAP-2	-54.17	n/a	2.0
Standard water filled capillaries run with Iceland Spar			
MEXIS-1	-56.58	n/a	2.0
MEXIS-4	-66.93	n/a	1.0
MEXIS-5	-61.37	1.61E-09	1.0
MEXIS-7	-58.10	6.82E-10	0.5
MEXIS-8	-98.87	4.00E-10	0.5
MEXIS-9	-49.06	3.30E-09	2.0
MEXIS-10	-53.71	1.66E-09	1.0
MEXIS-11	-66.66	n/a	
MEXIS-14	-106.92	n/a	1.0
MEXIS-15	-68.22	1.01E-09	1.0
MEXIS-17	-7.20	n/a	0.5
MEXIS-18	-75.74	7.94E-10	0.5
MEXIS-20	-77.13	n/a	1.0
MEXIS-21	-59.26	2.10E-09	1.0

*mean values for 60 samples

-77‰. The difference from the mean ranges from 2‰ to 14‰. The average δD agrees with δD value for DTAP (laboratory standard) of -58 ± 4‰. The slightly depleted average value of -61 ± 9 ‰ may result from fractionation effects from incomplete desorption of water from the calcite powder.

As another test of reproducibility of the method, sixteen growth layers of speleothems from Reed's Cave were analyzed in replicate, by analysis of slices taken as close as possible to the same level in the stalagmite. From the eleven layers which had sufficient water for isotopic analyses, four of these results agreed within the typical analytical error of 3 ‰ (Table 4.2). Groups of replicates are identified in the tables by color. Sample codes begin with the abbreviation for the speleothem (RC2 for sample 99902 and RC20 for sample 20000) and followed by an identification number for the layer number or height from base. Overall, the difference between replicate analyses ranges from 1 to 27 ‰. Two possible reasons for this are: a) incomplete recovery of water, resulting in isotopic fractionation; b) non-equivalence of the supposed replicates such that different growth periods are being averaged. Figure 4.4 shows the cross section of samples 99902 and 20000, where it is clear that a sample taken near the outer perimeter of the stalagmite may contain thousands more years of growth than a sample from the main growth axis. Results from adjacent growth layers show average differences which is comparable to estimate of reproducibility from analyses of crushed capillaries of water of less than 10‰.

Table 4.2. Fluid inclusion sample results.

Sample ID	δD (‰) VSMOW*	intensity*	Calculated volume (μL)*	Sample weight/g	$H_2O/CaCO_3$ (mg/g)*
RC20_0.6.7a	-150.27	n/a		1.02	
RC20_0-6.7	-120.45	4.09E-10	0.40	0.96	0.42
RC20_0-6.7b	-105.61	3.34E-10	0.36	0.45	0.82
RC20-174.25	-124.95	6.36E-10	0.52	0.57	0.93
RC20-174.25A	-117.60	6.47E-10	0.53	0.89	0.59
RC20-183.5	-99.04	4.09E-09	0.76	0.93	0.81
RC20-183.5A	-94.22	4.13E-09	0.84	1.25	0.67
RC20-183.5AS	-86.15	4.03E-09	0.75	0.71	1.05
RC20-33a	-82.71	1.99E-09			
RC20-33a	-109.97			0.56	
RC20-33a2	-92.84	7.13E-10	0.56	0.49	1.42
RC20-35	-64.98	3.13E-09			
RC20-35a	-120.48	6.50E-10			
RC20-35b	-82.90	3.01E-09			
RC20-40	-64.90	8.22E-10	0.62	1.06	0.59
RC20-40a	-98.98	7.51E-10	0.58	1.06	0.55
RC20-40B	-123.76	8.64E-10	0.64	0.52	1.24
RC20-41a	-122.84	5.70E-10	0.49	0.59	0.83
RC20-41b		1.03E-10	0.24	0.64	0.38
RC20-41c	-121.88	5.37E-10	0.47	0.78	0.61
RC20-42		7.14E-10	0.57	0.88	0.65
RC20-42a		3.60E-11	0.21	0.78	0.26
RC20-42b		4.40E-11	0.21	0.90	0.23
RC20-42c		4.03E-11	0.21	0.50	0.42
RC20-43				0.62	
RC20-43a				0.58	
RC20-44				0.78	
RC20-44a				0.82	
RC20-93.35	-114.37	3.53E-09	2.06	1.24	1.67
RC20-93.35A	-73.55	4.17E-09	2.40	1.21	1.98
RC20-93.35B	-116.75	9.12E-10	0.67	1.48	0.45
RC2-1	-122.07	8.90E-10	0.66	0.32	2.03
RC2-10OUT	-93.65	5.79E-09			
RC2-2&3IN	-104.06	1.03E-09	0.73	0.58	1.27
RC2-2&3OUT		6.26E-11	0.22	0.34	0.64
RC2-34OUT	-74.81	1.40E-09			
RC2-35	-93.73	5.67E-10			
RC2-35a	-73.67	5.76E-10			
RC2-4&5IN	-91.56	2.01E-09	1.25	0.41	3.04
RC2-4&5OUT	-82.75	8.49E-10	0.64	0.43	1.49
RC2-6&7IN		2.41E-10	0.51	0.55	0.93
RC2-6&7OUT	-108.16	9.47E-11	0.69	0.23	2.99
RC2-91	-39.87	2.96E-09	1.76	0.54	3.27
RC2-9OUT	-66.90	2.99E-09	1.77	0.45	3.97

Table 4.2. Fluid inclusion sample results.

Sample ID	δD (‰) VSMOW*	intensity*	Calculated volume (μL)*	Sample weight/g	$H_2O/CaCO_3$ (mg/g)*
RC2-OL-1	-129.37	2.88E-10	0.34	0.33	1.04
VR-1-13	-68.67	8.62E-10	0.64	1.10	0.58
VR-1-13a	-29.29	3.32E-09	1.95	0.85	2.29
VR-1-2	-22.69	7.84E-10	0.60	0.85	0.71
VR-1-24	-29.75	2.37E-09	1.44		
VR-1-25a	-36.49	8.01E-10	0.61	1.01	0.60
VR-1-26-1	-55.38	6.18E-10	0.51	1.07	0.48
VR-1-26-2	-46.88	6.25E-10	0.52	1.04	0.50
VR-1-27	-44.14	1.09E-09	0.76	0.98	0.78
VR-1-27a	-40.86	2.25E-09	1.38	0.70	1.98
VR-1-27b	-73.30	4.13E-10	0.41	0.44	0.93
VR-1-3	-55.40	4.53E-10	0.43	0.59	0.73
VR-1-4	-54.81	3.80E-10	0.39	0.82	0.48
VR-1-5a	-51.70	5.69E-10	0.49	0.70	0.70

*All missing data results from insufficient sample size - sample was too small to run or too small to produce dD value

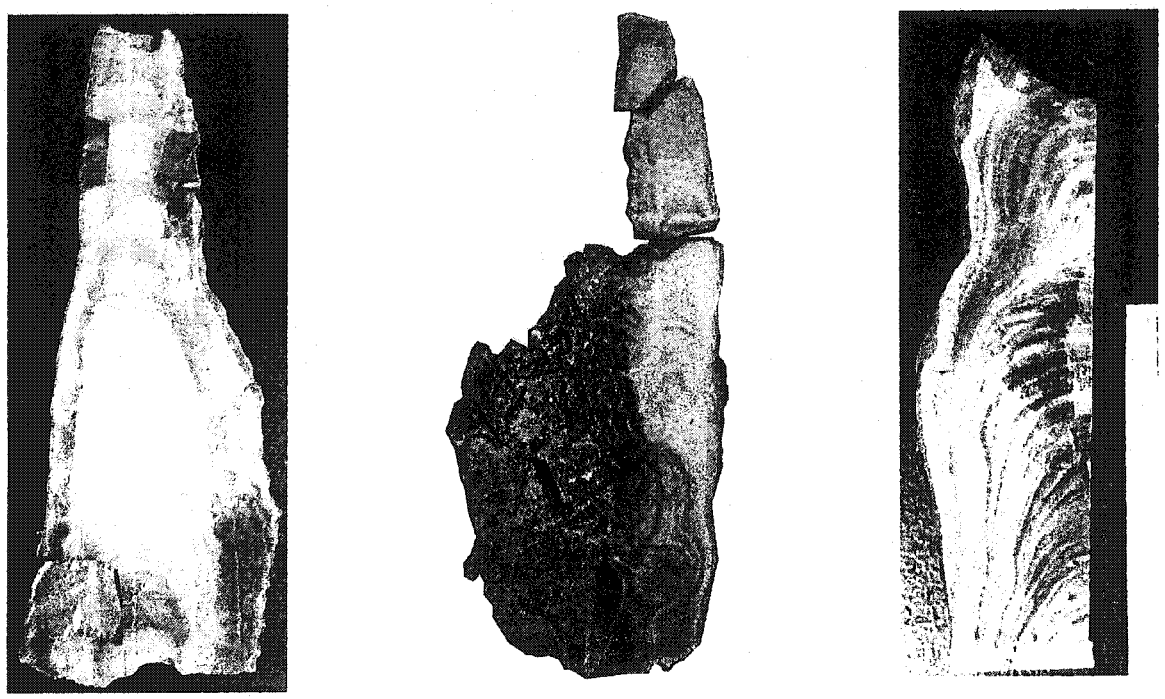

a b c

Figure 4.4. a) Reed's Cave 20000, b) Reed's Cave 99902 and c) Santa Cruz VR-1

To determine if leaks of atmospheric water vapor would contaminate samples, we attempted to collected water from the line without bringing the crushing cell and pyrex line down to vacuum. Three attempts failed to result in a measurable amount of water. We conclude that any small leaks had no effect on the isotopic values of collected water.

δD analyses can be offset if the proper zinc:water ratio is not used: the recommended ratio is of 50 mg Zn to 1 μL of water. We assume that the maximum water content of the speleothem is 0.1 wt %, and with a yield close to 100%, the sample sizes averaging 500 mg to 1g will give us extracted water volumes from 0.5 to 1.0 μL. We ran capillaries filled with 0.5 μL and 1.0 μL of DTAP water with 40 mg, 50 mg and 60 mg of zinc. These quantities gave reproducible and accurate results using standards of DTAP as small as 0.5 μl in capillaries with Iceland spar.

4.3.2. Analyses of speleothems

Sample weights ranged from 0.27 to 1.48 g. The number and volume of fluid inclusions varied between the growth layers so the wt % of water varied somewhat with sample size (Table 4.2). The results of δD analyses for the crushed calcite samples includes only the samples that were large enough to run on the mass spectrometer. Typically, samples less that 0.5 μl in size were too small for isotopic analysis. Of the 78 samples that were crushed and transferred to the zinc tubes, only 62 had enough water to collect δD data.

4.3.2.1. Reed's Cave, South Dakota

Cave dripwaters were sampled to determine spatial variation throughout the cave and whether there was a distinct seasonal signal in the isotopic composition of these waters. Results from oxygen and hydrogen analyses show a variation of up to 36‰ in the δD values and 5‰ in the $\delta^{18}O$ for drips (Table 4.3). This seasonal variation is well within the range expected for mid-continental precipitation (Rozanski et al. 1993). The range from -75 to -117 ‰ generally agrees with range of -70 to -102 ‰ (estimated from GNIP maps) of modern precipitation in this area, with cave drips slightly more depleted than the minimum of ~ -102 ‰ for precipitation. The more ^{2}H enriched waters in the range from -81‰ to -90‰ are found in samples that were collected from cave popcorn, an evaporative speleothem feature. These areas of the cave likely have less than 100 % humidity, which makes the waters unsuitable for study of equilibrium deposits. The modern drip water samples collected from the location of Wisconsin age speleothem samples 99902 and 20000 have a range of δD from -97 to -117 ‰ and $\delta^{18}O$ of -10.3 to -15.3‰ and falls slightly below the global meteoric water line (MWL) (Figure 4.5). The local MWL calculated from drip water at the sample sites in the cave is $\delta D = 8.0\ \delta^{18}O + 6.7$. This is within the expected range for mid-continental site in North America.

Forty-five samples from the two speleothems were crushed. Of these, 34 gave δD values, while 11 failed due to insufficient quantities of water. The average δD for the 34 samples is -97 ± 4 ‰ with a minimum value of -150 ‰ and a maximum value of -35 ‰ (Table 4.2). $\delta^{18}O$ values were calculated using the modern MWL and a hypothetical

Table 4.3. Results of dripwater analyses from Reed's Cave and Santa Cruz samples

SampleID	δD (‰) VSMOW	$\delta^{18}O$ (‰) VSMOW
Reed's Cave		
A1	-94.36	-11.85
A13	-99.77	-12.43
A34	-90.00	-12.42
A35	n/a	-12.21
A36	-81.09	-11.09
A45	-89.96	-12.23
A55	-103.21	-13.94
A63	-91.70	-12.05
A95	-94.13	-13.02
CCTR_82601	-90.11	-12.40
D65	-96.57	-12.68
NF-3_82601	-75.18	-10.35
NF-6	-93.48	-12.14
NF-12	-99.86	-13.25
NF-15	-117.02	-15.33
NF-18	-100.74	-13.59
NF-20	-105.48	-13.94
NF-20B	-102.22	-13.59
NF-20H1	-101.13	-13.58
NF-20H2	-102.16	-13.68
NF-33	n/a	-14.37
NFM-2	-108.70	-13.96
NFP-1	-98.93	-13.30
NFP-2	-99.51	-13.42
NFR-2	-96.76	-11.64
OM-20-3	n/a	-11.67
OM-20-4	-84.58	-11.87
RC-1	-88.76	-12.83
RC-2	-95.41	-12.19
RC-3	-90.18	-11.72
RC-5	-92.64	-12.30
RC-6	-90.00	-11.19
RC-7	-93.77	-12.29
RC-8	-84.75	-10.96
RC-9	-92.43	-11.86
RC-10	-95.36	-8.67
RC-13	-87.78	-11.12
SC-1	-101.67	-13.27
SC-3	-98.49	-12.79
TWC_82601	-111.41	-15.07
*Santa Cruz**		
VL-0-1	-38.22	-5.43

Table 4.3. Results of dripwater analyses from Reed's Cave and Santa Cruz samples

SampleID	δD (‰) VSMOW	$\delta^{18}O$ (‰) VSMOW
VL-0-1a	-36.46	-
VL-0-1b	-35.24	-
VL-0-1c	-38.46	-
VL-0-1d	-35.82	-
VL-0-1e	-34.30	-
VL-0-1f	-32.91	-

*only one oxygen analysis

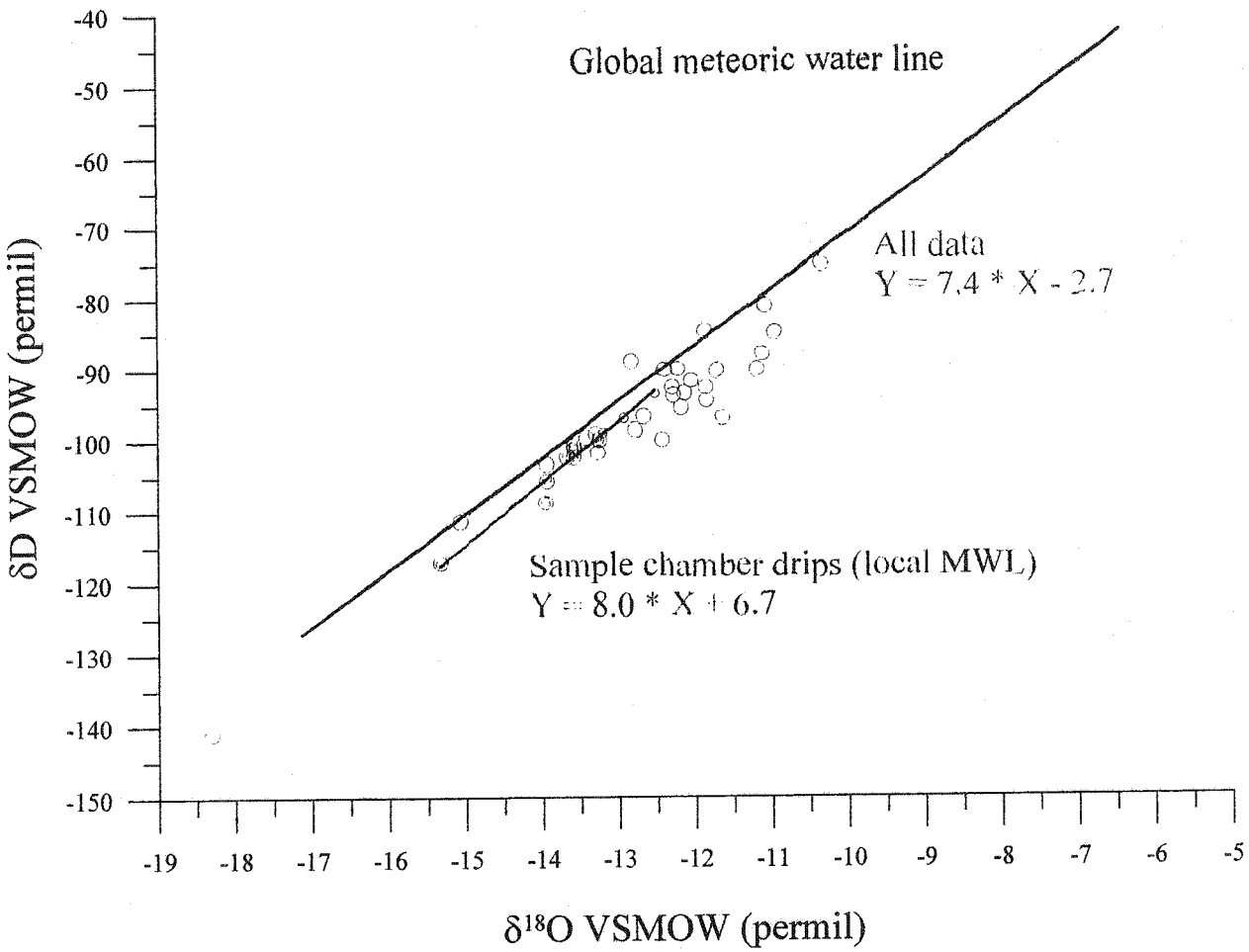

Figure 4. . δD and $\delta^{18}O$ of modern dripwaters plotted with global MWL.

glacial age MWL with $d_0 = 0$. Five samples with volumes less than 0.5 μL may have been fractionated during transfer of water from crushing cell to the zinc-filled pyrex tube.

4.3.2.2. Santa Cruz, CA

The 13 samples from the Santa Cruz speleothem give a mean δD of -47 ‰, with a range from -73 to -23 ‰ (Table 4.2). The mean value for modern cave drips is 37 ±1 ‰ from five repeat analyses of drips from one site. We would expect to see a similar average throughout the Holocene period. The full range of 51 ‰ for δD values from fluid inclusions is much higher than expected. $\delta^{18}O$ values were calculated using the global MWL and estimated local MWL. Two to three samples were run for each slice due to the larger diameter central growth axis for this speleothem (Table 4.2, Figure 4.4c). The difference between replicates done for 3 growth layers is 1‰, 9‰ and 40‰. This is also attributed to the problems described in the previous section, yet shows evidence of good reproducibility. It reemphasizes the requirements for careful sample cutting along the main axis of the growth layers.

4.3.2.3. Other sites

We also analyzed eight samples extracted from Rat's Nest Cave speleothem 8881020 and four samples from sample AF12 obtained from a cave in Jerusalem, Israel. None of these samples yielded sufficient water for analysis. Samples from other caves in Israel have been problematic due to small amounts of water (McGarry et al. 2002).

4.3.3. Variation in δD

The δD results clearly show that extraction and measurement of fluid inclusion water is very difficult. Preliminary results give some reproducible data and result in calculated temperature shifts that can be correlated with other proxy records. Analysis of small samples may also lead to unaccountable errors in δD values.

Atmospheric circulation patterns control relative contributions of moisture sources of different isotopic signatures to different regions (Charles et al. 1994, Nativ and Riggio 1990). The isotopic compositions of storm tracks in the Black Hills are determined by the relative contribution of Pacific and Gulf of Mexico air masses; the position of these air masses differs seasonally as well over long-term periods. There appears to be a good connection between the trajectory of these air masses and the isotopic composition of precipitation.. Measured δD values from fluid inclusions can give information on how the position of these air masses may have been different in the late Pleistocene although it may be difficult to distinguish these from temperature effects. The seasonal bias in the isotopic composition of recharge feeding different drip sites is likely controlled by some combination of both variables. More depleted values of δD may indicate a dominance of more depleted air masses as well as lower temperatures.

The δD values for the Reed's Cave speleothems show a range of values less than the estimated range for seasonal variation in $\delta^{18}O_{ppt}$ (Figure 4.6). The average δD value for sample 20000 is consistently lower than for sample 99902, even during coeval periods of growth. A previous paper (Serefiddin et al. 2002, Chapter 2) showed a similar difference in average $\delta^{18}O_{ct}$ values for these two samples and attributed this difference to

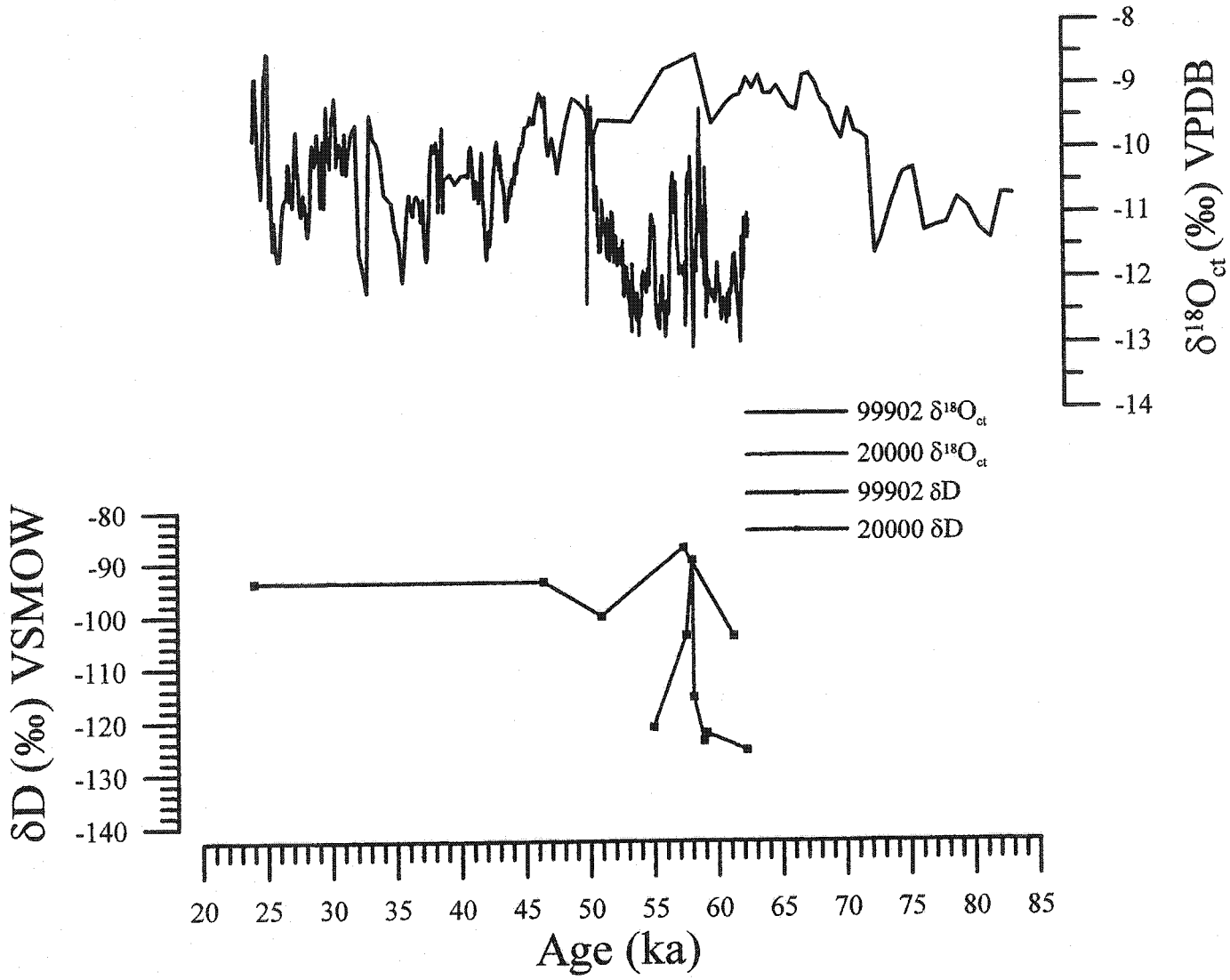

Figure 4.6. Comparison of $\delta^{18}O_{ct}$ records for samples 99902 and 20000 and δD from fluid inclusions (Table 4.2).

seasonality of recharge of drip waters (Chapter 2). Sample 20000 was likely formed from drips biased to winter precipitation (Chapter 2). This also explains the lower δD values. The range of δD values for sample 20000 is -65 to -150 ‰, more depleted than range of δD for sample 99902 of -40 to -129 ‰. There appears to be a slight enrichment of 10 ‰ in sample 20000 between 59 and 55 ka BP. This could indicate a short-term increase in the influence of Gulf of Mexico storm tracks. There is a similar enrichment of δD values in sample 99902 beginning at about 57 ka BP. The $\delta^{18}O_{ct}$ and δD values for these two speleothems agree at this point as well, which would explain the similar calculated temperatures. There is also evidence of warming in the $\delta^{13}C$ record at Crevice Cave in Missouri at this time (Dorale et al. 1998). The chronology for the change in 99902 is less certain due to weaker age control and lower resolution resulting from extremely slow growth rates over this interval.

Isotopic data from sample VR-1 in Vanishing River Cave, located on the central California Coast, could provide proxy data for climate change on the eastern Pacific margin. The δD values ranging from -23 to -47 ‰ are within expected values for δD measured from precipitation samples (IAEA 2001). The modern average δD from active drip sites in Vanishing River cave is - 37 ‰. The time period represented from the fluid inclusion data is from 7.7 to 0.5 ka BP (Figure 4.7). If the temperature dependent variation of δD in precipitation is the main control on the isotopic composition of these waters, these results can be interpreted as periods of temperatures colder and warmer than present. However, it is also possible that some of this variation is due to the amount effect (Rozanski et al. 1993). The amount effect is typically observed at sites between

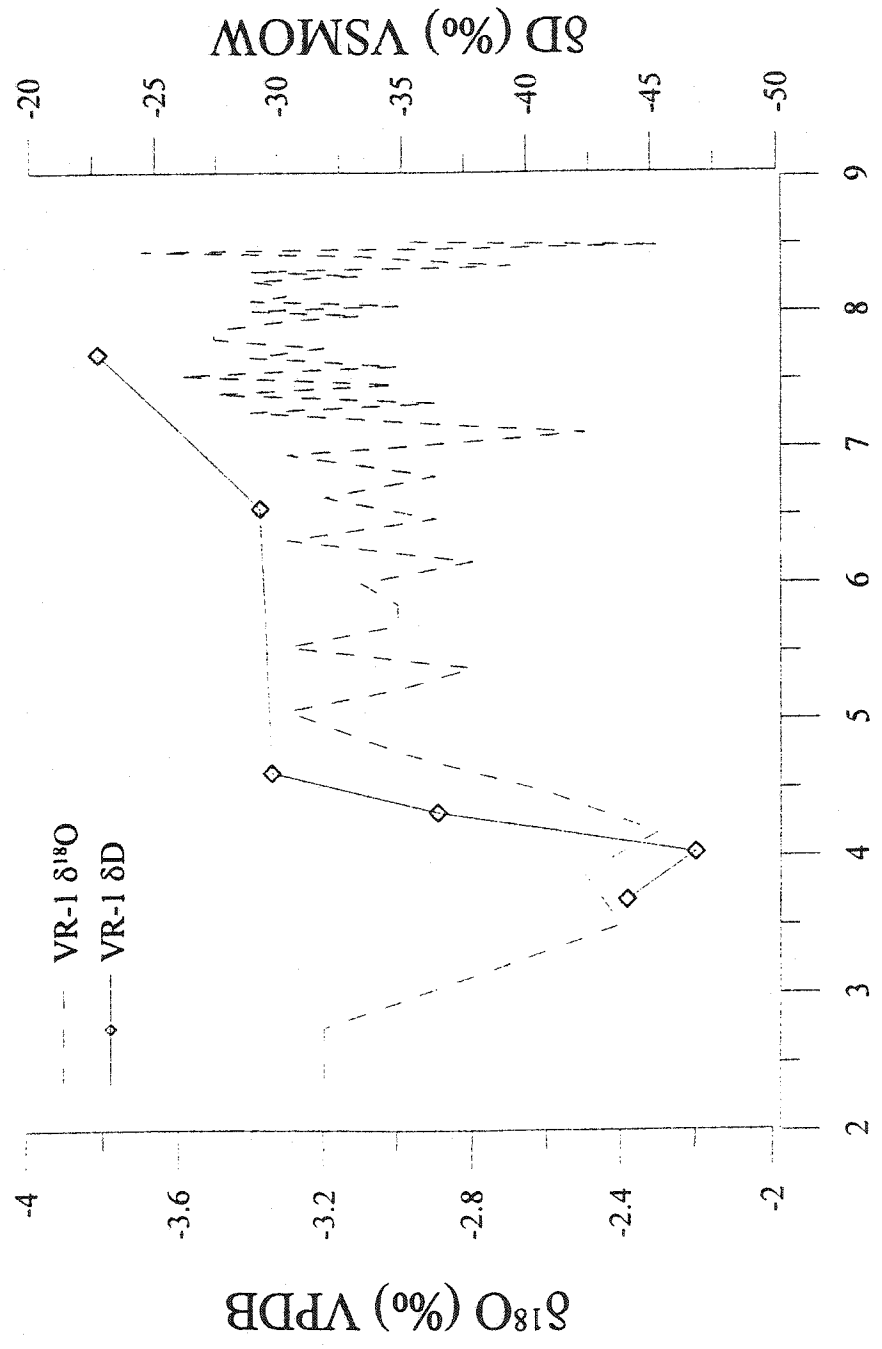

Figure 4.7. Comparison of $\delta^{18}O_{ct}$ records and δD from fluid inclusions for sample VR-1 (Table 4.2).

20° N and 20° S, but has been reported as far north as Israel (Bar-Matthews et al. 2000). If the amount of precipitation is controlling the δD composition of these waters, the more depleted values represent heavier rainfall periods and thus there are periods of more and less rainfall than modern during the Holocene. The δD value of -23 ‰ at 7.7 ka BP would indicate a period of decreased rainfall or warmer temperatures or a combination of these effects. This is consistent with the current climate regime in central and southern California that produces most of its rainfall during the winter. The δD values decrease with time, and dip below modern average δD at 3.7 to 4.0 ka BP with an average δD value of -45 ‰, indicating a period of cooler temperatures and/or increased rainfall. Increased rainfall from a strengthening of El Nino events is seen in modern coral records from the last 50 years in the western Pacific (Gagan et al. 1998). Marine sediment records from the Santa Barbara Basin (Hendy and Kennett 1999) also support cooler temperatures during this interval. On the other hand, pollen and lake level records in the Sierra Nevada record decreases in effective moisture after 6 ka BP (Anderson 1990, Thompson et al. 1993).

4.3.4. Paleotemperatures

Temperatures were calculated using the estimated $\delta^{18}O$ of fluid inclusions ($\delta^{18}O_{fi}$) and measured $\delta^{18}O_{ct}$ from the powders collected after crushing. The range of temperatures calculated for Reed's Cave use the modern MWL and estimated glacial age MWL relationship (Harmon and Schwarcz 1981). Table 4.4 shows temperatures calculated for Reed's Cave with $d_0 = 0$ (glacial age estimate) and $d_0 = 6.7$ (modern).

Table 4.4. Results from paleotemperature calculations for Reed's Cave speleothems 99902 (RC2) and 20000 (RC20).
Bold items omitted from graphs due to insufficient water (less than 0.5 μL), subzero or above modern temperature calculation.

Sample ID	Age (ka)	δD_{fi} (‰) VSMOW	$\delta^{18}O_{fi}$ (‰) (slope=8, d0=0)[a]	$\delta^{18}O_{fi}$ (‰) (slope=8, d0=6.7)[b]	$\delta^{18}O_{ct}$ (‰) VPDB	T[a] (deg. C) calculated	T[b] (deg. C) calculated
RC2-1	**61.90**	**-122.07**	**-15.26**	**-16.10**	**-9.03**	**-6.19**	**-8.18**
RC2-2&3IN	61.20	-104.06	-13.01	-13.84	-9.29	1.07	-1.56
RC2-4&5IN	**57.30**	**-91.56**	**-11.44**	**-12.28**	**-9.11**	**5.87**	**2.89**
RC2-4&5OUT	**57.30**	**-82.75**	**-10.34**	**-11.18**	**-9.11**	**10.12**	**6.85**
RC2-4&5avg	57.30	-87.15	-10.89	-11.73	-9.11	7.95	4.83
RC2-6&7OUT	50.90	-100.16	-12.52	-13.36	-9.47	3.32	0.52
RC2-9I	**48.30**	**-39.87**	**-4.98**	**-5.82**	**-9.66**	**39.21**	**34.44**
RC2-9OUT	**48.30**	**-66.90**	**-8.36**	**-9.20**	**-9.66**	**21.29**	**17.38**
RC2-10OUT	46.40	-93.65	-11.71	-12.54	-9.70	7.13	4.06
RC2-34OUT	**24.50**	**-74.81**	**-9.35**	**-10.19**	**-9.97**	**18.10**	**14.37**
RC2-35	24.00	-93.73	-11.72	-12.55	-9.19	5.18	2.25
RC2-35a	**24.00**	**-73.67**	**-9.21**	**-10.05**	**-9.19**	**15.25**	**11.67**
RC2-OL-1	**24.00**	**-129.37**	**-16.17**	**-17.01**	**-9.19**	**-7.98**	**-9.78**
RC20-174.25	**54.91**	**-124.95**	**-15.62**	**-16.46**	**-11.48**	**-0.28**	**-2.80**
RC20-174.25A	54.91	-117.60	-14.70	-15.54	-11.48	2.74	-0.02
RC20-34-1	57.71	-103.97	-13.00	-13.83	-11.50	9.10	5.90
RC20-34-2	**57.71**	**-97.84**	**-12.23**	**-13.07**	**-11.50**	**12.21**	**8.81**
RC20-35	**57.95**	**-64.98**	**-8.12**	**-8.96**	**-8.12**	**26.82**	**22.63**
RC20-35a	**57.95**	**-120.48**	**-15.06**	**-15.90**	**-15.06**	**-1.28**	**-3.72**
RC20-35b	**57.95**	**-82.90**	**-10.36**	**-11.20**	**-10.36**	**16.82**	**13.15**
RC20-35avg	57.95	-89.45	-11.18	-12.02	-11.18	14.12	10.69
RC20-93.35	58.06	-114.37	-14.30	-15.13	-10.86	2.00	-0.70
RC20-93.35A	**58.06**	**-73.55**	**-9.19**	**-10.03**	**-10.86**	**23.07**	**19.07**
RC20-93.35B	**58.06**	**-116.75**	**-14.59**	**-15.43**	**-10.86**	**1.02**	**-1.61**
RC20-40	**59.00**	**-64.90**	**-8.11**	**-8.95**	**-11.42**	**31.54**	**27.12**
RC20-40a	59.00	-98.98	-12.37	-13.21	-11.42	11.28	7.95

Table 4.4. Results from paleotemperature calculations for Reed's Cave speleothems 99902 (RC2) and 20000 (RC20).
Bold items omitted from graphs due to insufficient water (less than 0.5 μL), subzero or above modern temperature calculation.

Sample ID	Age (ka)	δD_{fi} (‰) VSMOW	$\delta^{18}O_{fi}$ (‰) (slope=8, d0=0)[a]	$\delta^{18}O_{fi}$ (‰) (slope=8, d0=6.7)[b]	$\delta^{18}O_{ct}$ (‰) VPDB	T[a] (deg. C) calculated	T[b] (deg. C) calculated
RC20-40B	**59.00**	**-123.76**	**-15.47**	**-16.31**	**-11.42**	**0.01**	**-2.54**
RC20-41a	59.14	-122.84	-15.36	-16.19	-11.72	1.33	-1.32
RC20-41c	59.14	-121.88	-15.24	-16.07	-11.72	1.73	-0.95
RC20-42	**59.27**	**2.06**	**0.26**	**-0.58**	**-12.04**	**92.38**	**85.67**
RC20_0.6.7a	**62.17**	**-150.27**	**-18.78**	**-19.62**	**-11.67**	**-8.27**	**-10.04**
RC20_0-6.7	62.17	-120.45	-15.06	-15.89	-11.67	2.18	-0.53
RC20_0-6.7b	**62.17**	**-105.61**	**-13.20**	**-14.04**	**-11.67**	**8.96**	**5.77**

[a] Calculated using MWL relationship $\delta D = 8\ \delta^{18}O + 0$

[b] Calculated using MWL relationship $\delta D = 8\ \delta^{18}O + 6.7$

Temperatures that are less than zero and greater than modern are assumed incorrect. It is unlikely that samples in the glacial and cooler MIS 3 interglacial are greater than modern temperatures. The range of acceptable temperatures is 0 to 8 °C using the modern MWL and 1 to 11 °C using the glacial age MWL. The MWL relationship for the modern central California Coast is not well constrained, so two separate values are used as well. A lower d_0 is seen in coastal and marine IAEA sampling sites and is the basis for our value of $d_0 = 4$ (Rozanski et al. 1993, Dansgaard 1969). Table 4.5 shows the temperatures calculated for the reduced d_0 and global MWL value of $d_0 = 10$. Using the same criteria as for the Reed's Cave temperature estimates, range of acceptable temperatures is 2 to 12 °C using the modern MWL and 0 to 11 °C using the modified age MWL

We expected all temperatures from Reed's Cave samples 99902 and 20000 to be lower than the modern value of 10 °C. Temperatures higher than modern or below zero may be due to fractionation as a result of incomplete water recovery. Incomplete recovery of water gave both positive and negative offsets in replicate samples. Samples with very low yields, usually less than 0.5 µl, also gave negative offset of up to 40 ‰ in analysis of capillary + Iceland spar (Table 4.1). This would lead to lower apparent temperatures of deposition.

As noted above, the $\delta^{18}O_{ct}$ records from the coeval period of growth in samples 99902 and 20000 show an offset in average $\delta^{18}O_{ct}$ and difference in magnitude of isotopic variation (Figure 4.6). In a previous paper (Chapter 2 of this thesis) we show how differences in seasonality and flow-paths of recharge can cause such differences.

Table 4.5. Results from paleotemperature calculations for Santa Cruz speleothem VR-1.
Bold items omitted from graphs due to insufficient water (less than 0.5 μL) or subzero temperature calculation.

Sample ID	Age (ka BP)	δD_{fi} (‰) VSMOW	$\delta^{18}O_{fi}$ (‰) (slope 8, d_0=10)[a]	$\delta^{18}O$ (‰) VPDB	T[a] (deg. C) calculated	$\delta^{18}O_{fi}$ (‰) (slope 8, d_0=4)[b]	T[b] (deg. C) calculated
VR-1-27a	**3.69**	**-75.92**	**-10.74**	**-3.21**	**-9.19**	**-9.99**	**-7.52**
VR-1-27b	**3.69**	**-73.30**	**-10.41**	**-3.38**	**-8.10**	**-9.66**	**-6.32**
VR-1-27	3.69	-44.14	-6.77	-3.27	1.80	-6.02	4.39
VR-1-26-1	4.03	-55.38	-8.17	-3.43	-2.12	-7.42	0.19
VR-1-26-2	4.03	-46.88	-7.11	-3.38	1.03	-6.36	3.57
VR-1-25a	4.33	-36.49	-5.81	-3.28	5.16	-5.06	7.97
VR-1-24	4.62	-29.75	-4.97	-3.29	8.37	-4.22	11.37
VR-1-13	**6.56**	**-68.67**	**-9.83**	**-3.20**	**-7.17**	**-9.08**	**-5.30**
VR-1-13a	6.56	-29.29	-4.91	-3.29	8.59	-4.16	11.60
VR-1-5a	**7.51**	**-51.70**	**-7.71**	**-2.99**	**-2.06**	**-6.96**	**0.25**
VR-1-4	**7.57**	**-54.81**	**-8.10**	**-3.28**	**-2.35**	**-7.35**	**-0.07**
VR-1-3	**7.64**	**-55.40**	**-8.17**	**-3.46**	**-2.04**	**-7.42**	**0.27**
VR-1-2	7.70	-22.69	-4.09	-3.20	11.54	-3.34	14.72

[a] Calculated using MWL relationship $\delta D = 8\ \delta^{18}O + 10$

[b] Calculated using MWL relationship $\delta D = 8\ \delta^{18}O + 4$

Minor evaporative effects can also cause an enrichment in record with respect to the other, but because the deposits were formed in equilibrium (as proved by Hendy test), it is unlikely that evaporative/kinetic fractionation has occurred. Paleotemperatures for these records give similar values and similar direction of change (Figure 4.8).

Temperatures were calculated using both the global MWL relationship and the modified glacial age MWL. The coeval part of the record shows a similar change in temperature, but the magnitude of increase is higher for sample 20000. We observe a temperature increase of 7 °C in sample 99902 and 8 °C in sample 20000 from 62 to 57 ka BP (Table 4.4). After 57 ka BP temperatures decrease by 8 °C at ~ 54 ka BP. The agreement in magnitude of temperature shift in the two coeval deposits is in striking contrast to the difference in their $\delta^{18}O_{ct}$ records. The magnitude of this temperature shift may, however, be somewhat exaggerated. For comparison, however, Anderson et al. (2000) observed cooling of up to 10 °C in the Colorado Plateau at the LGM, suggesting that temperature shifts of this magnitude may have occurred during the last glacial cycle.

The paleotemperature reconstruction for the Santa Cruz speleothem was expected to show a much smaller temperature change during the Holocene at this climatically moderated coastal location. It is not likely that temperatures would have deviated very much from the modern mean annual temperature of 11 °C. However, temperatures calculated from fluid inclusion-calcite pairs suggest a decrease of almost ~7 °C from 4.5 ka BP to 3.5 ka BP (Figure 4.9). Such a large decrease is not likely, although there is evidence of cooling after 6 ka from marine sediments in the Santa Barbara Basin (Hendy and Kennett 1999). The warmest temperatures which we obtained were calculated at ~ 8

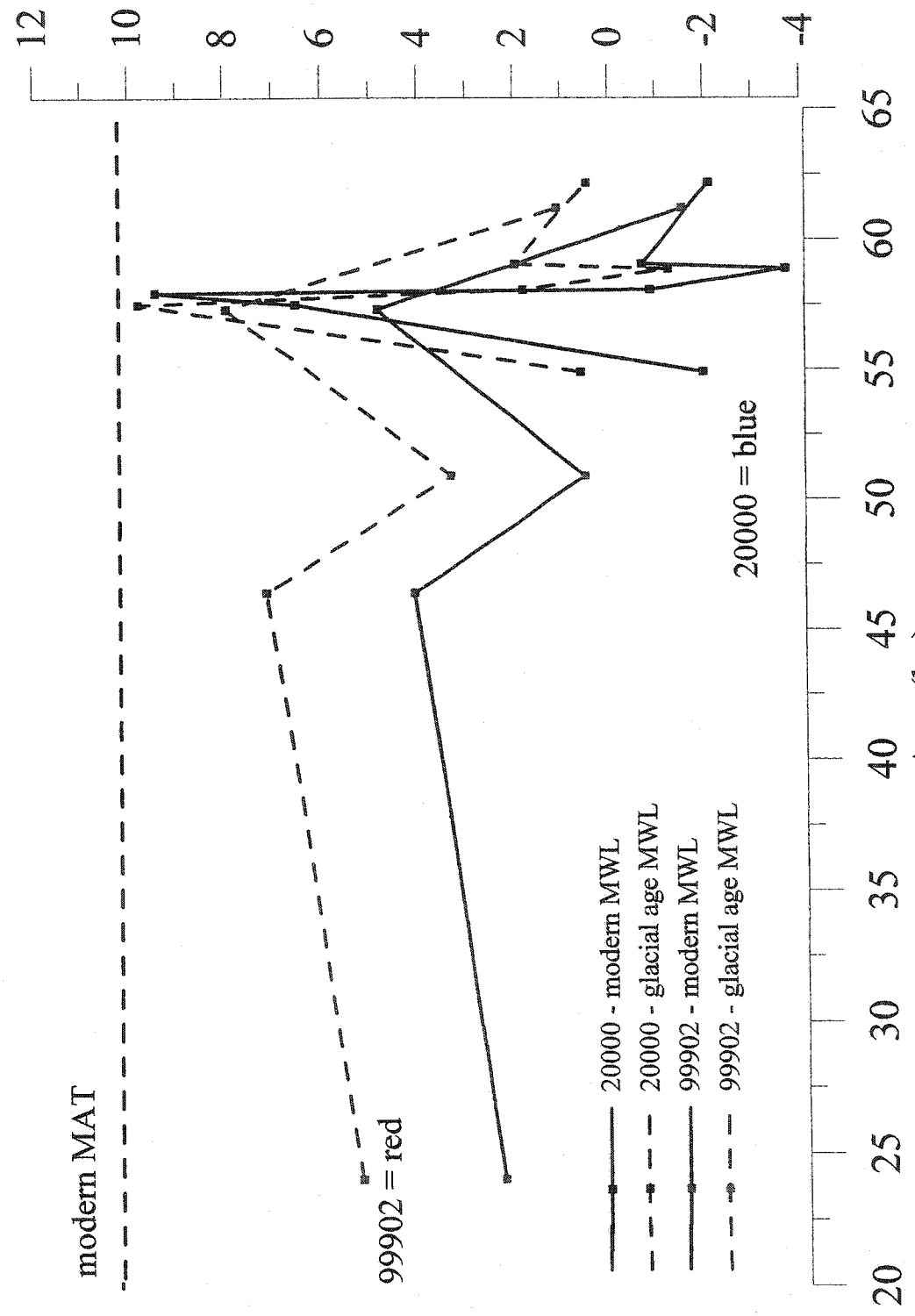

Figure 4.8. Paleotemperature records for sample 99902 and 20000 from fluid inclusion analyses (Table 4.4).

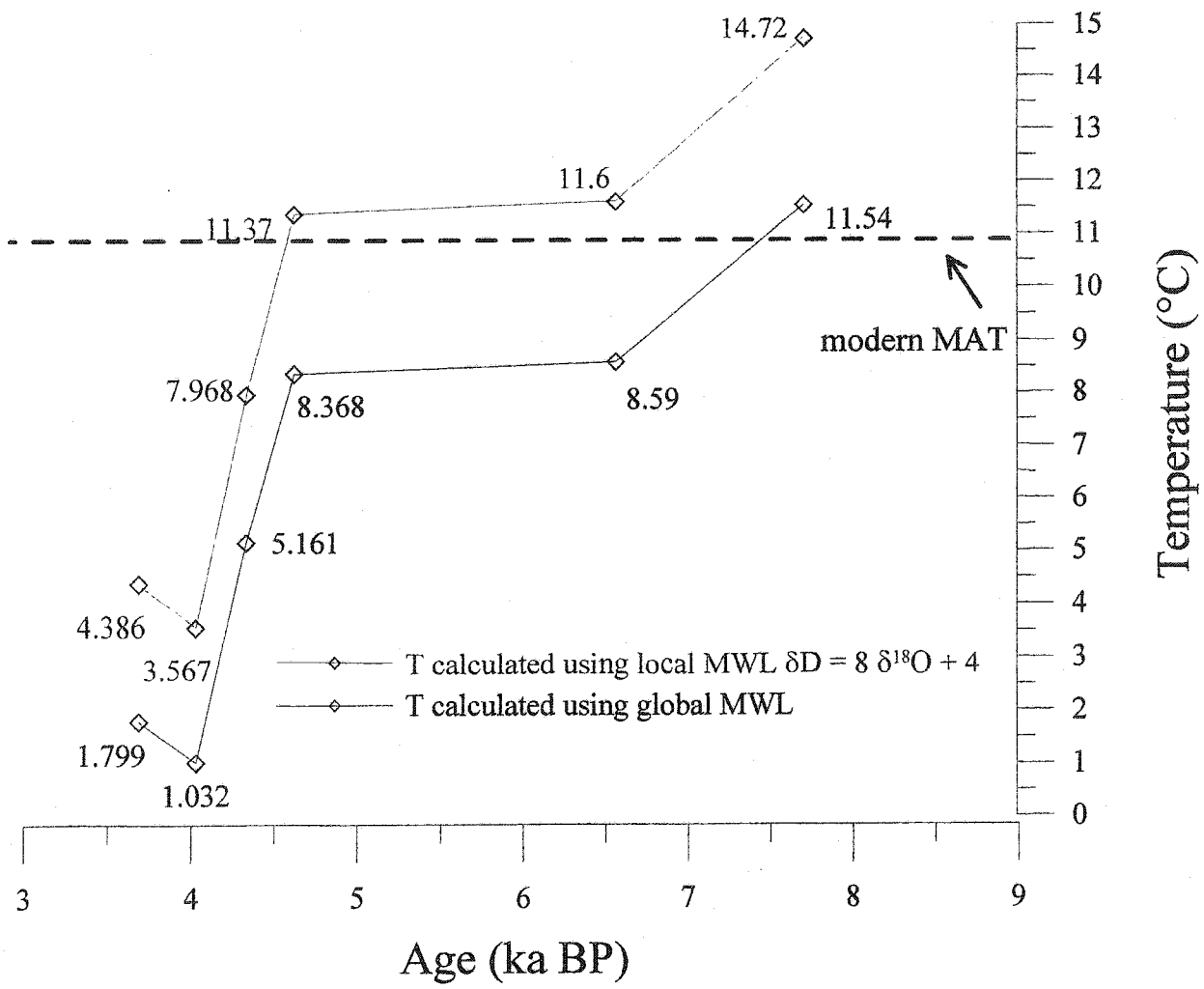

Figure 4.9. Paleotemperature record for sample VR-1 from fluid inclusion analyses (Table 4.5).

ka BP, at which time there is additional evidence for warming from the marine sediments (Pisias 1978). Again, the direction of temperature appears to agree with other proxy records, but the magnitude of change is problematic.

4.4 CONCLUSIONS

Variations in δD values over time as preserved in speleothem fluid inclusions are powerful recorders of past air mass composition and position and possibly of climate change. Late Pleistocene deposits from Reed's Cave, South Dakota show consistent depletion in ^{2}H in fluid inclusion waters. This is evidence of cooler temperatures and increased precipitation that may be due to changes in atmospheric circulation from ice sheet fluctuations or global ocean temperature gradients. Maximum δD values and a possible corresponding temperature increase in both Reed's Cave speleothems is seen at 57 ka BP. A trough in δD values at 54 ka BP correlates with a cooling event in the Mediterranean and in the Devil's Hole calcite record (Bar-Matthews et al. 1999, Winograd et al. 1997). Sample VR-1 from central California indicates a general Holocene cooling that began at least 8 ka BP and agrees well with Greenland ice core records and marine sediments off the Hawaii coast (Bond et al. 1997, Lea et al. get date). The decrease in temperature and/or increase in precipitation revealed by decrease in δD value in VR-1 appears to occur earlier than proxies from Santa Barbara basin that show a Holocene thermal maximum between 9 and 6 ka BP (Pisias 1978, Hendy and Kennett 1999). There may be a lag between these two records or weaker dating control in the

marine sediments, which may account for this offset. Although the δD records from Reed's Cave and Santa Cruz appear to be recording some component of global climate change, it is more useful to apply them towards understanding local or regional climate. Higher resolution records will be developed following more sample analyses and may give better insight into local climates.

We have analyzed two coeval stalagmites from Reed's Cave whose $\delta^{18}O_{ct}$ values differed by up to 3 ‰. If they had been deposited from water of identical isotopic composition, this would have implied a difference of at least 12 °C between their temperature of deposition, even though they were formed only a few meters apart in the same chamber. The analysis of fluid inclusions from these two deposits confirms there was a corresponding difference in hydrogen isotopic composition of drip waters feeding these deposits, which we assume to have been correlated to corresponding differences in $\delta^{18}O$, and which was the reason for the difference in $\delta^{18}O_{ct}$ between the samples.

There is evidence from the paleotemperature calculations that there were variations in the local relationship between $\delta^{18}O$ and δD (meteoric water line) during the late Pleistocene. Subzero temperatures and extreme magnitude of temperature change are calculated using the modern MWL for the Reed's Cave samples; these can only be resolved if the local MWL was changing throughout the period of these records. It may not be reasonable to use a constant MWL relationship for all fluid inclusion samples in the Pleistocene. Assumptions about past MWL relationships must be made to calculate $\delta^{18}O$ values for included waters until the $\delta^{18}O$ of waters can be measured directly.

We have also assumed that δD values are preserved over time and it remains a faithful record of δD of paleoprecipitation. Unless alternative proxy records for absolute paleotemperatures are developed to test these models, it will be difficult to ascertain the accuracy of this assumption. The results do show promise because we see correlation between direction of temperature change in coeval deposits and with other global proxy records.

4.5. ACKNOWLEDGEMENTS

The authors are grateful to the Cave Research Foundation for a grant to F. Serefiddin and the Natural Sciences and Engineering Research Council (Canada) for their support of this research, partly through a Special Project grant "Climate System History and Dynamics" and partly through operating grants to HPS and DCF. Special thanks to Dr. P. Rowe and Dr. P. Dennis at the University of East Anglia for their assistance with crusher design. Greg Stock and Dr. Jim Zachos provided sample material from Santa Cruz and unpublished isotope data. Steve Baldwin, Steve Langendorf, Sammi Langendorf and cavers from the Pahasapa Grotto in the Black Hills assisted with speleothem sample collection and collected all cave water samples.

4.6. REFERENCES

Anderson, R.S. (1980). Holocene forest development and paleoclimates within the central Sierra Nevada, California. *J. of Ecology* **78**: 470-489.

Anderson, R. S., Betancourt, J. L., Mead, J. I., Hevly, R .H. and Adam, D. P. (2000). Middle- and late-Wisconsin paleobotanic and paleoclimatic records from the southern Colorado Plateau, USA. *Palaeogeography, Palaeoclimatology, Palaeoecology* **155**, 31-57.

Bar-Matthews, M., Gilmour, M., Ayalon, A., Vax, A., Frumkin, A. and Hawkesworth, C. (2000). Variation of Palaeoclimate in the Eastern Mediterranean Region – As Derived from Speleothems in Various Climate Regimes in Israel. *Goldschmidt 2000; J. of Conference Abstracts* **5(2)**: 194-5.

Bar-Matthews, M., Ayalon, M., Kaufman, A. and Wasserburg, G.J. (1999). The Eastern Mediterranean paleoclimate as a reflection of regional events: Soreq Cave, Israel. *Earth and Planetary Science Letters* **166**, 85-95.

Bond, G., Showers, W., Cheseby, M., Lotti, R, Almasi, P. deMenocal, P., Priore, P., Cullen, R., Hajdas, I. and Bonani, G. (1997). A Pervasive Millennial-Scale Cycle in North Atlantic Holocene and Glacial Climates. *Science* **278**, 1257-1266.

Bryson, R. A. (1966). Air masses, streamlines, and the boreal forest. *Geographical Bulletin* **8**: 228-269.

Charles, C.D., Rind, D., Jouzel, J., Koster, R.D. and Fairbanks, R.G. (1994). Glacial-Interglacial Changes in Moisture Sources for Greenland: Influences on the Ice Core Record of Climate. *Science* **263**: 508-511.

Craig, H. (1961). Isotopic variations in meteoric waters. *Science* **133**: 1702.

Dansgaard, W. (1964). Stable isotopes in precipitation. *Tellus* **16**: 438-468.

Dennis, P. F., Rowe, P. J. and Atkinson, T. C. (2001). The recovery and isotopic measurement of water from fluid inclusions in speleothems. *Geochim. Cosmochim. Acta* **65(6)**: 871-884.

Dorale, J. A. (2000). A high-resolution record of climate and vegetation change from Crevice Cave, Missouri during the last interglacial-glacial cycle. Unpublished PhD thesis, University of Minnesota, Minneapolis, Minnesota.

Dorale, J. A., Edwards, R. L., Ito, E. and González, L. A. (1998). Climate and Vegetation History of the Midcontinent from 75 to 25 ka: A Speleothem Record from Crevice Cave, Missouri, USA. *Science* **282**, 1871-1874.

Dorale, J. A., Gonzalez, L. A., Reagan, M. K., Pickett, D. A., Murrell, M. T. and Baker, R. G. (1992). A High-Resolution Record of Holocene Climate Change in Speleothem Calcite from Cold Water Cave, Northeast Iowa. *Science* **258**: 1626-1630.

Edwards, R. L., Chen, J. H. and Wasserburg, G. J. (1986). ^{238}U-^{234}U-^{230}Th-^{232}Th systematics and the precise measurement of time over the past 500,000 years. *Earth and Planetary Science Letters* **81**, 175-192.

Frumkin, A., Ford, D. C. and Schwarcz, H. P. (1999). Continental oxygen isotopic record of the last 170,000 years in Jerusalem. *Quaternary Research* 51: 317-327.

Gagan, M.K., Ayliffe, L.K., Hopley, D., Cali, J.A., Mortimer, G.E., Chappell, J., McCulloch, M.T. and Head, M.J. (1998). Temperature and surface-ocean water balance of the mid-Holocene tropical Western Pacific. *Science* **279**: 1014-1018.

Gascoyne, M. (1992). Palaeoclimate determination from cave calcite deposits. *Quaternary Science Reviews* **11**: 609-632.

Gat, J. R. (1980). The isotopes of hydrogen and oxygen in precipitation. In *Handbook of Environmental Geochemistry, The Terrestrial Environment*, A, Vol. 1, pp. 21-47 (P. Fritz and J. C. Fontes (eds.). Amsterdam: Elsevier.

Genty, D., Plagnes, V., Causse, C., Cattani, O., Stievenard, M., Falourd, S, Blamarr, D., Ouahdi, R. and Van-Exter, S. (2002). Fossil water in large stalagmite voids as a tool for paleoprecipitation stable isotope composition reconstitution and paleotemperature calculation. *Chemical Geology* **184**: 83-95..

Goede, A., Green, D. C. and Harmon, R. S. (1986). Late Pleistocene palaeotemperature record from a Tasmanian speleothem. *Austr. J. Earth Sci.* **33**: 333-342.

Goede, A., Veeh, H. H. and Aycliffe, L. K. (1990). Late Quaternary palaeotemperature records for two Tasmanian speleothems. *Austr. J. Earth Sci.* **37**: 267-278.

Harmon, R.S. and Schwarcz, H.P. (1981). Changes in ^{2}H and ^{18}O enrichment of meteoric water and Pleistocene glaciation. *Nature (London)* **290**: 125-128.

Harmon, R. S., Schwarcz, H. P., and O'Neil, J. R. (1979). D/H ratios in speleothem fluid inclusions: a guide to variations in the isotopic composition of meteoric precipitation? *Earth and Planetary Science Letters* **42**: 254-266.

Hellstrom, J. C., M. T. McCulloch, and J. Stone. (1998). A detailed 31,000-year record of climate and vegetation change, from the isotope geochemistry of two New Zealand speleothems. *Quaternary Research* **50**: 167-178.

Hendy, I.L. and Kennett, J.P. (1999). Latest Quaternary North Pacific surface-water responses imply atmosphere-driven climate stability. *Geology* **27**: 291-294.

IAEA (2001). *GNIP Maps and Animations,* International Atomic Energy Agency, Vienna. Accessible at *http://isohis.iaea.org*

Jouzel, J., Lorius, C., Petit, J. R., Genthon, C., Barkov, N. I., Kotlyakov, V. M., and Petrov, V. M. (1987). Vostok ice core: a continuous isotope temperature record over the last climatic cycle (160,000 years). *Nature (London)* **329**: 403-408.

Jouzel J., Merlivat L., and Lorius C. (1982). Deuterium excess in an East Antarctic ice core suggests higher relative humidity at the oceanic surface during the last glacial maximum. *Nature* **299**: 688-691.

Nativ, R. and Riggio, R. (1990). Precipitation in the south High Plains: Meteorologic and isotopic patterns. *J. Geophys. Res.* **95**: 22559-22564.

Lauritzen, S. -E. and Lundberg, J. (1999). Calibration of the speleothem delta function: an absolute temperature record for the Holocene in northern Norway. *The Holocene* **9(6)**: 643-647.

Lea, D.J., Pak, D.K. and Spero, H.J. 2000. Climate impact of late Quaternary Equatorial Pacific sea surface temperature variations. *Science* **289** :1719-1724.

Linge, H., Lauritzen, S.-E., Lundberg, J., and Berstad, I.M. (2001). Stable isotope stratigraphy of Holocene speleothems: examples from a cave system in Rana, northern Norway. *Palaeogeography, Palaeoclimatology, Palaeoecology* **167**, 209-224.

Martinson, D. G., Pisias, N. G., Hays, J. D., Imbrie, J., Moore, T. C. and Shackleton, N. J. (1987). Age Dating and the Orbital Theory of the Ice Ages: Development of a High-Resolution 0 to 300,000-Year Chronostratigraphy. *Quaternary Research* **27**, 1-29.

Matthews, A., Ayalon, A., and Bar-Matthews, M. (2000). D/H ratios of fluid inclusions of Soreq Cave (Israel) speleothems as a guide to the Eastern Mediterranean Meteoric Water Line relationships in the last 120 Ky. *Chemical Geology* **166**: 183-191.

McGarry, S., Bar-Matthews, M., Matthews, A. and Ayalon, A. (2002) Palaeohydrology in the Eastern Mediterranean form speleothem fluid inclusion D/H analyses. *Geochim. Cosmochim. Acta* **66 (S1)**: A500.

Neff, U., S. J. Burns, A. Mangini, M. Mudelsee, D. Fleitmann, and A. Matter. (2001). Strong coherence between solar variability and the monsoon in Oman between 9 and 6 kyr ago. *Nature (London)* **411**: 290-293.

O'Neil, J. R., Clayton, R. N. and Mayeda, T. K. (1969). Oxygen isotope fractionation in divalent metal carbonates. *J. Chem. Phys.* **51**, 5547-5558.

Pisias, N. (1978). Paleoceanography of the Santa Barbara Basin during the last 8000 years. *Quaternary Research* **10**: 366-384.

Rozanski, K and Dulinksi, M. (1987). Deuterium content of European Paleowaters as inferred from isotopic composition of fluid inclusions trapped in carbonate cave deposits. IAEA-SM-299/99, Vienna, 565-578.

Rozanski, K., Araguás- Araguás, L., and Gonfiantini, R. (1992). Relation between long-term trends of oxygen-18 isotope composition of precipitation and climate. *Science* **258**: 981-985.

Rozanski, K., Araguás- Araguás, L., and Gonfiantini, R. (1993). Isotopic patterns in modern global precipitation. In *Climate Change in Continental Isotopic Records, Geophysical Monograph 78*. American Geophysical Union, Washington: 1-36.

Schwarcz, H. P. (1986). Geochronology and isotope geochemistry in speleothems. In *Handbook of Environmental Isotope Geochemistry* (P. Fritz and J. Fontes, eds.), 271-303. Amsterdam: Elsevier Publishers.

Schwarcz, H. P. and Yonge, C. J. (1983). Isotopic composition of paleowaters as inferred from speleothem and its fluid inclusions. In *Paleoclimates and Paleowaters: A collectionof Environmental Isotope studies*. IAEA STI/PUB/621: 115-133.

Schwarcz, H. P., Harmon, R. S., Thompson, P. and Ford, D. C. (1976). Stable isotope studies of fluid inclusions in speleothems and their paleoclimatic significance. *Geochim. Cosmochim. Acta* **40**: 637-665.

Serefiddin, F., Schwarcz, H. P., and Ford, D.C. Late Pleistocene paleoclimate in the Black Hills of South Dakota from isotope records in speleothems. Submitted to *Palaeogeography, Palaeocclimatology, Palaeoecology*.

Serefiddin, F., Ford, D.C., and Schwarcz, H. P. (2002). Late Pleistocene paleoclimate in the Black Hills of South Dakota from isotope records in speleothems. Paper presented at GSA Annual Meeting, Denver, Colorado.

Serefiddin, F., Schwarcz, H.P. and Ford, D.C. (2002). Paleotemperature reconstruction using isotopic variations in speleothem fluid inclusion water. *Geochim. Cosmochim. Acta* **66 (S1)**: A697.

Thompson, R.S., Whitlock, C., Bartlein, P.J., Harrison, S.P. and Spaulding, W.G. (1993). Climatic changes in the Western United States since 18,000 yr BP in H.P. Wright et al.

(eds.) *Global climates since the Last Glacial Maximum*, Univ. of Minnesota Press, 468-514.

Wang, Y. J., H. Cheng, R. L. Edwards, Z. S. An, J. Y. Wu, C. C. Shen, and J. A. Dorale. (2001). A High-Resolution Absolute-Dated Late Pleistocene Monsoon Record from Hulu Cave, China. *Science* **294**: 2345-2348.

Winograd, I. J., Landwehr, J. M., Ludwig, K. R., Coplen, T. B., and Riggs, A. C. (1997). Duration and Structure of the Past Four Interglacials. *Quaternary Research* **48**: 141-154.

Welker, J. M. (2000). Isotopic ($\delta^{18}O$) characteristics of weekly precipitation collected across the USA: an initial analysis with application to water source studies. *Hydrological Process* **14**: 1449-1464.

Yonge, C. J., Ford, D. C., Gray, J., and Schwarcz, H. P. (1985). Stable isotope studies of cave seepage water. *Chemical Geology* **58**: 97-105.

CHAPTER FIVE. CONCLUSION - SPELEOTHEMS AS PALEOCLIMATE PROXIES

5.1. OVERALL GOALS AND RESULTS

The goal of this work was to use existing and improved methods of analyzing speleothems for paleoclimatic research. Recent advances in radiogenic and stable isotope mass spectrometry allow the measurement of smaller sample sizes resulting in high resolution proxy data. The data for five speleothems from Reed's Cave, South Dakota were intended to give a record of climate change in central North America over the last 500,000 years, but lack of concordance between coeval samples in the caves revealed the difficulty of interpreting stable isotopes in speleothem calcite. The primary focus of this work is on the 1) improvement of extraction and measurement of δD in speleothem fluid inclusions., 2) investigation of intersample differences in $\delta^{18}O_{ct}$ for coeval periods of growth, 3) investigating intersite differences in drip water composition and 4) detecting sub-Milankovitch and millennial scale variation in $\delta^{18}O_{ct}$ records and comparison of these to other proxy records.

A new crushing cell design for the extraction of fluid inclusions has increased water recovery to over 90%, but the ongoing problem of contamination has masked this success. I hoped to use the new crushing cell design to provide high resolution data from paleoprecipitation samples. The analyses of δD in fluid inclusion water give results that are difficult to interpret. The variations in δD are important in their own right for studying paleoclimate, but I also attempted to calculate absolute paleotemperatures. The

temperature calculations showed changes that were larger than expected, but it is difficult to determine if this due to inaccuracies from experimental error or problems with estimating a MWL relationship for the past.

5.2. TOWARDS A BETTER UNDERSTANDING OF SPELEOTHEM ISOTOPE RECORDS

Previous studies of speleothems have focused on many different geographical areas with different types of climate, commonly using one speleothem sample from a cave. These single isotope records have shown both good and poor correlation with the more established marine sediment and ice core records. However, only recently have we seen the analysis of coeval speleothems within a cave (Bar-Matthews et al. 1999, Wang et al. 2001). The most probable reason for the absence of studies using coeval speleothems is that discordant $\delta^{18}O_{ct}$ records were believed to be due to kinetic fractionation in one of the speleothems. These intersample differences do not result in temperature (calculated) differences because of differences in the isotopic composition of fluid inclusion in these same growth layers. This suggests that kinetic fractionation may not be occurring.

We have studied five speleothems from Reed's Cave, of which two grew during the Wisconsin glacial period and three grew at different time slices between 550,000 and 150,000 years ago. The periods of growth which overlap for both sets of speleothems shows a divergence in the $\delta^{18}O_{ct}$ records (Figure 2.6, Figure 3.8). There are different

competing mechanisms controlling the variation of $\delta^{18}O_{ct}$ in speleothem calcite (from equation 2.1, Chapter 2): 1) changing $\delta^{18}O$ of seawater; 2) change in $\delta^{18}O_{ppt}$ with temperature; and 3) the temperature-dependent fractionation between calcite-water. From analyses of modern drip waters in the cave, we have discovered other factors that can lead to differences in coeval deposits, which appear to be a result of local differences in the long-term $\delta^{18}O$ of drip waters feeding the speleothem. This is attributed to a seasonal bias in the recharge of the drip site and is especially pronounced at a site like Reed's Cave where there is a large seasonal range of $\delta^{18}O$ of precipitation.

The overall relationship between $\delta^{18}O_{ct}$ and temperature ($\gamma = d(\delta^{18}O_{ct})/dT$) can be assigned to individual speleothems but not to the entire cave. The two Wisconsin age samples have an offset in the average $\delta^{18}O_{ct}$ and therefore in the value for γ. Sample 99902 clearly showed a negative γ. Sample 20000 is more difficult to interpret because it covers only 12,000 years and shows large oscillations in $\delta^{18}O_{ct}$ over this time. Comparing to modern $\delta^{18}O_{ct}$ values, we would assign it a positive γ because through most of the record, which is during the colder Wisconsin interval, $\delta^{18}O_{ct}$ is less than the modern average of -11 ‰. However, in part of the record $\delta^{18}O_{ct}$ is greater than the modern value, so it appears that $\gamma \approx 0$. The offset indicates different sources for the drips, and that 20000 is most likely forming from waters biased to winter precipitation. Its higher growth rate suggests higher drip rates than at the site of 99902.

Three mid-Pleistocene speleothems, all forming between ~ 450 and 375 ka, also have different γ values. The offset between samples 99900 and 99901 is as high as 6 ‰

during maximum interglacial conditions but appears to be reduced during the glacials. This is evidence that a bias towards winter precipitation gives more depleted $\delta^{18}O_{ct}$ values for 99900. It also indicates that $\delta^{18}O_{ct}$ for 99900 is being controlled by temperature dependent fractionation and $\delta^{18}O_{ct}$ for 99901 is more strongly controlled by temperature effects on $\delta^{18}O$ of precipitation. The Hendy tests in all speleothems show that they were formed in equilibrium, so the local environmental factors must play a strong role in controlling how $\delta^{18}O_{ct}$ varies over time. The character of the local infiltration site (and associated characteristics including topography and presence of vegetation) of water combined with the flow path of recharge to the drip site tells us if the speleothem is being formed from quickly infiltrating waters representative of one particular season (the rainy season) or slowly percolating waters with a long residence time that are well-mixed and therefore show no seasonal bias. Growth rate, trace element and other proxy data may also be valuable for determining the controls on stable isotope data.

5.3. PLEISTOCENE CLIMATE CHANGE IN CENTRAL NORTH AMERICA

This thesis focused on paleoclimate reconstructions in the Black Hills of South Dakota. The marked absence of pre-Holocene records makes these data very important for establishing some baseline information on paleoclimate in this area. The advance of the Laurentide ice sheet over surrounding areas during the last glacial maximum removed or disturbed Pleistocene-age lake deposits. Our records show that local climate was

highly variable during the mid-Wisconsin, particularly during MIS 3. More importantly, we found that the two deposits recorded climate in different ways. Although the $\delta^{18}O_{ct}$ records do not agree during their coeval period of growth, the paleotemperature calculations from measurements of δD in the fluid inclusions show similar change in and magnitude of temperature change. Speleothem 20000 gives a higher resolution record of climate over the 12,000 year interval of formation. It is sensitive to millennial-scale climate change and is showing a longer-term trend as well. Speleothem 99902 records slower growth in the early (pre 50,000 y) part of its growth, but as growth rate increases it show large magnitude oscillations in $\delta^{18}O_{ct}$ values. The growth rate of this speleothem increases during a period of ice sheet expansion leading up to MIS 2, which is clearly greater than the earlier MIS 4 glacial. This tells us that terrestrial proxy records are highly sensitive to short-term local climate change but record long term change as well. Comparisons with speleothems from Missouri and Soreq Cave prove this point. There are also strong similarities between the ice cores records and the Wisconsin age samples from Reed's Cave. A comparison of samples 99900 and 99901 showed high frequency variability in the $\delta^{18}O_{ct}$ equal to and greater than seen in the Devil's Hole thermal water calcite $\delta^{18}O_{ct}$ record and European pollen records. The long-term trends match very well, but the short-term oscillations differ at each site.

There is a strong indication that these deposits are not only responding to changes in temperature, but changes in storm tracks and moisture availability. This is evident in the mid-Pleistocene records as well. The older Reed's Cave speleothems show large oscillations in $\delta^{18}O_{ct}$ between the interglacial and glacial maxima. If we smooth the

records using the running average, we see isotope records with a shape much closer to the SPECMAP record (Figure 3.11). The timing on the Reed's Cave records are offset from SPECMAP, if we are looking at maxima and minima, but this is attributed to inaccuracies in the dating method in such old deposits. Improved sampling of individual layers and mass spectrometric techniques may solve these problems. Again, we do see that both local and global climate change is being recorded in these deposits.

The value of the mid-Pleistocene records for understanding the MIS 11 problem is not clear. There is evidence that MIS 11 is not as long and warm as previous workers believed (Poore and Dowsett 2001, Oppo et al. 1998, Imbrie et al. 1993). However, we show that it is a period of unstable climate in the mid-continent. It may be masking long-term climate extremes that are revealed in the marine records. Loess records in China and Russia also show that MIS 11 was not warmer than the MIS 5 interglacial. This highlights the problems in comparing terrestrial with marine proxy records. In order to calibrate global climate models we must have a better understanding of how different proxies respond to various forcing mechanisms.

5.4. PROGRESS IN FLUID INCLUSION ANALYSES

Fluid inclusions and their associated δD values are an important contribution to speleothem research because it can be used as an independent proxy and to calculate absolute paleotemperatures. The improvements in fluid inclusion water extraction enabled us to use smaller sample sizes, but the measurement of such small samples is still problematic. In the results that were able to reproduce, we measured expected δD values

that were more depleted than modern dripwaters, as expected for colder, glacial age samples. However, the temperature calculations were questionable. The absolute temperature change (decreasing towards LGM) measured within the Wisconsin glacial period was over 10°C in Reed's Cave, much higher than would be expected. Groundwater proxies from the Colorado Plateau showed similar, large magnitude changes for an entire interglacial/glacial cycle, but it is not clear if such a large shift could occur within MIS 3. This is probably explained by the assumptions made in converting the δD data to $\delta^{18}O_w$ data using the meteoric water line (MWL) relationship. Because the MWL for the late Pleistocene is not exactly known, we used the values as estimated by Jouzel et al. (1982) from ice core measurements. Glacial age precipitation is believed to have a lower d_0 than modern. The measured local MWL for Reed's Cave is $\delta D = 8\ \delta^{18}O + 6.7$, but using this value gives negative temperatures for our samples (Table 4.4). We used a $d_0 = 0$ for our calculations and this gave us positive temperatures. Surface waters must remain unfrozen to infiltrate into the aquifer and then the cave in order for speleothem deposition to occur. Similar, high magnitude shifts in temperature in a Holocene deposit from the central California Coast reflect similar problems. Large temperature shifts of up to 8 °C are calculated within 2-3 ka from the speleothem δD data. Marine sites are moderated by ocean, so even less likely to be showing such large changes in temperatures. The δD results may be more valuable as a tracer of storm tracks and shifts in seasonality of precipitation.

5.5. FUTURE WORK

Global climate models that will be used to predict future climate rely on proxy records for calibration. Currently, these models rely on the long-term marine and ice core records. These records are valuable in their own right, but are obscuring localized climate change, particularly in temperate, mid-continental areas. The influence of ice sheets and topography on the isotopic composition of storm tracks cannot be estimated from marine and high latitude data. Speleothems can be used to fill in the missing pieces of the paleoclimate story, but the mechanisms controlling their isotopic composition need to be better understood. This requires rigorous studies using multiple, preferably coeval speleothems from each cave site to determine if the speleothems are recording local or global climate, or both. It is also important to select cave sites that are located in areas with little other proxy data, such is the case in the Black Hills. With the advance in mass spectrometry for uranium-series dating, it is also possible to extend the range of dating past 500 ka, giving absolutely dated deposits far beyond what was possible before. We have presented data from central North America that provides new information about the mid-Pleistocene.

The improved fluid inclusion water techniques presented in this thesis show great promise but there are still some important issues that must be addressed before good paleotemperature records can be developed. High precision continuous flow isotope ratio mass spectrometers (CF-IRMS) using the chromium reaction method can measure nanoliter quanities of water and are needed for fluid inclusion analyses of sub-microliter size samples. The crushing cell that has been shown to recover over 90% of included

water from the samples can be used on-line with the CF-IRMS. Until better measurement of waters can be done, it is not clear if these δD values being measured are free of fractionation effects.

BIBLIOGRAPHY

Bar-Matthews, M., A. Ayalon, A. Kaufman, and G. J. Wasserburg. (1999). The eastern Mediterranean paleoclimate as a reflection of regional events; Soreq Cave, Israel. *Earth and Planetary Science Letters* **166**: 85-95.

Bond, G.C., Showers,W., Elliot, M., Evans, M., Lotti, R., Hajdas, I., Bonani, G., Johnson, S., Webb, R.S., Keigwin, L. D. (1999). The North Atlantic's 1-2 kyr climate rhythm; relation to Heinrich events, Dansgaard/Oescher cycles and the Little Ice Age. *Mechanisms of global climate change at millennial time scales, Geophysical Monograph 112*, 35-58.

Bryson, R. A. (1966). Air masses, streamlines, and the boreal forest. *Geographical Bulletin* **8**: 228-269.

Chen, J.H., Edwards, R.L., and Wasserburg, G. J. (1992). Mass spectrometry and application to uranium-series disequilibrium. In *Uranium-series disequilibrium; applications to Earth, marine, and environmental sciences*, Ivanovich, M. and Harmon, R.S. (eds). Clarendon: Oxford.

Dansgaard, W., Johnsen, S. J., Clausen, H. B., Dahl-Jensen, D., Gunderstrup, N. S., Hammer, C. U., Hvidberg, C. S., Steffensen, J. P., Sveinbjörnsdottir, A. E, Jouzel, J. and Bond, G. (1993). Evidence for general instability of past climate from a 250-kyr ice-core record. *Nature* **364**, 218-220.

Dorale, J. A. (2000). A high-resolution record of climate and vegetation change from Crevice Cave, Missouri during the last interglacial-glacial cycle. Unpublished PhD thesis, University of Minnesota, Minneapolis, Minnesota.

Gascoyne, M. (1992). Palaeoclimate determination from cave calcite deposits. *Quaternary Science Reviews* **11**: 609-632.

Imbrie, J. ; Berger, A. ; Boyle, E. A. ;Clemens, S. C. ; Duffy, A. ; Howard, W. R. ; Kukla, G. ; Kutzbach, J. ; Martinson, D. G. ; McIntyre, A. ; Mix, A. C. ; Molfino, B. ; Morley, J. J. ; Peterson, L. C. ; Pisias, N. G. ; Prell, W. L. ; Raymo, M. E. ; Shackleton, N. J. ; Toggweiler, J. R. (1993). On the structure and origin of major glaciation cycles; 2, The 100,000-year cycle. *Paleoceanography* **8(6)**: 698-735.

Jouzel J., Merlivat L., and Lorius C. (1982). Deuterium excess in an East Antarctic ice core suggests higher relative humidity at the oceanic surface during the last glacial maximum. *Nature* **299**: 688-691.

Li, W. -X., Lundberg, J., Dickin, A. P., Ford, D. C., Schwarcz, H. P., McNutt, R. and Williams, D. (1989). High-precision mass-spectrometric uranium-series dating of cave deposits and implications for palaeoclimate studies. *Nature (London)* **339**: 534-536.

Oppo, D. W., J. F. McManus, and J. L. Cullen. (1998). Abrupt climate events 500,000 to 340,000 years ago; evidence from subpolar North Atlantic sediments. *Science* **279**: 1335-1338.

Poore, R. Z. and H. J. Dowsett. (2001). Pleistocene reduction of polar ice caps; evidence from Cariaco Basin marine sediments. *Geology (Boulder)* **29**: 71-74.

Rutter, N., Ding, Z., And Liu, T. (1991). Comparison of isotope stages 1-61 with the Baoji-type pedostratigraphic section of north-central China. *Canadian J. Earth Sciences* **28**: 985-990.

Schwarcz, H. P. (1986). Geochronology and isotope geochemistry in speleothems. In *Handbook of Environmental Isotope Geochemistry* (P. Fritz and J. Fontes, eds.), 271-303. Amsterdam: Elsevier Publishers.

Schwarcz, H. P., Harmon, R. S., Thompson, P. and Ford, D. C. (1976). Stable isotope studies of fluid inclusions in speleothems and their paleoclimatic significance. *Geochim. Cosmochim. Acta* **40**: 637-665.

Stirling, C.H., Lee, D.C., Christensen, J.N. and Halliday, A.N. (2000). High-precision in situ ^{238}U-^{234}U-^{230}Th isotopic analysis using laser ablation multiple-collector ICP-MS. *Geochimica et Cosmochimica Acta* **64**: 3737-3750.

Wang, Y. J., H. Cheng, R. L. Edwards, Z. S. An, J. Y. Wu, C. C. Shen, and J. A. Dorale. (2001). A High-Resolution Absolute-Dated Late Pleistocene Monsoon Record from Hulu Cave, China. *Science* **294**: 2345-2348.

Wigley, T.M.L. and Brown, M.C. (1976). The physics of caves. In *The science of speleology*. T.D. Ford and C.H.D. Cullingford (eds)., 329-59. London: Academic Press.